Tetrahydrobiopterin: Nitric Oxide and Pulmonary Vascular Control

Manasi Nandi

A THESIS SUBMITTED IN FULFILMENT OF THE REQUIREMENTS OF THE UNIVERSITY OF L0NDON FOR THE DEGREE OF DOCTOR OF PHILOSOPHY

UNIVERSITY COLLEGE LONDON
JULY 2003

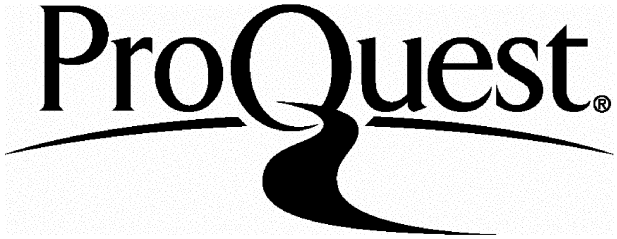

Abstract

GTP-cyclohydrolase 1 (GTP-CH1) catalyses the first and rate limiting step for the biosynthesis of tetrahydrobiopterin (BH_4), an essential cofactor for nitric oxide synthase (NOS). NOS, once active, generates nitric oxide (NO) an essential mediator of normal vascular tone and function. Suboptimal levels of BH_4 may render NOS inefficient and may additionally result in the generation of deleterious superoxide anions (O_2^-). GTP-CH1 is itself inhibited by BH_4, an effect mediated via the protein GTP-CH1 Feedback Regulatory Protein (GFRP).

There is mounting evidence correlating a dysfunction of the BH_4/NOS pathway with the vascular endothelial dysfunction observed e.g. atherosclerosis, but little evidence exists associating a dysfunction of this pathway with pulmonary hypertension (PH).

I have shown that GTP-CH1 protein expression is developmentally regulated in the porcine lung in the first few weeks of life, correlating with functional effects of supplemented BH_4 on isolated pulmonary arteries. GTP-CH1 protein expression is unchanged in animals exposed to hypobaric exposure (a model of persistent pulmonary hypertension of the newborn (PPHN)) when compared to their age matched controls and GTP-CH1 localisation appeared unchanged both developmentally and in PPHN. Thus GTP-CH1 levels do not appear to be implicated in the profound endothelial dysfunction observed in animals with PPHN.

However, studies performed on the GTP-CH1 deficient mouse mutant (*hph-1*) indicate that these mice exhibit the structural characteristics of a pulmonary hypertensive phenotype when compared to the C57BL/6xCBA wild types.

Finally, GFRP over expression in isolated endothelial cells attenuates inducible NOS (iNOS) mediated NO generation following cytokine stimulation, an effect likely to be mediated via direct inhibition of BH_4 biosynthesis.

In summary, these studies have demonstrated that regulation of BH_4 via GTP-CH1 or GFRP, affects the NOS pathway both *in vitro* and *in vivo* and that sub optimal levels of BH_4 may contribute towards the development of PH.

Acknowledgements

First and foremost I would like to express my deepest gratitude to Dr James Leiper and Professor Patrick Vallance, whose knowledge, expertise and guidance made this thesis possible. I would also like to thank the Medical Research Council for financially supporting my PhD.

I have been fortunate enough to have collaborated with a number of people during my PhD and in particular, I would like to thank Dr Alyson Miller for establishing the protocol used for the *Hph-1* studies, her knowledge and proficiency has been vital for this study and more importantly, her moral support over the past year has been invaluable. I am also grateful to Dr Simon Heales for allowing me to use the *Hph-1* strain and the equipment at the Institute of Neurology. I would also like to thank Dr Christian Hesslinger (Frankfurt University) for performing the GTP-CH1 activity measurements and Professor Steven Gross and Mark Crabtree for teaching me the BH_4 detection assay and making me feel so welcome during my Bogue Fellowship at Cornell University, New York in 2002.

Dr Alison Hislop has also been vital in both teaching and in the proofreading of this thesis, along with Professor S.G. Haworth and Professor Patrick Vallance. I am also very grateful to everyone in the BHF labs at the Rayne Institute, UCL, for all their help, in particular Dr Caroline Smith, Dr Francesca Arrigoni and Dr Aroon Hingorani.

Finally, I am indebted to my family and friends, in particular Elizabeth Foley, Emma Buttle and Lyndsey Clegg, whose continual love, support and generosity throughout my PhD, but especially over the last few months, has been immeasurable.

Publications

Tetrahydrobiopterin enhances pulmonary arterial relaxation after birth
Manasi Nandi, Francesca Arrigoni, James Leiper, Patrick Vallance, Sheila Haworth.
British Pharmacological Society Meeting, Imperial College, London. (Dec 2001)
Published in: Proceedings Supplement of the British Journal of.
Pharmacology March 2002 Volume 135 no.199P

Tetrahydrobiopterin deficient mouse mutant (hph-1) displays a pulmonary hypertensive phenotype.
M.Nandi, A. Miller, S. Haworth, S. Heales, P.Vallance
British Pharmacological Society Winter Meeting, Brighton. (Jan 2003)
Published in: British Journal of Pharmacology Volume 138, April 2003,
65P.

Early life changes in GTP-cyclohydrolase 1 contribute to pulmonary vascular endothelium-dependent relaxation.
Manasi Nandi, James Leiper, Christian Hesslinger, Alison Hislop,
Patrick Vallance, Sheila Haworth

Submitted

TABLE OF CONTENTS

TABLE OF FIGURES

Abbreviations

12-24h	12-24 hour old piglet
14d	14 day old piglet
3d	3 day old piglet
3H	3 day old piglet exposed to hypobaric hypoxia
A	Adult pig
AAAH	Aromatic amino acid hydroxylase
ACh	Acetylcholine
AD	Alveolar duct
ADMA	asymmetric dimethylarginine
BH_4	(*6R*)-5,6,7,8-Tetrahydrobiopterin
cNOS	Constitutive NOS (i.e.eNOS and nNOS)
CO_2	Carbon dioxide
DDAH	Dimethylarginine dimethylamino hydroxylase
DNA	Deoxyribonucleic acid
DRD	Dopa responsive dystonia
eNOS	Endothelial NOS
ET	Endothelin
F	Fetal piglet
FAD	Flavin adenine dinucleotide
FMN	Flavin mononucleotide
GFRP	GTP-CH1 feedback regulatory protein
GTP	Guanosine Triphosphate
GTP-CH1	GTP-cyclohydrolase 1
H_2O_2	Hydrogen peroxide
Haem	Iron protoporphyrin IX
Hph-1	Hyperphenylalanaemic mouse mutant
IFNγ	Interferon gamma
iNOS	Inducible NOS

L-NMMA	N^G–monomethyl L-arginine
LPS	Lipopolysaccharide
LV+S	Left ventricle plus septum
MnTMPyP	Manganese(III)tetrakis(1-methlyl)porphyrin pentachloride
NADPH	Nicotinamide adenine dinucleotide phosphate
NB	Newborn piglet
nNOS	Neuronal NOS
NO	Nitric Oxide
NOS	Nitric Oxide Synthase
O_2^-	Superoxide anion
$ONOO^-$	Peroxynitrite
PGI_2	Prostacyclin
PH	Pulmonary hypertension
PPHN	Persistent pulmonary hypertension of the newborn
PVR	Pulmonary vascular resistance
RB	Respiratory bronchiole
RNA	Ribonucleic acid
RTP	Room temperature and pressure
RV	Right ventricle
SDS	Sodium dodecyl sulphate
SEM	Standard error of the mean
sEnd 1	Murine skin endothelial cells
SNP	Sodium nitroprusside
SOD	Superoxide dismutase
TB	Terminal bronchiole
TNFα	Tumour necrosis factor alpha
U46619	9,11-Dideoxy-11α,9α-epoxymethanoprostaglandin $F_2\alpha$

CHAPTER 1

General Introduction

Adult lung anatomy and physiology

The respiratory system in mammals is composed of airways that carry air from the atmosphere to the alveoli within the lungs, and a dual supply of blood vessels, comprising the pulmonary circulation and the bronchial circulation, that allow gaseous exchange to occur and provides oxygen and nourishment to the lung, respectively. The bronchial circulation operates under the high pressure of the systemic circulation whilst the pulmonary circulation is a low-pressure system. The pulmonary circulation has developed as a high flow, low resistance vascular bed, to protect the thin blood gas barrier from high intravascular pressures that would otherwise promote oedema formation (Morrell and Wilkins, 2001). Inspired air reaches the alveolar surface by passing though a series of branching airways that stem from the main airways (bronchi) and become progressively more numerous and narrower in diameter, a branching pattern which provides a large surface area within a small volume, increasing the efficiency of gas exchange. The bronchi are so called based on their size and the presence of cartilage within the wall. In humans, as the bronchi divide and narrow into progressively smaller airways, the walls no longer contain cartilage, and are termed bronchioli (Figure 1.01). All airways have a smooth muscle layer beneath the epithelium thereby allowing the airways to change diameter and length, and the amount of this muscularisation decreases as the airways become smaller in diameter (Stocks and Hislop, 2002). Accompanying the airways and branching along side them are the pulmonary arteries, carrying blood from the right heart to the capillaries for gaseous exchange. Blood returns to the left atrium via pulmonary veins.

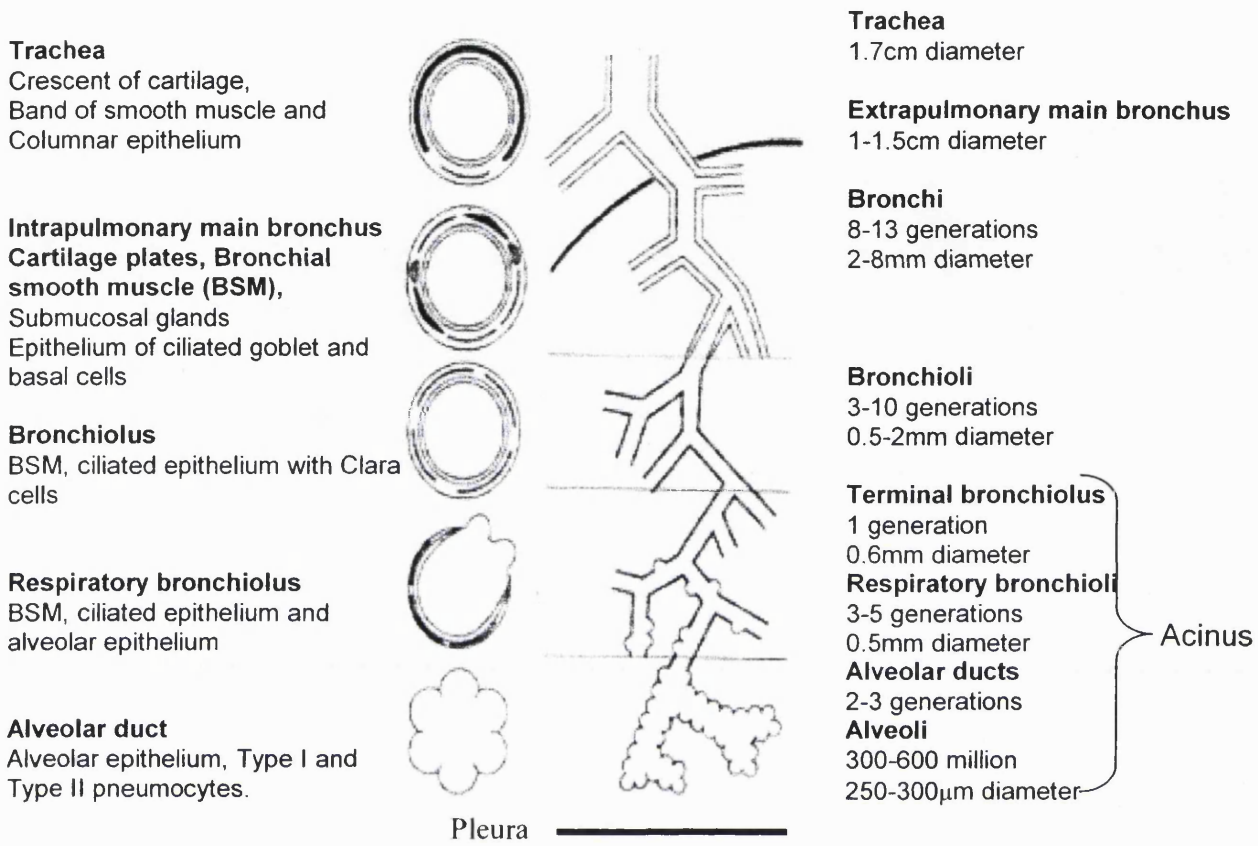

[1]Figure 1.01 Number and dimensions of airways in the human adult lung and structure of the airway wall

[1] Taken from Stocks and Hislop Chapter 3 in Drug Delivery to the Lung, Ed. Visgaard H; Smaldone GC and O'Callaghan C. Vol. 162 in Lung Biology in Health and Disease series. Exec. Ed. Claude Lenfant. Marcel Dekker, Inc.

Structure of arteries

The walls of an artery are composed of three distinct layers: the tunica intima, tunica media and tunica adventitia (Figure 1.02). The tunica intima is the innermost layer and is made up of a layer of endothelial cells adhering to a connective tissue basement membrane with elastic fibres. It has been demonstrated that the endothelium is an important regulator of vascular tone as it is involved in the release of a variety of vasoactive mediators (see figure 1.03).

The next layer, the tunica media, is primarily composed of spindle shaped smooth muscle cells embedded in a matrix of elastin and collagen, providing support for the vessel in addition to changing the lumen diameter to regulate blood flow and pressure. Finally, the tunica adventitia forms the outermost layer acting as a connective tissue sheath. This layer is composed of varying amounts of elastin and collagen and furthermore contains cell types including fibroblasts and tissue macrophages (Figure 1.02).

Pulmonary arteries run alongside the bronchial airway, subdividing into terminal branches, which lead to a vast capillary network enveloping the alveoli, where gaseous exchange occurs. Structurally, these arteries consist of an endothelial cell layer, a medial layer containing elastic laminae and smooth muscle cells and an adventitial layer. All arteries conduct blood throughout the body but depending on the size and composition of the vessel, serve differing roles. Elastic arteries have the greatest lumen diameters (e.g. lobar pulmonary artery) and, as the name suggests, are rich in parallel elastic laminae, allowing the vessels to expand and accommodate large volumes of blood.

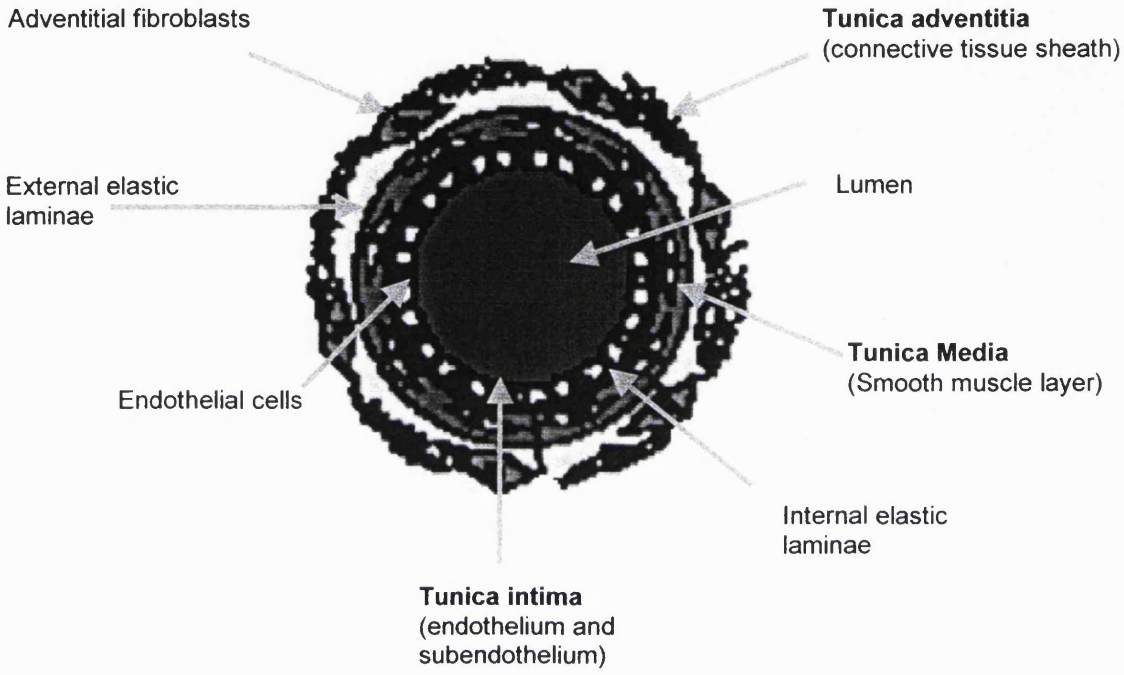

[2]Figure 1.02 Schematic representation of blood vessel structure showing the three distinct layers.

Progressing peripherally along the arterial pathway, as the external diameter decreases, the elastic laminae within the media decrease in number and gradually the proportion of smooth muscle cells increase (muscular arteries). Finally the elastic laminae further decrease in the smallest of arteries and the media is almost entirely composed of smooth muscle (resistance arteries), these vessels have a relatively thick wall in relation to their diameter and provide the chief resistance to blood flow.

[2]Doug Simmonds, Modified from Pulmonary Circulation: Basic Mechanisms to Clinical Practice, Imperial College Press 2001

Within the subgroup of resistance arteries the entirely muscular wall (fully muscular resistance arteries) gets progressively thinner until the muscle becomes incomplete around the circumference and exists as a spiral which, in cross section, appears as a crescent. The artery is then termed a partially muscular artery. Further to the periphery in the smallest arteries, the muscle disappears leaving only a single elastic lamina outside the endothelium (non muscular). Overall the pulmonary arterial system is a low resistance system consisting of comparatively thin walled vessels that have larger internal diameters compared with the systemic circulation. This structural difference provides relatively low resistance to flow allowing handling of the large blood volume at perfusion pressures that are low compared with the systemic circulation.

Development of the pulmonary vasculature

The intra-uterine (fetal) pulmonary circulation is very different from the extrauterine "adult" pulmonary circulation. Major alterations of the circulation occur at birth to allow a change from an entirely placental to an entirely pulmonary dependent system of gaseous exchange. In the fetus, all nutritional and oxygen requirements are met by the placenta and the lungs are largely bypassed. Oxygenated blood from the maternal circulation enters the fetus via the umbilical vein, entering the inferior vena cava and then the right atrium of the heart. This oxygenated blood is then directed through a fetal channel, the foramen ovale (communication between right and left atria), to the left side of the heart from where it is pumped through the aorta into the fetal systemic circulation. Some of the placental blood passes into the pulmonary arteries via the right ventricle. However as the lungs are not used for gaseous exchange in the fetus (and only require a small blood supply for growth,

oxygenation and metabolic functions), approximately 90% of this blood is diverted into the aorta via the ductus arteriosus (vessel connecting pulmonary artery and aorta) (Rudolph, 1979). Overall, the fetal pulmonary arterial system exists in a high resistance state and the arteries have comparatively thick walls and small lumen diameters compared to that seen after birth.

After birth, the placental circulation is no longer required and the fetal channels close. Furthermore there is a substantial increase in blood flow through the lungs and the pulmonary circulation changes from a high resistance system to a low resistance system as a result of the lung expansion following air breathing. This fall in pulmonary vascular resistance (PVR) allows for up to a ten-fold rise in pulmonary blood flow, which ensures that the lung can assume its postnatal role in gas exchange (Ghanayem and Gordon 2001). This dramatic fall in PVR is additionally associated with the establishment of a gas liquid interface in the lung, increased oxygen tension, rhythmic distension of the lung (respiration), shear stress and the production of vasoactive products including nitric oxide (NO) and prostacyclin (PGI_2) (potent vasodilators) (Abman, 1999).

The first breath results in the pulmonary alveoli opening up and blood from the right heart fills the pulmonary vasculature within the lungs, thereby reducing the pressure on the right hand side of the heart. Conversely, the pressure in the left hand side of the heart increases as more blood is returned from the well vascularised pulmonary tissue via the pulmonary veins, to the left atrium leading to a high blood pressure in the aorta. The right ventricular wall, which is about as thick as the left ventricular wall *in utero,* gradually becomes relatively

thinner due to the decreased pressure and does not increase in thickness as rapidly as the left ventricle. At birth, a considerable amount of structural reorganisation occurs within the pulmonary vasculature, with the PVR falling and blood flow increasing. This is achieved by an increase in the endothelial and smooth muscle cell surface volume, and as cells spread in the vessel wall, the lumen diameter increases and resistance falls (Haworth and Hislop 1981). In the pig model, by 24 hours after birth, the rapid decrease in total PVR diminishes to 50-60% of the systemic vascular resistance, reaching adult values within 2-4 week of age (Haworth and Hislop 1981).

1.04 Persistent Pulmonary Hypertension of the Newborn

In cases where the normal adaptation of the pulmonary vasculature does not occur and neonates fail to achieve or sustain the normal decrease in PVR, persistent pulmonary hypertension of the newborn (PPHN) may occur (Gersony, 1984). PPHN is the result of an elevated pulmonary vascular resistance usually caused by hypoxia. Venous blood can be diverted to some degree through persistent fetal channels (i. e. the ductus arteriosus and foramen ovale) into the systemic circulation (right to left shunting), bypassing the lungs thereby increasing the severity of systemic arterial hypoxemia (Abman, 1999). Increased muscularisation and luminal narrowing potentiate the pulmonary vascular obstruction thereby further contributing to the pulmonary hypertension. PPHN is a problem in neonatal intensive care and contributes to morbidity and mortality in both term and preterm neonates.

One consistent finding in both neonates with PPHN and in cases of adult pulmonary hypertension, is that a number of structural and functional changes occur in the pulmonary vascular wall including abnormal vasoreactivity and proliferation of vascular smooth muscle cells and hypertrophy, and it is believed that the pulmonary vascular remodelling and the abnormal pulmonary vasoconstriction contribute to the elevations in pressure and resistance (Jeffery and Wanstall 2001).

1.05 Animal models of pulmonary hypertension

The pulmonary vascular remodelling observed in pulmonary hypertension has been characterised in a variety of animal models. This includes the adult rat model of hypoxia induced pulmonary hypertension, in which adult rats are placed in a hypobaric chamber maintained at a pressure of 380 mmHg and develop hypobaric induced pulmonary hypertension (Hislop and Reid 1976; Hislop and Reid 1977). These animals show an increase in the thickness of all three layers of the pulmonary vessels occurring as a result of hypertrophy (growth) and hyperplasia (proliferation) of the predominant cell types within each layer (fibroblasts, smooth muscle cells and endothelial cells) (Hislop and Reid 1976; Hislop and Reid 1977; Jeffery and Wanstall 2001). Furthermore there is an observed increase in medial thickness of the smooth muscle layer in the pulmonary arteries at all levels of the pulmonary arterial tree and extension of muscle into the small pulmonary arteries (resistance arteries), which normally do not contain any smooth muscle cells, by light microscopy. The mechanisms leading to increased muscularisation are not entirely clear, although it has been suggested that the muscle arises from the differentiation of

pericytes or intermediate cells (intermediate between smooth muscle and pericytes) into smooth muscle cells (Reid and Meyrick 1980).

In terms of studying the effects of hypoxia induced pulmonary hypertension in the newborn period, the rat model is perhaps not the best experimental animal to use for elucidating the nature of the pulmonary remodelling in human pulmonary hypertension as there are important structural differences between the human and rat lung and pathological reactions to hypoxia differ significantly to those found in human disease (Heath 1992). A better model is the porcine model of PPHN. PPHN can be mimicked in the porcine lung by placing newborn piglets in a hypobaric chamber which is essentially a chamber attached to a vacuum pump, resulting in an internal atmospheric pressure of 50.4kPa. The use of chronic hypobaric hypoxia enables the study of pathophysiological functional and structural changes, which are in keeping with human PPHN (Haworth and Hislop 1982). These piglets develop right ventricular hypertrophy and have a reduced arterial oxygen saturation compared with normoxic control piglets because they continue to shunt right to left through the foramen ovale and ductus arteriosus (Tulloh *et al.*, 1997). This model will be discussed in greater detail in the following chapters.

1.06 Pulmonary vascular remodelling in the neonatal period

A variety of physical and chemical stimuli influence the pulmonary vascular remodelling that occurs after birth and in PPHN. The physical stimuli include stretch and shear stress (due to increased blood flow), which in turn may activate stretch sensitive ion channels or act upon shear stress response elements thereby potentially regulating protein synthesis

(Jeffery and Wanstall 2001). In addition to physical stimuli, a variety of vasoactive mediators may play a role in the failure of the PVR to fall after birth in PPHN. Broadly speaking, either there is 1.) a failure to release or to sustain release endogenous vasodilators including nitric oxide, prostacyclin, endothelium derived hyperpolarizing factor and adenosine or 2.) there is an increase in the release of vasoconstrictors including endothelin and leukotrienes (Abman 1999) most of which are released from the endothelium or 3.) both factors are operative suggesting that the endothelium may be dysfunctional in cases of PPHN.

1.07 The functional role of the endothelium

Initially thought to be a layer of inert cells lining the lumen of blood vessels, the endothelial cell layer has since been proven to be a dynamic, heterogeneous multifunctional organ playing a variety of roles including the regulation of vascular tone via the generation of potent vasoconstrictors and vasodilators and maintenance of the patency of the vessels via the release of anti-platelet and anti-thrombotic agents. The vascular endothelium forms the permeability barrier between circulating blood cells and the underlying vascular tissue and is thus in a unique position to respond to circulating factors, blood elements or environmental stresses and then serve as a signal integrator and transducer to modulate events in the vasculature via paracrine effects (Vane *et al.*, 1990).

The seminal study performed by Furchgott and Zawadski in 1980 established the importance of the endothelium. They observed that denuding the endothelial lining of the rabbit aorta resulted in the loss of acetylcholine (ACh) induced relaxation, whilst the dilator

effects of glyceryl trinitrate and contractile effects of noradrenaline remained intact. It was thus concluded that the endothelial cell layer needed to be intact in order for ACh to exert its effect. It was subsequently shown that this ACh-induced relaxation was mediated by the presence of a diffusible factor released from endothelial cells, termed endothelium derived relaxing factor (EDRF) which had a biological half life of a few seconds (Furchgott, 1984).

The identity of EDRF was not established until 1987 when it was shown to be indistinguishable from nitric oxide (NO) (Palmer *et al.* 1987). Furthermore, in man, inhibitors of NO synthesis such as L-NG monomethylarginine (L-NMMA) have been shown to partially reduce the vasodilatory response to ACh in blood vessels as well as causing a reduction in local blood flow (Vallance *et al.*, 1989). The importance of NO is now well established and will be discussed further.

In addition to NO, a second vasoactive mediator released from endothelial cells that appears to be especially important in the vasoregulation of the perinatal lung is endothelin (ET-1) (Yanagisawa *et al.* 1988). ET-1 is derived from preproendothelin-1, which undergoes proteolysis within the endothelial cell resulting in the generation of big endothelin, which is subsequently cleaved by the action of ET converting enzyme (ECE) forming the vasoactive product ET-1. The contractile effects of ET-1 are mediated through the ET_A and ET_B receptors located on the smooth muscle cell, whilst dilatory effects are mediated via activation of the ET_B localised to the endothelial cell. As far as the effects of ET-1 on the pulmonary circulation are concerned, the largest body of evidence suggests that ET-1 serves primarily as a potent vasoconstrictor (Wang and Coceani, 1992). The two substances NO

and ET-1 appear to be particularly important in the vasoregulation of the perinatal lung, but endothelial cells release a number of other mediators which are summarised in Figure 1.03 below.

[3]Figure 1.03 Endothelium derived factors

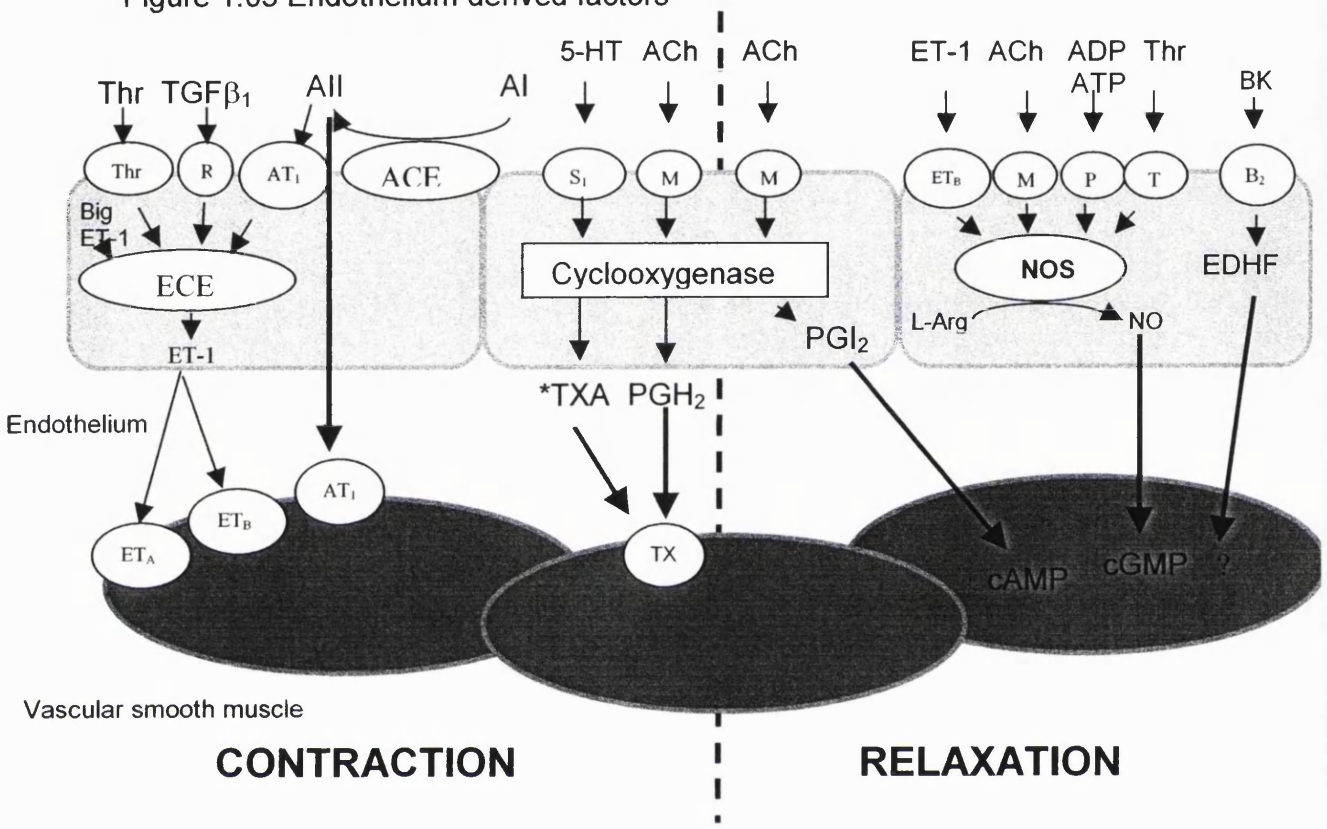

Endothelium derived contractile and relaxant vasoactive substances: **Big ET**, Big endothelin; **Thr,** thrombin; **T**, thrombin receptor; **TGFβ$_1$**, transforming growth factor; **ECE**, endothelin converting enzyme; **AII**, angiotensin II; **AI**, angiotensin I; **ACE**, angiotensin converting enzyme; **AT-1**, angiotensin receptor; **ET-1**, endothelin I; **ET$_A$ and ET$_B$** endothelin receptors A and B; **5-HT**, 5-hydroxytryptamine; **S$_1$,** 5HT receptor; **ACh**, acetylcholine; **M**, muscarinic receptor; **PGI$_2$**, prostacyclin; **PGH2**, prostaglandin H$_2$; **TXA$_2$**; Thromboxane (*mainly derived from platelets) **TX**, thromboxane receptor; **ADP**, adenosine diphosphate; **ATP**, adenosine triphosphate; **P**, purine receptor; BK, bradykinin; **B$_2$**, bradykinin receptor; **EDHF**, endothelium derived hyperpolarizing factor; **NOS**, nitric oxide synthase; **L-Arg**, L-arginine; **NO**, nitric oxide; **cAMP**, cyclic AMP; **cGMP**, cyclic GMP

[3] Modified from The Endothelium in Cardiovascular Disease, Chapter 1; ed Luscher, T.F. Springer and Vascular Endothelium in Human Physiology and Pathophysiology, Ed. Vallance and Webb; Harwood Academic Publishers.

1.08 Nitric oxide and the endothelium

NO is synthesised from L-Arginine (Palmer *et al.*, 1988) utilizing molecular oxygen to generate NO and L-citrulline as a co product (Palmer and Moncada, 1989). It is now well established that NO can be produced from a number of cell types other than endothelial cells and the enzyme responsible for catalysing this reaction is nitric oxide synthase (NOS), of which three isoforms have been identified, neuronal NOS (nNOS or NOS I), endothelial NOS (eNOS or NOS III), and inducible NOS (iNOS or NOS II). eNOS and nNOS are constitutively active enzymes, thus responding to fluxes in intracellular calcium (Ca^{2+}), whilst iNOS has the Ca^{2+} /calmodulin tightly bound within its structure with such high affinity that it is bound over the entire physiological range of intracellular Ca^{2+} levels and the activity of iNOS is therefore independent of Ca^{2+} fluxes (Cho *et al.*, 1992).

1.09 Neuronal NOS (nNOS)

nNOS was the first NOS isoform to be purified and cloned (Bredt *et al.*, 1991). Although initially thought to be released by brain cells, it has also been shown to be present in many different parts of the body including areas of the spinal cord, peripheral vasomotor nerves, skeletal muscle and in epithelial cells of the lung and uterus (Fostermann *et al.*, 1994). nNOS has also been shown to be present in non-adrenergic-non-cholinergic (NANC) inhibitory neurones purified from rat anococcygeus muscle (Mitchell *et al.* 1991). NO produced from nNOS mainly serves as a neuromodulator although other functions including neurotoxic effects (which may be implicated in neurogenerative diseases such as Parkinson's disease) have been demonstrated (Canals *et al.*, 2001).

1.10 Inducible NOS (iNOS)

iNOS was first purified and cloned from an immunoactivated murine macrophage cell line (Lowenstein *et al.*, 1992). iNOS has been detected in all nucleated cells in the cardiovascular system including vascular endothelial and smooth muscle cells as well as in inflammatory cells such as mast cells and fibroblasts (Papapetropoulos *et al.* 1999). Unlike the other two NOS isoforms, iNOS does not require calcium to bind in order for the enzyme to become active but iNOS expression is transcriptionally regulated following cytokine or bacterial lipopolysaccharide stimulation and this expression can be induced in a variety of cell types including cardiac myocytes and endocardial cells (Schulz *et al.*, 1992, Smith *et al.*, 1993). On the whole, cells derived from rodents tend to produce more NO from iNOS following cytokine stimulation compared to human cells (Nathan and Xie 1994).

1.11 Endothelial NOS (eNOS)

eNOS protein was originally purified and cloned from bovine vascular endothelial cells (Nishida *et al.*, 1992) and is the isoform responsible for producing endothelium derived relaxing factor (NO) and thus plays an essential role in the cardiovascular system. eNOS has also been shown to be present in cardiac myocytes and platelets (Balligand *et al.*, 1993, Sase and Michel 1995). Most importantly, eNOS displays a constitutive activity responsible for generating low levels of NO in the basal state providing a continuous supply of NO to the vascular smooth muscle cells hence aiding the maintenance of normal vascular tone and systemic blood pressure (Rees *et al.*, 1989).

1.12 NO and PPHN

There is a large amount of evidence to suggest that NO is a key player in both the structural remodelling and in the abnormal vasoconstriction seen in pulmonary hypertension. Indeed neonates suffering from PPHN can be successfully treated with NO inhalation therapy (Kinsella *et al.*, 1992), although there are inherent risks associated with inhalation of NO as it is typically administered in combination with oxygen, leading to the generation of harmful NO oxides and/or free radicals. NO provides both anti thrombotic and anti constrictive effects as it is released into the lumen of vessels (where it prevents platelet aggregation) and into the smooth muscle layer where it relaxes vascular smooth muscle (Moncada *et al.*, 1991). Thus NO can modulate pulmonary vascular tone and impaired NO production may contribute towards the development of pulmonary hypertension. Additionally NO inhibits the mitogenesis and proliferation of vascular smooth muscle in cultured rat vascular smooth muscle cells (Garg and Hassid 1989).

Studies performed on a porcine model of PPHN have shown decreased expression of eNOS protein and immunostaining and a reduction in the proportion of constitutive NOS activity compared with age matched controls, alongside an absence of endothelium dependent vasodilatation to ACh (Hislop *et al.*, 1997; Arrigoni *et al.*, 2002, Tulloh *et al.*, 1997). Other studies using a porcine model have shown that newborn piglets exposed to a different model of chronic hypoxia (normobaric, 10% O_2) developed pulmonary hypertension and exhibited reduced responses to agents that stimulated or reduced the release of NO (Fike and Kaplowitz 1994; Berkenbosch *et al.*, 2000; Fike and Kaplowitz 1996) and furthermore have demonstrated a significant decrease in exhaled NO output,

plasma concentrations of nitrite and eNOS protein from chronically hypoxic newborn piglets (Turley *et al.*, 2003; Fike *et al.*, 1998). eNOS protein expression and mRNA expression have also been shown to be decreased in different animal models of PPHN including prenatal ligation of the ductus arteriosus in the lamb and congenital diaphragmatic hernia in the rat (Shaul *et al.*, 1997; North *et al.*, 1995).

However, species differences appear to exist regarding the role of NO in the regulation of pulmonary vascular tone and must be taken into account when interpreting data (Adnot *et al.*, 1995) as other animal models of hypoxia, in particular rodents, have shown increased eNOS expression activity and/or increased release of NO to endothelium dependent vasodilators following hypoxic exposure (Isaacson *et al.*, 1994; Muramatsu *et al.*, 1996; Resta and Walker, 1996; Sato *et al.*, 1999). The majority of the rodent studies were conducted in adult animals and it has been suggested that the effects of hypoxia may be different between adult and newborn, in so far as the contribution of NO to the regulation of pulmonary vasomotor tone changes with postnatal age (Shaul et al., 1993; Zellers and Vanhoutte 1991).

Possible mechanisms explaining the loss of endothelium dependent relaxation observed in hypobaric induced pulmonary hypertension includes either the inability of the vascular smooth muscle to relax in response to NO or impaired synthesis or release of NO from the endothelial cell layer. However, NO donors such as SNP elicit similar concentration dependent vasodilation in lungs from both normal and pulmonary hypertensive (hypoxic) rats, suggesting the response of the smooth muscle is unaltered by chronic hypoxia (Adnot *et al.*, 1991; Carville *et al.*, 1993; Eddahibi *et al.*, 1992). It is therefore more likely that

impaired synthesis or release of NO results in endothelial dysfunction seen following hypoxic/hypobaric exposure.

NO biosynthesis and NOS activity are therefore important targets for treatment of PPHN and one possible approach would be to investigate the regulation of NOS cofactors as these may have direct influences upon NO generation and hence manipulation of cofactors may lead to alternative therapies.

1.13 Structure of NOS

NOS isoforms, once active, exist as a homodimer consisting of two identical monomeric subunits, which can be functionally and structurally divided into two major domains, the C-terminal reductase domain and the N-terminal oxygenase domain (Knowles and Moncada 1994). NOS catalyses the formation of NO from L-arginine and molecular oxygen, with nicotinamide adenine dinucleotide phosphate (NADPH) behaving as an electron donor in a reaction involving the five electron oxidation of the terminal guanidine nitrogen of arginine. Both monomeric subunits of NOS also contain tightly bound cofactors (6*R*)-5,6,7,8-tetrahydrobiopterin (BH_4), flavin adenine dinucleotide (FAD), flavin mononeucleotide (FMN) and iron protoporphyrin IX (haem) (Figure 1.04).

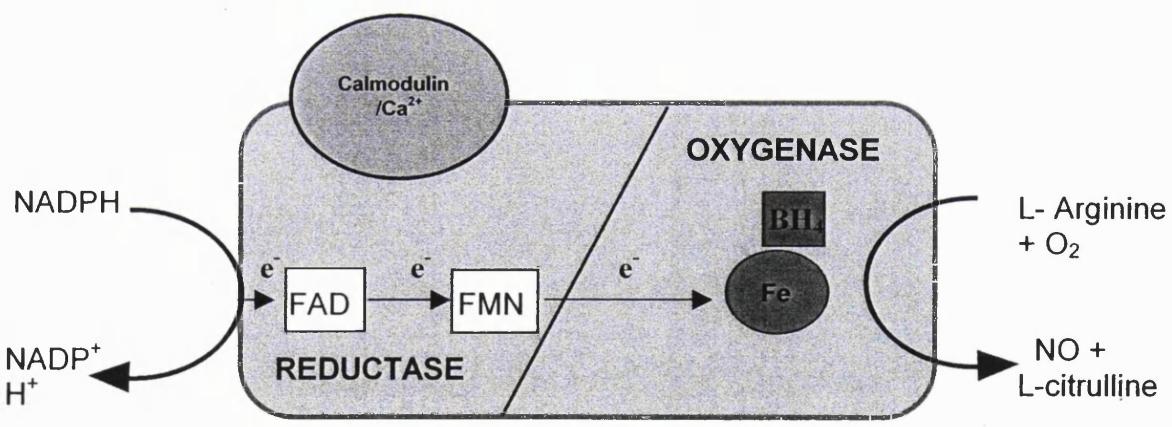

Figure 1.04 Schematic representation of a NOS monomer showing cofactors and electron transfer.

1.14 6*R*-L-erythro-5,6,7,8-tetrahydrobiopterin

6*R*-L-erythro-5,6,7,8-tetrahydrobiopterin (BH_4) was first identified as an electron donating co-factor for the aromatic amino acid hydroxylases (AAAH), including phenylalanine hydroxylase, tyrosine hydroxylase and tryptophan hydroxylase involved in the synthesis of the neurotransmitters L-Dopa, noradrenaline and 5-hydroxytryptamine (Kaufman 1963 and Hoshiga *et al.*, 1993). However Kwon *et al.*, 1989 and Tayeh and Marletta, 1989, demonstrated that BH_4 is also an essential co-factor for NOS activity, with all three isoforms of NOS requiring BH_4 as a crucial cofactor for full activity, and hence BH_4 has important biological implications within the cardiovascular system (Tayah and Marletta 1989; Kwon *et al.*,1989; Werner-Felmeyer *et al.*, 1990; Schmidt *et al.*, 1992). The Km of BH_4 for NOS is several orders of magnitude lower than that for the AAAH's (100-600μM for AAAH's and 0.03-0.1μM for NOS) (Katusic 2001).

BH_4 biosynthesis proceeds primarily via the *de novo* pathway in a Mg^{2+}-, Zn^{2+}-, and NADPH-dependent reaction from GTP via two intermediates, 7,8-dihydroneopterin triphosphate and 6-pyruvoyl-5,6,7,8-tetrahydropterin (Figure 1.05). The first and rate limiting enzyme in the *de novo* pathway is GTP cyclohydrolase 1 (GTP-CH1) (Nichol *et al.*, 1985). In addition to the *de novo* pathway for BH_4 synthesis from GTP, mammalian cells also have the capacity to regenerate BH_4 from pre-existing dihydropterins. BH_4 is unstable and is readily oxidised to form dihydropterin, and it is believed that the salvage pathway allows recycling of these excess dihydropterins (Figure 1.05). The pterin salvage pathway comprises the two enzymes sepiapterin reductase and dihydrofolate reductase and exogenously added sepiapterin can also be converted by sepiapterin reductase to 7,8-dihydrobiopterin, which is

further reduced to BH_4 by the action of dihydrofolate reductase. Additionally, endogenous sepiapterin and 7,8-dihydrobiopterin are detectable in tissue and cell homogenates, arising via the degradation of tetrahydrobiopterin intermediates from the *de novo* BH_4 synthetic pathway e.g. 6-lactoyl tetrahydropterin. (Nichol *et al.*, 1985).

L-Sepiapterin is a light sensitive compound, which when administered exogenously, is incorporated into cells where it is intracellularly reduced to BH_4 via the salvage pathway (Nichol *et al.*, 1985, Tsutsui *et al.*, 1996). Unlike BH_4 itself, sepiapterin is less sensitive to oxidation and hence is superior to direct application of BH_4 as a means of increasing intracellular concentrations of the cofactor (Werner-Felmayer *et al.*, 1993). Sepiapterin is now a commonly used pharmacological tool to study the effects of BH_4 supplementation in a number of systems. Exogenous administration of sepiapterin to cytokine treated brain endothelial cells and rat aortic smooth muscle cells almost doubles NO synthesis, an effect arising from conversion of sepiapterin to BH_4 via the salvage pathway and not by sepiapterin acting directly as a NOS cofactor (Gross *et al.*, 1991; Gross and Levi, 1992). Diaminohydropyridine (DAHP) a GTP-CH1 inhibitor has been shown to decrease the production of Nitrite in cells following cytokine stimulation and sepiapterin administration has been shown to prevent this effect in murine fibroblasts and brain endothelial cells (Werner-Felmeyer *et al.*, 1990; Gross *et al.*, 1991). Functionally, addition of sepiapterin to intact canine middle cerebral arteries, resulted in 300 fold increase in the levels of intracellular BH_4, demonstrating that sepiapterin is able to be taken up into vascular endothelial cells and utilized in the salvage pathway to generate BH_4 in an *in vitro* system. The endothelium also contained almost 80% of the total amount of BH_4 in arteries

incubated with sepiapterin suggesting that, at least in cerebral arteries, endothelial cells have a high capacity to synthesize BH_4. However, this study also demonstrated that sepiapterin alone (24 hour treatment) actually attenuated calcium ionophore (A23187) mediated endothelium dependent relaxation of the arteries but improved the relaxations when administered in conjunction with superoxide dismutase (SOD), and concluded that auto oxidation of BH_4 and subsequent formation of superoxide anions (O_2^-) explained these findings (Tsutsui *et al.,* 1996). Vasquez-Vivar *et al.*, (2002a) performed studies on aortas from hypercholesterolaemic (HL) rabbits and found that although sepiapterin supplementation restored BH_4 levels to normal in the aortas from HL rabbits whilst having no effect in control animals, long term sepiapterin administration worsened the endothelium dependent relaxations of the HL aortas an effect resulting again from enhanced O_2^- generation, consistent with the findings by Tsutsui *et al.*, (1996). Endothelial function has, however, been improved following acute administration of sepiapterin to vessels in a number of studies (Tiefenbacher *et al.*, 2000; Bagi and Koller 2003, Marinos *et al.*, 2001).

The importance of BH_4 in relation to NO synthesis has been demonstrated in a variety of cell lines. Selective inhibitors of enzymes in the BH_4 biosynthetic pathway abolish NO generation in cytokine treated endothelial cells (Gross *et al.,* 1991) vascular smooth muscle cells (Gross and Levi 1992) and fibroblasts (Werner *et al.*, 1991). Repletion of BH_4 reverses this inhibition and increases the rate of NO synthesis in endothelial cells (Rosenkranz-Weiss *et al.*, 1994). Functionally, Kinoshita *et al.*, (1997) showed that inhibiting BH_4 biosynthesis, using the GTP-CH1 inhibitor 2,4-diamino-6-hydroxypyrimidine, impaired endothelium-dependent relaxation of cerebral blood vessels. It was concluded that decreased intracellular

levels of BH_4, reduced endothelium-dependent relaxations and that superoxide (O_2^-) production (resulting from activation of dysfunctional eNOS), was responsible for the impairment of endothelial function. NO generation can therefore be impaired by reduced BH_4 cofactor availability either by impaired synthesis of any of the enzymes required in the *de novo* or salvage pathways or by accelerated oxidation under conditions of oxidative stress.

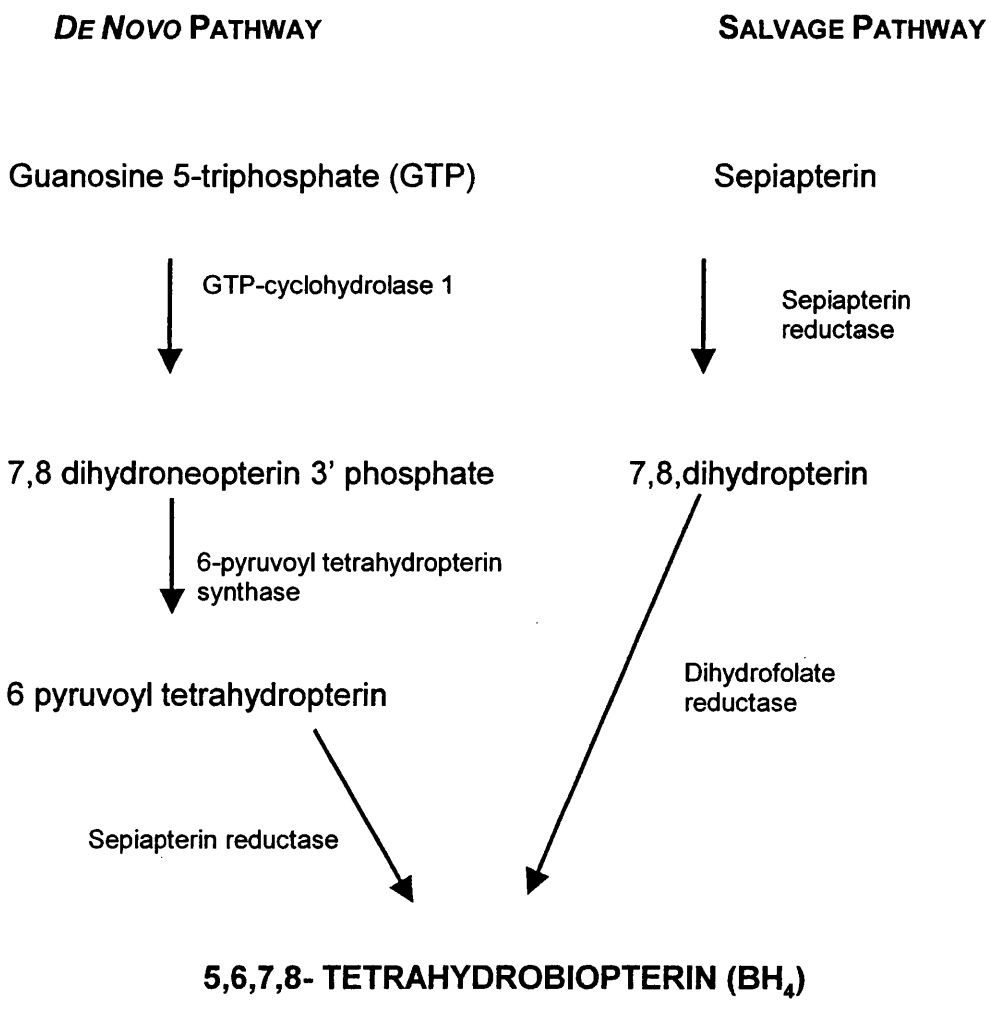

Figure 1.05 The de novo and salvage pathways for tetrahydrobiopterin biosynthesis.

1.15 Tetrahydrobiopterin, reactive oxygen species and endothelial dysfunction

NO is released immediately on synthesis and the bioavailability of NO is determined by the balance between the activity of NOS and the catabolism of NO. The *in vivo* half-life of NO is mainly determined by its reaction with oxyhaemoglobin and O_2^- (Beckman and Koppenol 1996). Catabolism of NO by its reaction with O_2^- is an important mechanism underlying endothelial dysfunction and oxidative vascular injury, described in many vascular diseases and the O_2^- anion is able to rapidly react with NO to produce peroxynitrite ($ONOO^-$), high concentrations of which are highly toxic (Beckman *et al.*, 1990). Cyclooxygenase, NADH oxidoreductase and xanthine oxidase are thought to also be sources of O_2^- production in the dysfunctional endothelium and may lead to the production of peroxynitrite ($ONOO^-$) via a rapid reaction between NO and O_2^- (Cosentino *et al.*, 1994; Mohazzab *et al.*, 1994; Griendling *et al.*, 2000; Sanders *et al.*, 1997). Indeed, human studies have shown that reduced NO mediated vasorelaxations in arteries and veins from patients with vascular disease risk factors, is associated with increased O_2^- formation (Guzik *et al.*, 2000). Cosentino and Luscher (1999), suggested that decreased BH_4 availability might be responsible for the dysfunction of NOS, causing a shift in the balance between the production of protective NO and deleterious reactive oxygen species. Various studies have demonstrated that a close relationship exists between the availability of BH_4 and NO synthesis in both endothelial and vascular smooth muscle cells, indeed intracellular levels of BH_4 have been shown to be controlled by the generation of both NO and O_2^- (Schmidt *et al.*, 1996). Partially oxidised analogues of BH_4 have been shown to enhance the rates of O_2^- formation from purified eNOS in the presence of saturating L-arginine concentrations, implying that the ratio of

reduced and oxidised biopterin may be physiologically important in determining the rates of NO production versus uncoupled O_2^- formation from eNOS (Vasquez Vivar *et al.*, 2002 (b)). Furthermore, purified nNOS has also been shown to act as a source of O_2^- (Pou *et al.*, 1992).

There are several possible reasons as to why the availability of BH_4 may be decreased in endothelial dysfunction, including reduced expression of GTP-CH1 as demonstrated in coronary vessels of diabetic rats (Meininger *et al.*, 2000). Additionally BH_4 can be rapidly oxidised by $ONOO^-$ implying that the associated increase of NOS dependent O_2^- and $ONOO^-$ generation would further deplete BH_4 levels (Milstein and Katusic 1999). Finally Vasquez-Vivar *et al.*, 2000, demonstrated that 7,8,dihydrobiopterin, an oxidized BH_4 derivative, can enhance O_2^- formation from eNOS. *In vivo* studies have been conducted to establish the effects of BH_4 supplementation in both clinical and experimental models, to investigate whether endothelial function can be restored. BH_4 supplementation using either sepiapterin or BH_4 directly, restored endothelial dysfunction in long term smokers (Ueda *et al.*, 2000), hypercholesterolemics (Stroes *et al.*, 1997, Fukuda *et al.*, 2002) and atherosclerosis (Tiefenbacher *et al.*, 2000).

1.16 NOS as a generator of O_2^- and the role of BH_4

Mechanisms of the precise action of BH_4 have been proposed, including stabilisation of the structure of the active NOS dimer (Giovanelli *et al.*, 1991, Wever *et al.*, 1997) and, at high concentrations, inducing allosteric modification of NOS increasing the affinity for L-Arginine (Liu and Gross 1996). Furthermore, it has been demonstrated that binding of the first molecule of BH_4 to a NOS dimer has an anticooperative effect on the binding of the second molecule of BH_4 (Gorren *et al.*, 1996).

However the largest body of evidence points towards BH_4 behaving as an electron donor in the synthetic reaction (Wei *et al.*, 2001, Wei *et al.*, 2002), and sub optimal concentrations of BH_4 (or the presence of BH_2) have been shown to reduce the formation of nitric oxide, favouring the 'uncoupling' of NOS leading to NOS mediated reduction of oxygen and formation of O_2^-.(Katusic 2001, Cosentino and Luscher 1999, Vasquez Vivar 1999).

The proposed mechanism by which NOS generates O_2^- is explained by considering the reactions within the NOS dimer. A flow of NADPH derived electrons from the reductase domain to the oxygenase domain follows the formation and binding of a calcium/calmodulin complex (for eNOS and nNOS). Once the electrons reach the oxygenase domain, the iron group of heme is reduced from Fe(III) to Fe (II) and this facilitates molecular oxygen (substrate) binding to the heme Fe(II) group (Fig 1.06 Part A) forming a transient ferrous-dioxygen complex (Figure 1.06 Part B), which is further reduced to form a hydroxylating heme iron (IV)-oxo species which hydroxylates the

guanidine nitrogen of the second substrate, L-Arginine (Figure 1.06 Part C), forming N-hydroxy-L-arginine (NOHA) which in turn is oxidised to produce NO and L-citrulline (Figure 1.06 Part D) (Wei *et al.* 2002). The proposed mechanism via which O_2^- may be generated lies in the fact that the ferrous dioxygen complex may dissociate in the absence of BH_4 thereby forming O_2^- and regenerating heme iron (III) (Vasquez Vivar *et al.*, 1998) (Figure 1.06 Part E).

Thus, one of the main mechanisms by which BH_4 works is to aid electron transfer from the ferrous dioxygen complex to reduce it to the hydroxylating heme iron (IV)-oxo species, which subsequently reacts with L-Arginine. However if there is insufficient BH_4 available, this reaction may not be able to take place and hence the O_2^- group can dissociate from the ferrous dioxygen complex (Figure 1.06 Part E).

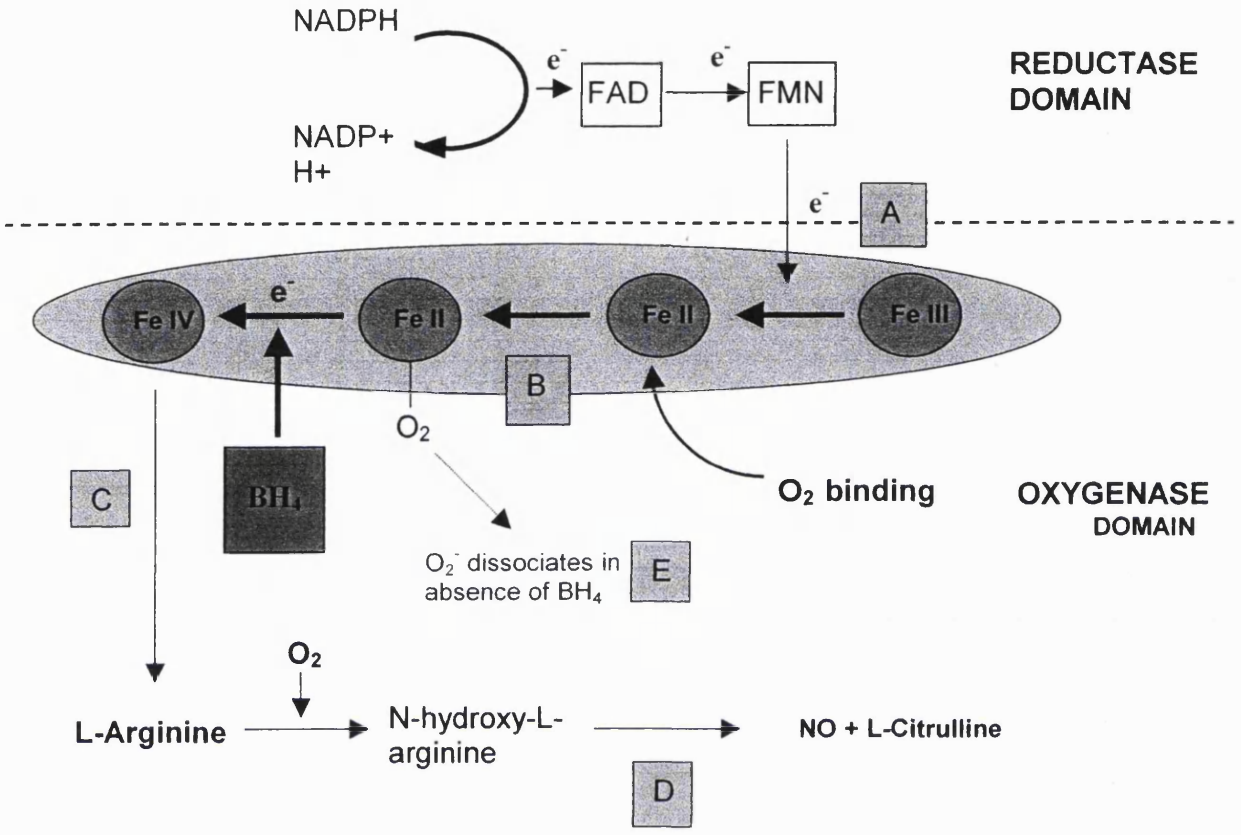

Figure 1.06 Schematic illustrating role of BH_4 in NOS activation.
A flow of electrons from the reductase domain enter the oxygenase domain (A) reducing Haem bound Fe (III) to (Fe II), oxygen binds to the Fe (II) complex forming a transient ferrous dioxygen complex (B). BH_4 is believed to aid electron transfer from this complex producing Fe (IV) which is essential for hydroxylation of the guanidine nitrogen of L-Arginine (C). This results in NO and L-citrulline generation (D). Lack of BH_4 may cause O2- to dissociate from the ferrous dioxygen complex (E).

1.17 Structure of GTP- cyclohydrolase 1

GTP-cyclohydrolase 1 (GTP-CH1) is the first and rate-limiting enzyme in the biosynthesis of BH_4 in vertebrates and insects (Nichol *et al.*, 1985) and BH_4 levels in mammalian cells are mainly determined by GTP-CH1 activity (Auerbach *et al.*, 2000). The crystal structure of GTP-CH1 from *Escherichia coli* was elucidated by Nar *et al.*, 1995. The enzyme exists as a decamer formed by face-to-face association of two pentamers, with the legs (formed by N-terminal pairs of monomers) of one pentamer clasping the 'body' of the other. The decamer is a toroid of subunits, with 10 equivalent active sites being located at the periphery of the toroid and each catalytic site being located at the interface of three adjacent subunits (see Figure 1.07).

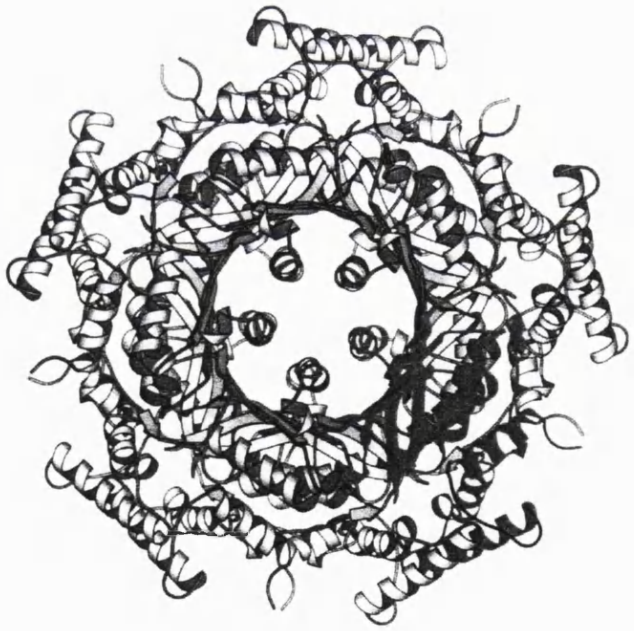

Figure 1.07 Crystal structure of GTP-CH1 elucidated by Nar *et al.*, 1995

1.18 Diseases arising from BH_4 deficiency and mutations in GTP-CH1

As mentioned earlier, BH_4 serves as an electron donating cofactor for the AAAH's, hence insufficiency of BH_4 can result in the inability of L-phenylalanine to be converted to L-tyrosine and L-tyrosine to L-Dopa. Homozygous mutations of the GTP-CH1 gene have been recognised as a rare cause of hyperphenylalanaemia and the resulting deficiency of BH_4 (and hence decreased activities of phenylalanine, tyrosine and tryptophan hydroxylase) gives rise to a progressively deteriorating neurological disorder including severe movement and muscle disorders, mental retardation, hypersalivation and hyperthermia (Thony, 2000; Muller *et al.*, 2002).

Heterozygous mutations in the GTP-CH1 gene have been shown to be closely associated with dopa responsive dystonia (DRD) and certain cases of mild hyperphenylalanemia or atypical phenylketonurea (PKU) (Muller *et al.*, 2002; Ozelius and Breakefield 1994 and Thony *et al.*, 2000). Mild forms of PKU (i.e. atypical PKU) have been shown to be responsive to phenylalanine-BH_4 loading, i.e. BH_4 lowered blood phenylalanine levels and significantly enhanced phenylalanine oxidation whereas in the same study patients with severe PKU (where there are mutations in the gene encoding phenyalanine hydroxylase (PAH)) remained unresponsive to BH_4 (Lindner *et al.*, 2001). However it has been suggested that BH_4 responsiveness is determined by the specific mutation in the PAH gene and that the effectiveness of BH_4 therapy is dependent upon the type of mutation (Lindner *et al.*, 2001; Muntau *et al.*, 2002).

In terms of the localisation of GTP-CH1, immunohistochemical staining performed on brain sections revealed that it is predominantly localised to tyrosine hydroxylase expressing cells within specific brain regions, consistent with it's role in BH_4 biosynthesis (Hwang *et al.*, 1998). GTP-CH1 mRNA and protein expression were not pronounced in neurons or endothelial cells that constitutively expressed NOS, but two possible explanations could account for this. Firstly there may be low levels of BH_4 utilised by NOS in these cells compared with the high levels required by AAAH's (and hence less detectable by immunohistochemistry) and secondly it may be possible that BH_4 is transported into NOS containing cells from AAAH cells (Hwang *et al.*, 1998).

The majority of the literature regarding GTP-CH1 has focused on its role in neurodegenerative disorders and in PKU and less has been documented upon the direct link between GTP-CH1 availability and BH_4 biosynthesis in terms of endothelial function, although the importance of BH_4 in terms of NOS activation and endothelial function is becoming increasingly more evident.

1.19 GTP-CH1 and endothelial dysfunction

Several studies have shown a correlation between GTP-CH1 levels and BH_4 availability in various models of endothelial dysfunction including the spontaneously diabetic BB rat (Meininger *et al.*, 2000) and in atherosclerosis, where it has been proposed that decreased expression of GTP-CH1 may be involved in the pathology of the reduced BH_4 generation seen in atherosclerosis, as sepiapterin (a generator of BH_4 independent of GTP-CH1) significantly improved endothelium dependent relaxations to different agonists in

atherosclerotic vessels of both human and porcine origin (Tiefenbacher *et al.*, 2000). A variety of investigations of GTP-CH1 in intact endothelial cells have also been conducted. Gene transfer of GTP-CH1 has been shown to augment intracellular BH_4 in human endothelial cells and furthermore enhanced NO generation in an eNOS-specific manner with the most salient finding being that GTP-CH1 gene transfer appeared to increase eNOS homodimerisation (Cai *et al.*, 2002). Other studies have shown that in human umbilical vein endothelial cells (HUVECs) cytokine stimulate the production of tetrahydrobiopterin with subsequent elevation of eNOS activity (Rosenkranz-Weiss *et al.*, 1994; Werner-Felmeyer *et al.*, 1993). A further study demonstrated that cytokines could induce functionally significant venous hyporesponsiveness to vasoconstrictors in humans via the release of NO generated by eNOS and not iNOS (Bhagat *et al.*, 1999a). These studies concluded that this stimulatory effect was mediated by increased enzymatic activity of GTP-CH1 (thereby increasing BH_4 availability for eNOS). This cytokine induced increase in GTP-CH1 in human umbilical vein endothelial cells (HUVECs) has been shown to result from increased levels of GTP-CH1 mRNA and it may be possible that cytokines also affect GTP-CH1 mRNA stability (Katusic *et al.*, 1998).

1.20 GTP-CH1 deficient mouse model

Knockout of the BH_4-dependent enzyme tyrosine hydroxylase is embryonically lethal in mice and hence it is likely that inactivation of all BH_4 dependent enzymes would be similarly lethal. However, a mouse model of GTP-CH1 and BH_4 deficiency has been created by chemical mutagenesis (induced by N-ethyl-N'-nitrosourea) of spermatological stem cells in a breeding scheme that selected for recessive mutations giving rise to hyperphenylalanemia

(McDonald and Bode 1988). This mutation does not alter the sequence within the reading frame of GTP-CH1 but appears to reduce steady state levels of GTP-CH1 mRNA and it is likely that the defect resides in the regulatory region of the GTP-CH1 gene (Gutlich *et al.*, 1994).

The hyperphenylalanaemic (*hph-1*) mouse shows a 90% reduction in enzymatic activity of GTP-CH1 and a 50% BH_4 deficiency in the brain (Hyland and Bola 1989 and Hyland *et al.*, 1996). Phenotypically these animals suffer from hyperphenylalanemia due to deceased activity of GTP-CH1, in the first few weeks of life and are unable to metabolise phenylalanine in response to a phenylalanine challenge in adult life (Maeda *et al.*, 2000). It is unusual that the *hph-1* mice do not experience the severe pathology usually associated with GTP-CH1 deficiency, although *hph-1* mice and patients with Dopa responsive dystonia (DRD) are very similar, neurochemically (Gross *et al.*, 2000). DRD is a rare autosomal dominant dystonia caused by mutations in the GTP-CH1 gene in about 50% of cases and clinically patients suffer from mild movement disorders (this may explain the slight movement disorders in the *hph-1* mice) and involuntary sustained muscle contractions or abnormal postures to much more serious movement disorders or rigor. In most cases however, there is a dramatic therapeutic response of symptoms to treatment with L-Dopa (Muller *et al.*, 2002). *Hph-1* mice additionally have an apparent impairment of brain NOS activity, which can be corrected by peripheral administration of BH_4 resulting in an increase in the activity of the cGMP/NO pathway (Canevari *et al.*, 1999). Work has been published on the neurological phenotype but relatively little is known about the consequences of this mutation on the cardiovascular system of *hph-1* mice, although a study performed by

Cosentino *et al.*, (2001) demonstrated significantly elevated systolic blood pressure and significantly lower intracellular levels of BH_4 in isolated aortas in the *hph-1* mice compared to the wild types.

1.21 GTP-CH1 Feedback Regulatory Protein

It has been known for a number of years that GTP-CH1 is inhibited by BH_4, but a study performed by Harada *et al.*, (1993) demonstrated that BH_4 was unable to inhibit the activity of pure recombinant GTP-CH1 *in vitro* and that another protein present in rat liver extracts, conferred BH_4 dependent inhibitory sensitivity to GTP-CH1. Following purification and cloning, this protein was found to consist of 9.5kDa subunits with the cDNA containing an open reading frame encoding 84 amino acids (Milstien *et al.*, 1996) and more recent purification and cloning studies revealed that the protein was made up of five identical subunits forming a pentamer of 52kDa (Yoneyama *et al.*, 1997). This protein was termed GTP-CH1 feedback regulatory protein (GFRP) and in the presence of bacterially expressed rat GFRP, BH_4 was found to elicit a concentration dependent and complete inhibition of recombinant GTP-CH1 (Milstien *et al.*, 1996). It is believed that 2 molecules of the pentamer GFRP bind to 1 molecule of the decamer GTP-CH1 to form a complex (Yoneyama and Hatakayama 1998).

GFRP functions as both a positive and negative regulator of GTP-CH1 and this tight regulation of GTP-CH1 ensures that intracellular BH_4 levels are maintained at and below those needed by BH_4 requiring enzymes (Harada *et al.*, 1993). BH_4 induces the formation of the inhibitory GTP-CH1/ GFRP complex and it is thought that GFRP and BH_4 inhibit the

enzyme activity of GTP-CH1 by decreasing its maximum velocity whilst having little effect on the affinity of GTP, indicating non-competitive inhibition (Yoneyama and Hatakayama 1998) (Figure 1.08).

BH_4 is the first enzyme for the biosynthesis of phenylalanine hydroxylase, the main enzyme of phenylalanine metabolism. To ensure efficient degradation of phenylalanine by phenylalanine hydroxylase, GTP-CH1 activity and hence BH_4 biosynthesis is stimulated by phenylalanine, but not by the other substrates of BH_4 dependent enzymes, and it is believed that the presence of phenylalanine is responsible for the formation of a stimulatory protein complex between GFRP and GTP-CH1, reversing the inhibitory effects of GFRP (Harada *et al.*, 1993) (Figure 1.08).

BH_4 binds to the GTP-CH1/GFRP complex with a K_d of 4 ± 0.8 μM and furthermore, binding is enhanced by dGTP, whereas phenylalanine binds with a K_d of 94 ±8μM and does not require any additional cofactor for binding (Yoneyama and Hatakeyama, 2001). In addition BH_4 binds weakly to GTP-CH1 but not to GFRP whilst phenylalanine binds weakly to GFRP and not GTP-CH1, indicating that the binding sites of BH_4 and phenylalanine may be composed of residues on GTP-CH1 and GFRP respectively (Yoneyama and Hatakeyama, 2001). Studies on the crystal structure of GTP-CH1 and GFRP have shown that the pentamer, GFRP, forms five phenylalanine-binding cavities to accommodate the phenyl group whereas GTP-CH1 has no such cavity for phenylalanine binding (Maita *et al.*, 2002). BH_4 on the other hand is able to bind to free GTP-cyclohydrolase 1 but not to free GFRP (Yoneyama and Hatakeyama, 2001).

Studies have consistently shown that under the influence of proinflammatory stimuli such as lipopolysaccharide or interferon gamma, GTP-CH1 mRNA expression is upregulated whilst GFRP mRNA expression is downregulated (the cytokine specific effect altering depending on cell type studied), thereby favouring BH_4 synthesis (Werner *et al.*, 2002 and Gesierich *et al.*, 2003).

Recombinant human GFRP stimulates recombinant human GTP-CH1 in the presence of phenylalanine and mediates feedback inhibition by BH_4 consistent with previous findings using rat enzymes (Werner *et al.*, 2002, Harada *et al.*, 1993). Cell studies have shown LPS down regulated GFRP expression whilst GTP-CH1 was upregulated, rendering the GTP-CH1 activity in the cells independent of metabolic control by phenylalanine, again consistent with the role of providing enough BH_4 for optimal iNOS activation following cytokine treatment (Werner *et al.*, 2002). In hepatocytes, pre-treatment of cells with the NO donor S-nitroso-*N*-acetyl-D-L-penicillamine (SNAP) resulted in increased NO production following cytokine treatment, without changing iNOS expression. This effect which was thought to occur as a result of suppressed GFRP and increased GTP-CH1 activity, resulting in an elevated cellular BH_4 leading to the promotion of iNOS activation (Park *et al.*, 2002). However, apart from these studies, relatively little has been published on the functional role of GFRP on NO production. It would therefore be interesting to investigate whether changes in the expression of GFRP can influence BH_4 production and hence NO production *in vitro* or *in vivo*.

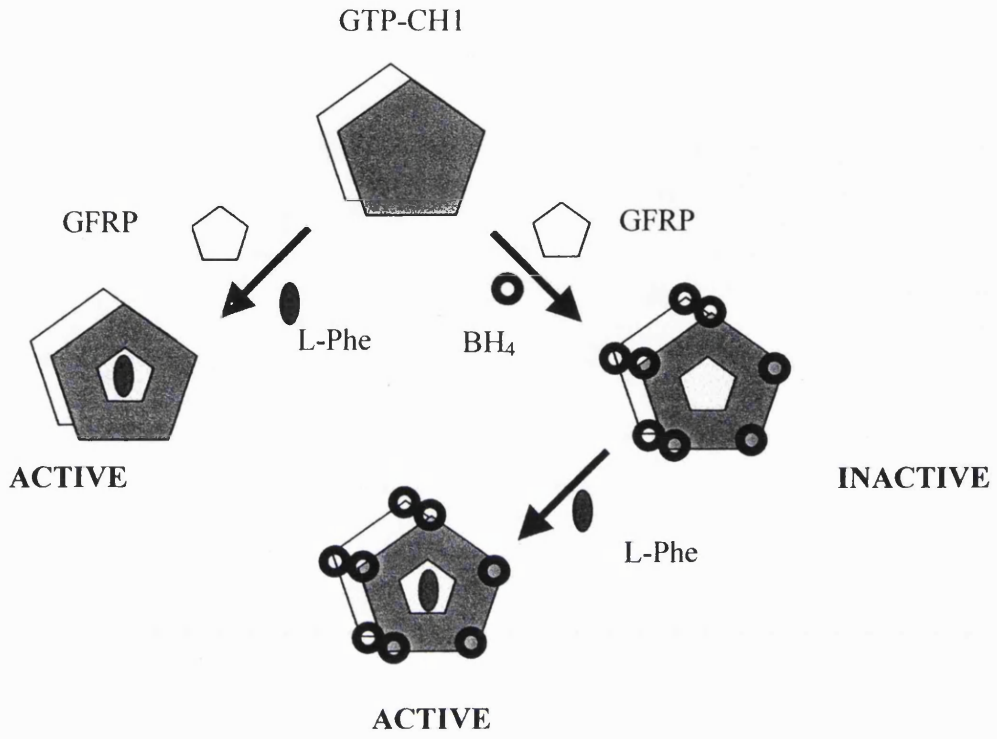

[4]**Figure 1.08** The GFRP/GTP-CH1 complex. BH_4 mediates feedback inhibition through the formation of an inhibitory complex of GFRP and GTP-CH1. L-Phenylalanine can form a stimulatory complex between GFRP and GTP-CH1 thereby promoting BH_4 synthesis. BH_4 is an essential cofactor for Phenylalanine hydroxylase, L-phenylalanine build up will thus require increased levels of BH_4 to promote conversion to L-tyrosine. The inactive complex inhibits formation of BH_4, active complex promotes formation of BH_4.

[4] Modified from Gross *et al.*, 2000. Tetrahydrobiopterin: An essential cofactor of Nitric oxide synthase with an elusive role. In: Nitric Oxide Biology and Pathobiology. San Diego, CA: Academic, 2000 p. 167-187

AIMS OF THESIS

It is becoming increasingly apparent that the NO pathway is a key component in normal endothelial function, and that a dysfunctional endothelium, as observed in a number of pathological conditions including hypertension, may be associated with a dysfunction in the activity of NOS and subsequent biosynthesis of NO. BH_4 levels and excess O_2^- may contribute towards this dysfunction. The overall objective of the studies within this thesis was to investigate how the regulation of the BH_4 pathway (Figure 1.09) affects NOS activity with particular reference to its role in the control of pulmonary vascular tone and PPHN. BH_4 concentration seems to be crucial in determining whether or not NOS generates O_2^- and hence the effects of SOD were also investigated.

- The first model to be investigated will be the developing porcine pulmonary vasculature over the neonatal period, and the null hypothesis of the study:

  Regulation of the GTP-CH1/BH_4 pathway and O_2^- generation affects pulmonary endothelial responses in the neonatal period.

- The second model is the porcine model of PPHN. This model has been well characterised and demonstrates markedly impaired endothelium dependent relaxations when compared to the age matched healthy control.

  Regulation of the GTP-CH1 BH_4 pathway and O_2^- generation affect endothelial responses in hypobaric induced pulmonary hypertension and

failure of the pterin pathway contributes towards the failed adaptation that characterises PPHN.

- The third study will utilise a mouse model of GTP-CH1 and BH_4 deficiency (*hph-1*) to determine whether an inborn deficiency of GTP-CH1 and BH_4 can contribute towards the progression of pulmonary hypertension in these mice.
- **Hph-1 mice display the structural characteristics of a pulmonary hypertensive phenotype.**
- Finally, the role of GFRP in determining BH_4 bioavailability for NOS function will be investigated using an endothelial cell line.
- **GFRP overexpression will reduce intracellular BH_4 and nitrite production from sEnd1 cells both pre and post cytokine+LPS treatment.**

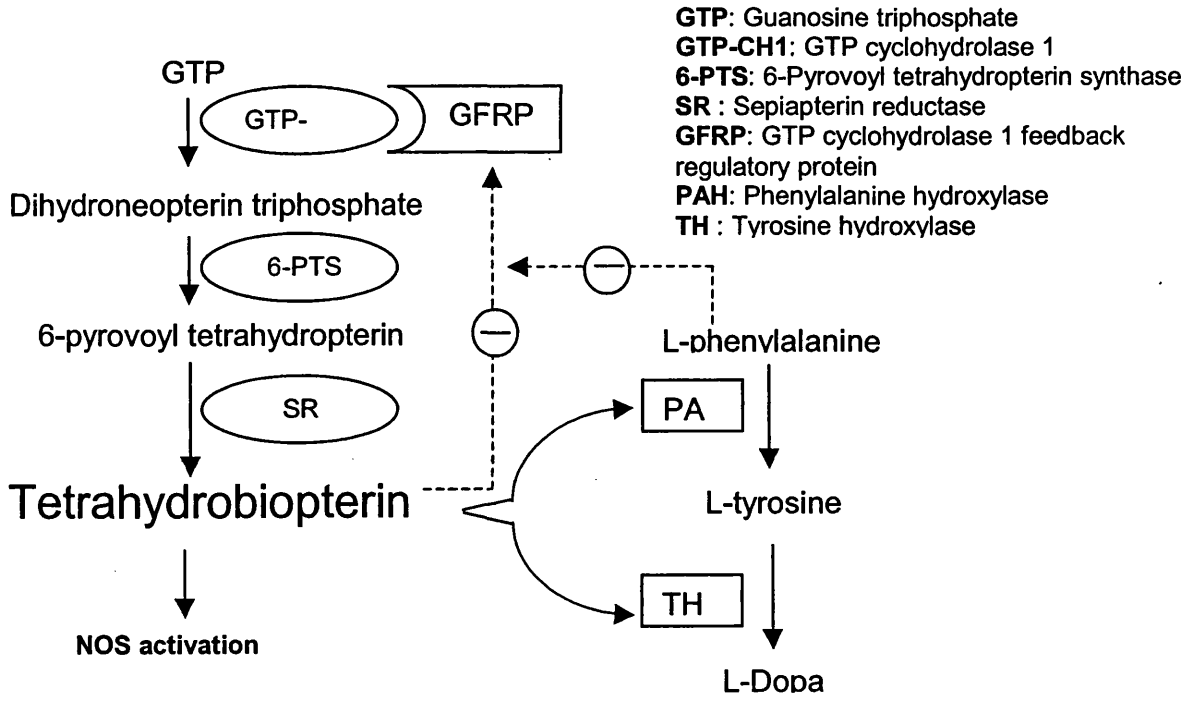

Figure 1.09 Components of the BH_4 pathway

CHAPTER 2

Materials and Methods

Section 2.1 Functional studies on porcine pulmonary arteries

2.1.01 Acquisition of porcine lung tissue

Lungs were obtained from Large White piglets and studied by age in the following groups: fetal (usually one week preterm), newborn 12-24 hour, 3 day old, 14 day old and adult. Pigs were killed with an overdose of pentobarbitone (100 mg/kg) with the exception of adult pigs, which were killed with captive bolt. Fetal piglets were delivered by Caesarian section one-week preterm and were prevented from air breathing by placing a rubber sheath over their snouts, and killed immediately. The fetal piglets along with the 12-24 hours, 3 day and 14 day old piglets were obtained from Boltons Park Farm, Potters Bar. Newborn animals were obtained from the Royal Veterinary College, Camden and adult tissue was obtained from Fresh Tissue Supplies, Surrey. All lung/heart blocks were removed as soon as possible after death and immersed in chilled Krebs-Henseleit solution (NaCl 119mM, KCl 4.7mM, $NaHCO_3$ 25mM, $MgSO_4$, KH_2PO_4 1.2mM and glucose 11mM plus $CaCl_2$ 2.5mM) until subsequent use.

All animals received humane care in compliance with the British Home Office Regulations and with the *Principles of Laboratory Animal Care* formulated by the National Society of Medical Research and the "Guide for the Care and Use of Laboratory animals" published by the National Institutes of Health [DHEW Publication No. (NIH) 80-23, Revised 1996, Office of Science and Health reports, DRR/NIH, Betheseda, MD 20892]. These studies were carried out under a Home Office License.

2.1.02 Organ chamber pharmacology

The axial intrapulmonary arteries were dissected under a microscope, from one upper lobe per animal. The adventitia was carefully removed ensuring that the endothelium was still intact. Arterial rings each of approximately 2-3mm in length were cut from the axial vessel distal to the first branch.

Each ring was suspended between 2 tungsten wire stirrups, and mounted in a 5ml organ chamber containing Krebs-Henseleit solution plus calcium, maintained at 37°C and gently gassed with 95% O_2, 5% CO_2. Recordings were made via an isometric force transducer linked to a PC data acquisition system (Figure 2.1.01). Once suspended in the organ chamber, arterial rings were taken up to 1 gram of tension (based on previous length tension study data) and allowed to equilibrate for 1 hour with approximately 3 washes of Krebs-Henseleit. Following the equilibration period, K125 (125mM potassium chloride in Krebs-Henseleit) was added to all vessels to test the viability of the arterial rings. If vessels did not contract to K125 or if their response was poor compared to the remaining vessels from the same animal, they were not used. The K125 was subsequently washed out and replaced with Krebs-Henseleit solution and the tissues allowed to return to their resting baseline tension.

Functional studies investigating the effect of sepiapterin (BH_4 precursor) and Mn(III) tetrakis (1-methyl-4-pyridyl)porphyrin pentachloride (MnTMPyP) (SOD mimetic) were subsequently performed as described in the protocol sections of Chapter 4.

2.1.03 Preparation of reagents

Although sepiapterin is a better means of supplementing BH_4 in experimental systems due to the unstable nature of BH_4, it is still relatively unstable, reacting rapidly with oxygen (especially in solution). Sepiapterin was therefore made up in the dark, in oxygen free water at room temperature (soluble at 0.17g per 100g water at 22°C) and stored at –20°C with fresh aliquots being used in each experiment. MnTMPyP was made up in water at a stock concentration of 10mM, aliquoted and stored at -20°C until use, with a fresh aliquot being used for each experiment. All other pharmacological reagents used in the functional studies were cumulatively diluted in fresh calcium free Krebs Henseleit on the day of experimentation from frozen stocks (10^{-1} M stock for ACh and SNP, 10^{-2} stock for U46619). Diluted reagents were kept on ice and in the dark throughout the experiment as, in general, coloured compounds such as sepiapterin, MnTMPyP and SNP tend to be light sensitive.

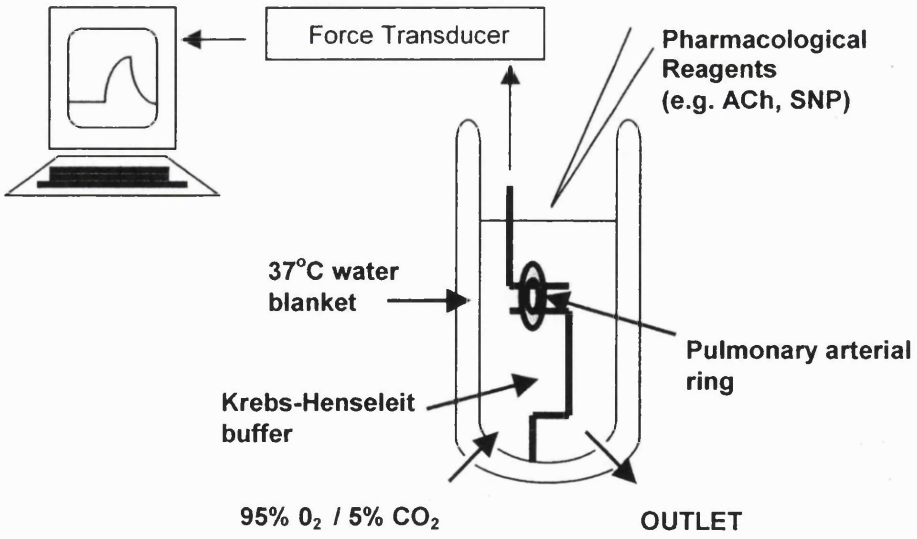

Figure 2.1.01 Standard organ chamber set up

2.1.04 Pharmacological reagents

Sepiapterin

A detailed account of the published effects of sepiapterin is given in Chapter 1. The main points of note are that a number of studies have been conducted using sepiapterin as a tool for upregulating BH_4 and increased BH_4 levels have been measured in isolated vessels treated with sepiapterin (Tsutsui *et al.*,1996). However, long term (~24 hours) exposure of isolated vessels to sepiapterin resulted in a deterioration of endothelium dependent relaxations (Tsutsui *et al.*, 1996; Vasquez Vivar *et al.*, 2002) whilst acute administration restored endothelial dysfunction seen in a number of disease states (Tiefenbacher *et al.*, 2000, Bagi and Koller 2003; Marinos *et al.*, 2001). It was postulated that the deleterious effects of sepiapterin were due to auto oxidation of BH_4 resulting in O_2^- generation.

MnTMPyP

Mn(III) tetrakis (1-methyl-4-pyridyl)porphyrin pentachloride or MnTMPyP is a SOD mimetic. Three isoforms of SOD have been identified in eukaryotic cells, intracellular Cu/Zn SOD, Mn SOD, bound to the mitochondrial matrix, and extracellular Cu/Zn SOD, localised on the cell surface. (Kira *et al.*, 2002, Fridovich, 1983). Endogenous levels of Cu/Zn SOD have been shown to be critically important in protecting NO from destruction by O_2^- anions in a variety of isolated blood vessels (MacKenzie and Martin 1998). The reason as to why a SOD mimetic rather than native SOD should be used in experimental studies is due to the shear size of SOD, rendering it too large to penetrate cellular membranes. A variety of low molecular weight, cell permeable SOD mimetics have

therefore been developed including a class of metal-based SOD mimetics such as the metalloporphyrins. MnTMPyP is one such metalloporphyrin and has been shown to be stable, active and non-toxic *in vivo* (Patel and Day 1999) and furthermore is cell permeable. The manganese moiety functions in the dismutation reaction by being reduced from Mn(III)TPy to Mn(II)TPy by cellular reductants with a subsequent reductive scavenging of O_2^- (Gardner *et al.*, 1996). In a thorough study performed by MacKenzie and Martin (1998) a variety of SOD mimetics were assessed to determine their effectiveness in restoring NO dependent vasodilator function in isolated rabbit aortic strips following exposure to oxidant stress. Of the seven compounds tested, MnTMPyP was the only SOD mimetic that restored the NO dependent relaxation in conditions of both intracellular and extracellular oxidant stress. However, a more recent study suggested that MnTMPyP might also produce superoxide anions that scavenge NO (MacKenzie *et al.*, 1999) and effect which may be dependent on the prevailing MnTMPyP oxidation-reduction pathways (Gardner *et al.*,1996). There is therefore compelling data both supporting and opposing the beneficial effects of sepiapterin and MnTMPyP on endothelial function. This study would allow us to determine the effects of acute administration of both sepiapterin and MnTMPyP on porcine pulmonary arteries over the age range fetal through to adult.

Section 2.2 Determination of protein expression and localisation using antibodies.

2.2.01 General principles of SDS-polyacrylamide gel electrophoresis

SDS-polyacrylamide gel electrophoresis (SDS-PAGE) is a standard technique for separating polypeptides by size to enable them to be probed with an antibody by Western blotting. It works on the principle that a protein sample heated to 100°C for 10 minutes in loading buffer (see appendix) containing sodium dodecyl sulphate (SDS) (strong anionic detergent) and β-mercaptoethanol (a strong reducing agent) results in dissociation of the protein into denatured polypeptides which bind to the SDS, forming SDS-polypeptide complexes. These complexes are loaded into a pre-cast gel, which consists of a stacking gel (pH 6.8) set over a resolving gel (pH 8.8). The gel, containing the SDS-polypeptide complexes is submerged into an electrophoresis tank (Biorad) containing an ionic running buffer (see appendix) and voltage passed through (200V), resulting in the size separation of the SDS-polypeptide complexes on the resolving gel.

2.2.02 General principles of Western blotting

Western blotting is the standard technique for establishing the expression of a protein within cell lysates or tissue. Once polypeptides have been separated using SDS-PAGE, the polypeptides are electrophoretically transferred onto a methanol presoaked nitrocellulose membrane (Hybond P, Amersham) using six sheets of Whatmann paper per gel, presoaked in blotting solution (see appendix) in a semi-dry blotter. Once transferred, the membrane is blocked in 5% non fat milk (w/v) made up in phosphate buffered saline solution containing 1% polyoxyethylene-sorbitan monolaurate (Tween 20, Sigma) (PBST) to minimise non-specific binding and subsequently exposed to a primary antibody specific for the protein of interest, diluted in PBST or PBST containing 5% milk powder (as specified) for either 1-2 hours at room temperature and pressure (RTP) or overnight at 4°C. Following this incubation period the membrane is thoroughly washed in 6 x 15 minute washes in PBST and incubated with a secondary antibody linked to horseradish peroxidase (HRP) diluted in PBST for 1-2 hours RTP, which binds to the primary antibody. Following incubation with the secondary antibody, the membrane is again thoroughly washed in 6 x 15 minute washes of PBST after which immunoreactivity is visualised using a chemiluminescent substrate that detects HRP (ECL Plus - Amersham) (Figure 2.2.01).

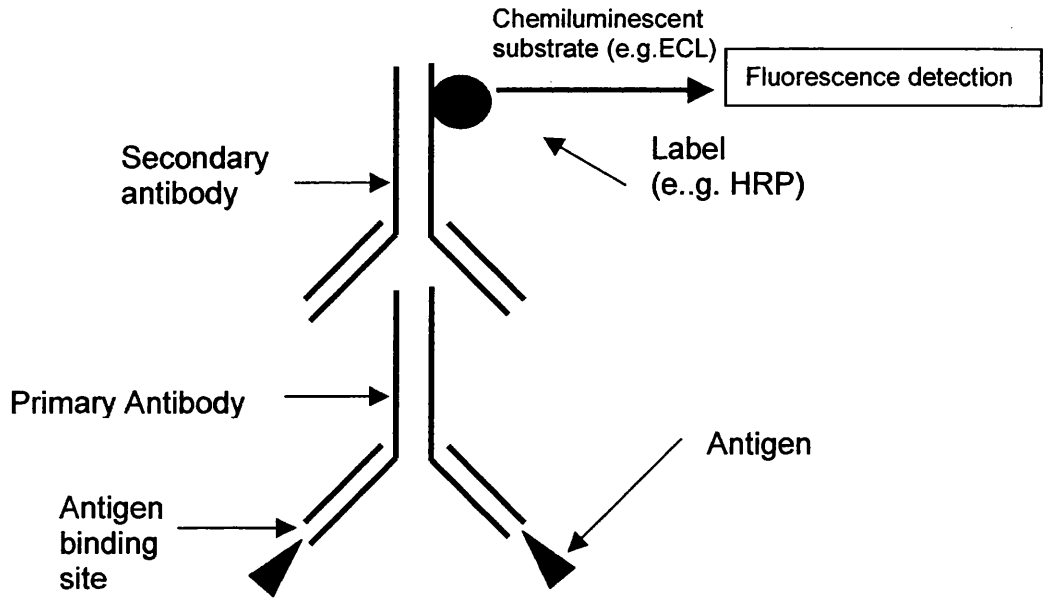

Figure 2.2.01 Schematic representation of antibody interactions in Western blotting leading to detectable fluorescence.

2.2.03 Protein assay

In order to correct for protein concentration in experiments, a standard colorimetric assay based on the Bradford assay (Bradford, 1976) was carried out on cell and tissue extracts. A standard curve of bovine serum albumin (BSA, Promega), made up by serial dilution in distilled water (or appropriate solution where specified) in the range 1μg/ml to 25μg/ml, was loaded with a blank, in duplicate on a clear 96 well plate. Protein samples (from cell or tissue samples) were diluted sufficiently to ensure they were in the range of the standard curve and loaded in quadruplicate into separate wells. Bradford reagent (Biorad) was added in a 1:5 dilution to each of the samples including the standard curve and pipetted up and down to ensure the two solutions were thoroughly mixed. Absorbance was measured at

OD_{595} on a SoftMax platereader and protein concentration of samples calculated against the standard curve, by firstly subtracting the blank, and finally multiplying by the dilution factor.

2.2.04 General principles of Immunohistochemistry

Immunohistochemistry is a well-established technique using antibodies specific for a protein of interest to detect antigens within tissues or cells thereby establishing the localisation of the protein of interest. Using a similar principle to Western blotting, a secondary antibody with a biotinylated tag binds to the primary antibody and a streptavidin-biotin-HRP complex binds to the tag on the secondary antibody. Immunoreactive staining is visualised using an agent that recognises the avidin-biotinyated HRP (Figure 2.2.02). There are however a number of constraints associated with this type of experiment. Firstly, cells or tissues must be fixed for this technique and fixation processes are often highly damaging to the antigenic structure. Ideally, perfect fixation would immobilize the antigens within the tissue whilst retaining the authentic cellular and subcellular architecture resulting in no change in epitope structure. However, no fixation methods are perfect and hence many epitopes are often masked or altered by certain fixatives. One example is the effects of formaldehyde or paraformaldehyde, which may block the ability of an antibody to bind to an antigen by modifying amino acid side chains. If these chains are part of an epitope, the antibodies will not be able to interact. Formaldehyde and paraformaldehyde react with the primary amines of lysine establishing a cross link that stabilizes the antigen display, however this fixation often denatures the antigen thereby causing the loss of denaturation sensitive epitopes.

Additionally, unlike Western blotting where the identity of an immunoreactive band can be confirmed by its size, immunohistochemistry tells you nothing about the identity of the protein, and hence it is vital that a well-characterised specific antibody is used. Other factors which influence the strength of the signal obtained include how the antigen is displayed in its local environment. In general antigens that are easy to detect present a large number of identical antibody binding sites in a small local environment, thereby allowing multiple antibody-antigen interactions to take place and hence making detection more simple. Furthermore, how easily an antibody can get to the antigen will determine the strength of the signal, thus it is vital that the tissue is treated in a suitable manner to optimise this. It is also essential that suitable negative controls be used to correct for background and non-specific staining.

The immunohistochemical techniques used in these studies have been optimised to ensure that many of these constraints can be overcome. Two different techniques have been used, immunohistochemistry of frozen and wax sections. The detailed protocols of these two methods will be described in more detail in Chapters 4 and 5.

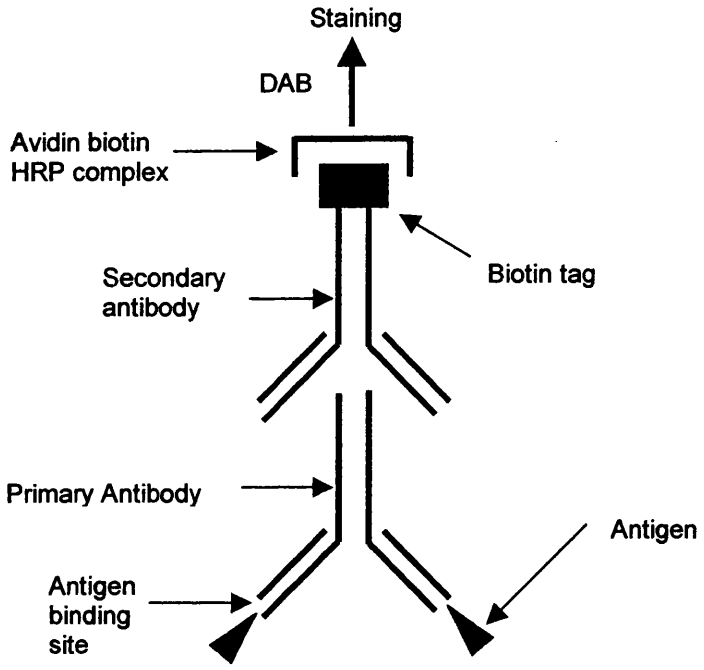

Figure 2.2.02 Schematic representation of interactions leading to detectable staining in immunohistochemistry.

2.2.05 Preparation of lung tissue fractions for SDS-PAGE and Western blotting.

The cardiac lobes from porcine lungs were snap frozen in liquid nitrogen as soon as possible after death. The lobes were then homogenised using a polytron grinder, in cold assay buffer 1 (50mM Tris HCl, pH 7.4 containing 0.1mM EDTA, 0.1 EGTA, 0.1% β-mercaptoethanol and the protease inhibitors 1μM Pepstatin A, 2μM Leupeptin and 1mM phenylmathanesulfonyl fluoride) in a ratio of 1 gram tissue: 5ml buffer. The homogenate was centrifuged at 150 x g at 4°C for 10 minutes to remove larger particles and then

ultracentrifuged at 100,000x g for 60 minutes at 4°C. The supernatant (soluble fraction) was then removed, the protein concentration determined using a standard protein assay, aliquoted and stored at -80°C until required.

In order to obtain the particulate (membrane bound) fraction, the pellet obtained following untracentrifugation was homogenised in buffer 1 containing 1M KCl, to remove associated cytosolic proteins from 'true' membrane bound proteins. The homogenate was ultracentrifuged at 100,000 x g for 30 minutes at 4°C, the supernatent discarded and the pellet rehomogenised in buffer 1 containing 10mM 3-3[(3-cholamidopropyl) dimethylammonio]-1-propanesulphonate (CHAPS). CHAPS buffer solubilises membrane bound proteins. The homogenate was mixed gently at 4°C for 30 minutes and centrifuged for a further 30 minutes at 100,000 x g. Samples were then centrifuged at 100,000 x g for 30 minutes and the supernatant removed, the protein concentration determined using a standard protein assay, aliquoted and stored at -80°C until required.

2.2.06 Tissue preparation of frozen sections for immunohistochemistry

Immunostaining studies on mammalian tissues are often carried out on frozen sections as this is the gentlest method of sample preparation and tends to preserve tissue structure and antigens. Blocks of lung tissue and extrapulmonary arteries, together with aorta, main bronchus and atrium were surrounded by embedding compound (OCT Brights, Cambridge, U.K.) on cork disks and snap frozen in isopentane cooled in liquid nitrogen. The blocks were then stored at -80°C. Subsequently, serial 10-μm cryostat sections were cut from each

block and thaw mounted on glass slides coated with Vectabond (Vector Laboratories, Peterborough, UK). Slides were kept frozen at -80°C until further use.

2.2.07 Immunohistochemical staining of porcine lung frozen sections

For immunohistochemical staining, slides were removed from -80°C storage and maintained at 20-25°C, for 2-3 minutes until no moisture droplets were visible. Slides were then immersed for 20 minutes in cooled acetone for fixing. Following the acetone incubation, slides were dried and then washed in PBS for 2 x 5 min washes on a rotating platform. After washing, slides were immersed in 0.3% H_2O_2 in 100% methanol for 30 minutes at room temperature and pressure (RTP) (this step blocks endogenous peroxide activity which is essential, as the final method of detection is peroxidase based). Slides were subsequently washed with PBS for 3 x 5min washes. Each section was outlined using a waterproof pen (PAP pen) and sections on each slide were then blocked for non specific binding using protein blocker (DAKO) for 30 minutes RTP. The DAKO blocker was washed off with 3x5min washes of PBS after which sections were incubated with the primary antibody diluted in PBS, overnight at 4 °C. After overnight incubation, the primary antibody was washed off in 3x5min washes of PBS and slides subsequently incubated for 30minutes at RTP with a biotinylated secondary antibody (DAKO) diluted in PBS. Excess secondary antibody was washed 3x5 min washes of PBS. Streptavidin biotinylated horseradish peroxidase complex (ABC - Amersham) was added to all sections in a 1:200 dilution. This was then followed by a stringent 3 x 10 min wash in PBS. Slides were then stained with Diaminodenzidine (DAB) tablets (Sigma) made up to manufacturers instruction, and brown staining observed under a light microscope. DAB is a reagent,

which, in the presence of horseradish peroxidase, yields an intense brown product that is insoluble in both water and alcohol. Once stained, slides were immersed in distilled water to stop the DAB reaction. Slides were not left for any longer than 1 minute with DAB. Negative controls were treated in the same way with the exception that the primary antibody was omitted.

2.2.08 Counterstaining

Counterstaining is performed on slides following immunostaining for the protein of interest to help differentiate the various cell types or subcellular structures seen following immunostaining. Slides were immersed in Ehrlich's hemotoxylin (BDH) for 1 minute after which they were quickly washed in water and then soaked briefly in acid alcohol. The slides were then washed continuously under running water for 10 minutes after which they were placed in 70% alcohol for 1 min x 2; absolute alcohol 3-5 minutes x 2; and 10 minutes histoclear x 2. Slides were finally dried and fixed in DPX for light microscopy.

Section 2.3 GTP-CH1 activity measurements

2.3.01 GTP-CH1 activity assay

The activity of GTP-CH1 can be assayed in a relatively straightforward manner and the principle of GTP-CH1 activity measurement is as follows. Formation of 7,8-dihydroneopterin triphosphate (7,8-NH2-TP), the product of GTP-CH1 is oxidised to neopterin triphosphate a fluorescent compound detectable on a 96 well plate reader (excitation 360nm, emission 465nm). The phosphate group of neopterin triphosphate is then cleaved by alkaline phosphatase resulting in the generation of neopterin, a second fluorescent compound that is readily detectable by HPLC. The levels of neopterin and neopterin triphosphate fluorescence directly correlate with GTP-CH1 activity (Figure 2.3.01). As the next enzyme down stream of GTP-CH1 requires Mg^{2+}, assays of GTP-CH1 activity are performed in the presence of EDTA and 7,8-dihydroneopterin triphosphate will accumulate even in the presence of high 6-pyrovoyl tetrahydropterin synthase activity. It is also essential that a highly purified alkaline phosphatase is used to cleave the neopterin triphosphate as crude phosphatase preparations sometimes containing substantial GTP-CH1 activity (Figure 2.3.01).

2.3.02 Preparation of lung homogenates for GTP-CH1 activity measurements

Porcine cardiac lobes from all age groups (F, NB, 12-24 hr, 3d, 14d, A and 3H) were snap frozen as soon as possible after death, crushed under liquid nitrogen and homogenised in 250µl Tris Buffer (50 mM, pH 8.0) containing 2.5mM EDTA by mechanical stirring (80g) in a tissue grinder (Braun, Melsungen, Germany) and centrifuged (13,000 rpm, 10 minutes). Protein concentrations were determined by Bradford assay (Bio-Rad Laboratories, Munich, Germany) according to manufacturer's instructions. The detailed protocol of the GTP-CH1 activity measurements in porcine lung homogenates are described in the following results chapters.

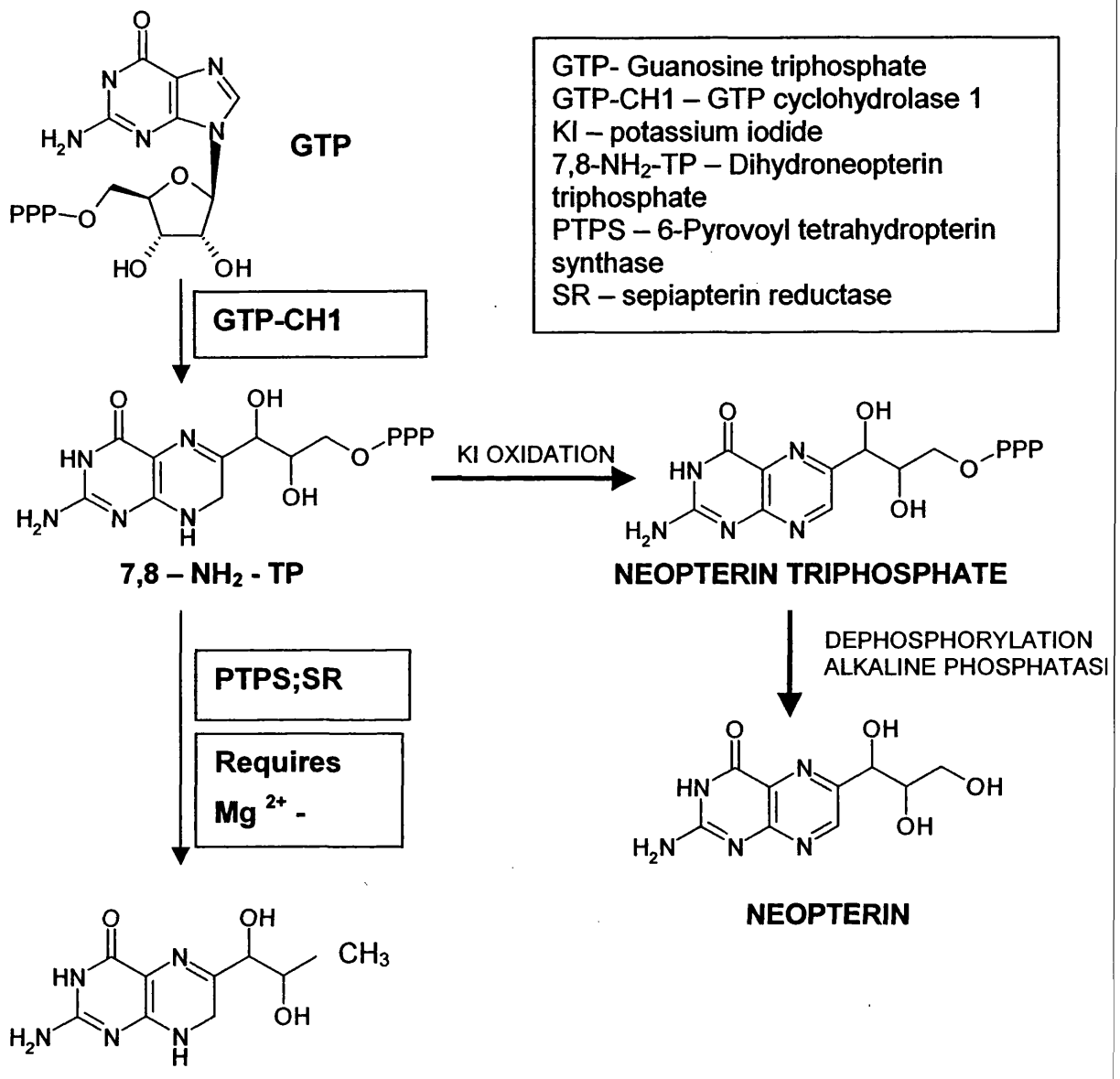

Figure 2.3.01 Reaction mechanism for GTP-CH1 activity assay

Section 2.4

Development of a GFRP over expressing cell line and standard molecular biological techniques

2.4.01 Reverse transcription

Reverse transcription (RT) was performed using Ready-To-Go™ You-Prime first-Strand Beads (Amersham) which utilize Moloney Murine Leukemia Virus (M-MuLV) reverse transcriptase to generate first strand cDNA. Typically, 1μl RNA was heated with 29μl of diethyl pyrocarbonate (DEPC, Sigma) treated water (RNAse free water), to 65°C for 10 minutes and chilled on ice for 2 minutes. The reaction mixture was transferred to a fresh RT-PCR tube containing the RT-beads and 0.2μl of reverse oligonucleotide primer added. After incubation at RTP for 1 minute, tubes were mixed by gentle vortex followed by centrifugation and incubated at 37°C for 1 hour.

2.4.02 Polymerase Chain Reactions

DNA sequences were amplified by Polymerase Chain Reaction (PCR). Typically, PCR reactions contained oligonucleotide primers at 1pmol/μL (Sigma-Genosys), 0.1mM dNTPs, 1.5mM $MgCl_2$, Taq DNA polymerase 0.025U/μL and 10 X PCR buffer (all from Invitrogen) in a final volume of 25μL. Amplification conditions were typically 94°C for 5 minutes; 30 cycles of 94°C (10s), *60°C (10s), 72°C (30s); and 72°C for 5 min, unless otherwise stated, and carried out in a Techne Genius automated thermocycler. In certain cases, PCR reactions were performed using Expand High Fidelity PCR system (Roche) according to manufacturer's instructions. This kit consists of an optimised PCR system,

which increases the overall efficiency and yield of the reaction whilst minimising the risk of introducing a sequence error.

* Annealing temperature chosen was typically 4°C lower than oligonucleotide primer melting temperature.

2.4.03 Agarose gel electrophoresis

Products of PCR or restriction digests were analysed by agarose gel electrophoresis. Agarose (0.6-2% w/v) (Invitrogen) was made up in 1X TBE (10X TBE stock diluted in distilled water - Invitrogen) and melted by heating to >60°C. Ethidium bromide (Sigma) was added to a final concentration of 0.2mg/mL. Gel loading solution (6X) (Sigma) was added to DNA samples and loaded onto a gel along with a 1kB plus DNA ladder (Invitrogen). Samples were electrophoresed in 1X TBE buffer at 100V for ~30 min or until bands were sufficiently separated to visualise fragment of interest. DNA fragments were visualised using a UV transilluminator.

2.4.04 Purification of DNA bands from agarose gels

PCR products or restriction enzyme digestion products were excised and purified from agarose gels using a Qiaquick gel extraction kit (Quiagen) according to manufacturer's instructions. DNA fragments were excised from gels with a scalpel and incubated for 10 min at 50°C in 300μL/100mg gel of buffer QG to solubilize the agarose. One volume of isopropanol was then added to the sample and mixed to increase the yield of DNA fragments <500bp and >4Kb. Samples were then applied to Qiaquick columns and

centrifuged for 1 min to bind DNA. Columns were then washed with 0.5mL buffer QG to remove traces of agarose and 0.75mL of ethanol-containing buffer PE to remove salt. DNA was eluted with 30μL of distilled water.

2.4.05 TOPO TA cloning

PCR products amplified by Taq DNA polymerase (and therefore containing A overhangs) were directly inserted into pCR2.1--TOPO using a TOPO TA Cloning kit (Invitrogen). The linearised vector has single overhanging T residues and ligation with Taq polymerase PCR products using topoisomerase occurs efficiently within 5 minutes at room temperature. 2μL of gel-extracted PCR product was added to 1μL vector and 2μL sterile water. The reaction was incubated for 5 minutes at room temperature before transformation into TOP10 One Shot competent cells (Invitrogen). 2μL of the TOPO-cloning reaction was transferred to a vial of One Shot cells and mixed gently. The cells were incubated on ice for 30 minutes prior to heat-shocking for 30s at 42°C. Tubes were then transferred immediately to ice for 2 minutes and shaken horizontally for 30 minutes at 37°C after addition of 250μL SOC medium. 150μL of each transformation was spread on LB plates (Miller's Luria Broth - Sigma) treated with 40μL 40mg/mL X-gal (5-Bromo-4-chloro-3-indolyl β-D-galactoside - Sigma) for blue/white screening. Plates were incubated overnight at 37°C.

2.4.06 Restriction enzyme digests

Restriction enzyme digests were incubated for 1-2h at 37°C in a 10μL reaction volume containing plasmid DNA, 10U of the restriction enzyme (Roche or Promega) and the corresponding enzyme reaction buffer.

2.4.07 Ligation reactions

Digested vector DNA was incubated with insert DNA in a 1:3 molar ratio. Reactions contained 1X ligase buffer (50mM Tris-HCl, 10mM $MgCl_2$, 1mM ATP, 1mM dithiothreitol (DTT), 5% (w/v) polyethylene glycol-8000) and 1U of T4 DNA ligase (Invitrogen) giving a final volume of 10μL. Reactions were incubated at 4°C overnight. 5μL or 10μL of the reaction was then used to transform 50μL or 100μL, respectively, of competent DH5α *E.coli* cells (Invitrogen).

2.4.08 Transformation of competent *E.coli* cells

DH5 α competent cells (Invitrogen) were transformed according to instructions. Cells were slowly thawed on ice and aliquoted into pre-chilled 1.5mL eppendorf tubes. Ligation reactions were then added to the cells and gently mixed before returning to ice for 30 min. Cells were then heat-shocked by incubation at 42°C for 1 min and immediately returned to ice for a further 2 min. 450μL or 900μL of LB medium was then added to 50μL or 100μL of cells, respectively. Cells were then shaken horizontally at 37°C for 30 min and then collected by centrifugation at 13,000 rpm for ~30s in a bench top microfuge. The cells were

then resuspended in 100μL and spread on LB agar plates containing 100μg/mL ampicillin and finally incubated overnight at 37°C.

2.4.09 Preparation of plasmid DNA – miniprep

Colonies of transformed DH5α cells were picked from agar plates and inoculated into 3mL of LB medium containing 100μg/mL ampicillin. Cultures were incubated at 37°C overnight, shaking. Plasmid DNA was then isolated from 2.5mL of overnight culture using a Qiaprep Spin Miniprep Kit (Qiagen). The remaining 0.5mL was mixed with 0.5mL of sterile 50% (v/v) glycerol and stored at –80°C. In brief, the protocol for plasmid purification was as follows. Bacterial cells were pelleted by centrifugation at 13,000 rpm for ~30s and resuspended in 250μL of resuspension buffer. The cells were then lysed under alkaline conditions by mixing with 250μL lysis buffer until the solution was slightly clear. Denatured proteins, chromosomal DNA and cell debris were precipitated by mixing the lysate with 350μL neutralisation buffer and removed by centrifugation at 13,000 rpm for 10 min. The supernatants were then applied to Qiaprep spin columns and centrifuged for 30-60s to allow binding of plasmid DNA to the silica-gel membrane of the column under the high-salt conditions of the neutralisation buffer. Columns were washed with buffer PB to remove trace endonucleases and buffer PE to remove salts. DNA was eluted in low salt conditions with 50μL of buffer EB (10mM Tris-CL, pH8.5).

2.4.10 Larger scale preparation of plasmid DNA – Midiprep

Larger preparations of ultrapure DNA (up to 100μg) were obtained from 50mL or 100mL cultures of transformed *E.coli* cells using a Qiafilter Plasmid Midi Kit (Quiagen) according to manufacturer's instructions. The principles of the purification procedure are essentially the same as those for the Qiaprep Spin Miniprep Kit but clearing of lysates was achieved by filtration through a Qiafilter cartridge instead of centrifugation. Plasmid DNA was purified using a Qiagen tip packed with Qiagen resin and precipitated with isopropanol to obtain an ultrapure preparation suitable for use in transfection and sequencing. DNA concentrations in midipreps were determined by measuring absorbance at 260nm in a CECIL 2020 UV spectrophotometer. One unit of absorbance at 260nm is equivalent to 50μg/mL of double-stranded DNA.

2.4.11 Ethanol precipitation

In order to prepare DNA samples for sequencing, ethanol precipitation was carried out as follows. To the total DNA extract, one tenth of the volume of 3M NaAcetate pH 5.2 and two and a half times the volume of 100% ethanol were added (i.e. for 20μl DNA sample, 2μl NaAcetate and 50 μl ethanol were used). Subsequently, incubation on dry ice for 10 minutes followed by centrifugation at 14,000rpm for 15 minutes at 4°C resulted in a pellet. The supernatent was discarded and the pellet washed with 70% ethanol followed by a second spin at 14,000rpm for 15 minutes. Finally the supernatent was removed and the pellet allowed to air dry before being sent off for sequencing.

2.4.12 Cloning and expression of human kidney GFRP cDNA

First strand cDNA synthesis of GFRP was performed using human kidney poly A^+ RNA as a template (Clontech) and was primed using an oligonucleotide complementary to the 3' UTR of human GFRP [GGT GCC CCG TCT GCA AATC] with reverse transcription beads (Amersham). Subsequently, PCR amplification of the cDNA was performed using oligonuceotide primers complementary to residues 3-17 downstream of an inserted ***EcoR1*** site [GATC ***GAA TTC*** CCC TAC CTG CTC ATC] and residues 255-236 downstream of an inserted ***Sal 1*** restriction site [CTGA ***GTC GAC*** TCA CTC CTT GTG CAG ACA CCAC] (94°C 10 secs; 55°C 10 secs and 72°C 30 secs 30x cycles) giving rise to a 0.25 kB product. The GFRP human sequence was analysed beforehand to confirm that Eco R1 and Sal 1 restriction sites did not exist in the coding region.

The 0.25kB product was gel purified (Quiagen) and Topo A cloned into pCR TOPO 2.1 (Invitrogen). Successfully cloned colonies were picked, cultured and the DNA extracted using a miniprep kit (Quiagen). The DNA samples were then restriction digested with Eco R1 and Sal 1 for 2 hours after which they were run out on a 1.5% agarose DNA gel. This gave rise to two bands (2.1kB and 0.25kB) corresponding to the TOPO vector and insert respectively (Figure 2.4.01). These DNA samples were ethanol precipitated and sequenced using the T7 forward primer (MWG Biotech) to confirm that no mutations had been introduced during amplification. Sequencing results showed a 99.6 % alignment with human GFRP.

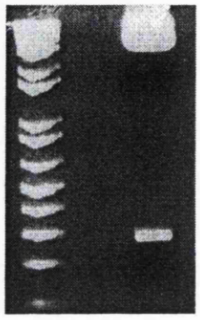

Figure 2.4.01 Gel image of GFRP/TOPO digested with Eco R1 and Sal 1

GFRP-pcDNA 3.1 Hygro construct development

Two oligonucletide primers (GFRP 4 and 5) complementary to residues 98-118 downstream of an inserted ***Hind III*** restriction site and N-Myc tag [***AAG CTT*** AAC ATG GCC GAA CAA AAA CTC ATC TCA GAA GAG GAT CTG GGC GGC CCC TAC CTG CTC ATC AGC ACC] and residues 349-328 downstream of an inserted ***Xho 1*** restriction site [CTGA ***CTC GAG*** TCA CTC CTT GTG CAG ACA CCA C] were produced. Using GFRP/TOPO as a template, and the primers GFRP 4 and GFRP 5, PCR amplification using Expand Taq (Boeringer) (94°C 10 secs; 40°C 10 secs; 72°C 30 secs x 20 cycles) gave rise to a band approximately 310kB in size. The 310kB band was subsequently gel purified, digested with Xho 1 and Hind III (Promega) and ligated with pcDNA 3.1 Hygro (pre cut with Xho1 and HindIII). The ligation was transformed into DH5α cells, colonies cultured in 3ml LB Amp and DNA extracted using the Quiagen miniprep kit. The products were later digested with Xho 1 and Hind III and run out on a 1.5% agarose gel with each giving rise to two bands one at 5.6kb and one at 310kb,

corresponding to the pcDNA 3.1Hygro vector band and Myc tagged GFRP insert respectively (Figure 2.4.02).

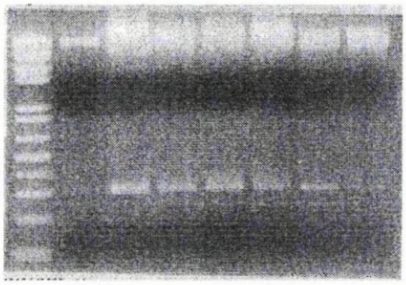

Figure 2.4.02 Gel image of GFRP/pcDNA 3.1 Hygro miniprep digests using Xho 1 and Hind III

The sample corresponding to the brightest band on the gel was then ethanol precipitated and sequenced (MWG Biotech) using the BGH reverse and T7 forward primers to confirm that no mutations had been introduced during amplification. Both sequencing results showed a 100% alignment with human GFRP (Figure 2.4.03a and b).

```
202 gagaagagccttgggaaacaacttttatgaatactacgtcgatgaccctc
    ||||||||||||||||||||||||||||||||||||||||||||||||||
101 GAGAAGAGCCTTGGGAAACAACTTTTATGAATACTACGTCGATGACCCTC

252 cccgcatagtcctggacaagctggaacgcaggggcttccgtgtgctgagc
    ||||||||||||||||||||||||||||||||||||||||||||||||||
 51 CCCGCATAGTCCTGGACAAGCTGGAACGCAGGGGCTTCCGTGTGCTGAGC
```

Figure 2.4.03a Alignment of sequenced GFRP Myc/pcDNA 3.1 Hygro, using the BGH reverse primer, versus derived human GFRP nucleotide sequence.

```
            .         .         .         .         .
98  ccctacctgctcatcagcacccagatccgcatggaggtgggccccactat 147
    ||||||||||||||||||||||||||||||||||||||||||||||||||||
61  CCCTACCTGCTCATCAGCACCCAGATCCGCATGGAGGTGGGCCCCACTAT 110
            .         .         .         .         .
148 ggtgggcgatgaacagtcggatccagagctgatgcagcatctgggggctt 197
    ||||||||||||||||||||||||||||||||||||||||||||||||||||
111 GGTGGGCGATGAACAGTCGGATCCAGAGCTGATGCAGCATCTGGGGGCTT 160
            .         .         .         .         .
198 caaagagaagagccttgggaaacaacttttatgaatactacgtcgatgac 247
    ||||||||||||||||||||||||||||||||||||||||||||||||||||
161 CAAAGAGAAGAGCCTTGGGAAACAACTTTTATGAATACTACGTCGATGAC 210
            .         .         .         .         .
248 cctccccgcatagtcctggacaagctggaacgcaggggcttccgtgtgct 297
    ||||||||||||||||||||||||||||||||||||||||||||||||||||
211 CCTCCCCGCATAGTCCTGGACAAGCTGGAACGCAGGGGCTTCCGTGTGCT 260
```

Figure 2.4.03b Alignment of sequenced GFRP Myc/pcDNA 3.1 Hygro, using the T7 forward primer, versus derived human GFRP nucleotide sequence.

2.4.13 sEnd1 cells

sEnd 1 cells (skin endothelioma cells) were originally isolated from murine hemangiomas (benign tumours) induced by developing tumour forming mice using a neomycin resistant retroviral vector expressing the middle T oncogene (Williams *et al.*, 1988). When a retrovirus infects a cell, it injects its RNA into the cytoplasm of that cell along with the reverse transcriptase enzyme. The cDNA produced from the RNA template contains the virally derived genetic instructions and allows infection of the host cell to proceed. Once isolated and cultured, these endothelioma cells have been shown to retain endothelial cell morphology and express specific endothelial cell markers (Williams *et al.*, 1988). Under normal conditions, in culture, sEnd 1 cells express eNOS and make low but detectable levels of NO (nitrite levels measured by Greiss assay), and following cytokine (interferon gamma - IFN γ, tumour necrosis factor alpha -TNF α) + lipopolysaccharide (LPS) treatment for 24 hours, express iNOS and produce higher levels of NO (Leiper *et al.*, 2002). Furthermore, stable cell lines overexpressing different proteins have been successfully created, using a similar methodology to that described for the generation of GFRP over expressing cells, in sEnd 1 cells (Leiper *et al.*,2002; Achan *et al.*, 2002).

2.4.14 Myc Tag

Epitope tags are useful for labelling proteins for detection using immunoblotting. The tags are usually small and tend not to affect the protein's biochemical properties. The Myc tag is perhaps the most widely used epitope tag system. The monoclonal antibody specific for the Myc tag is the 9E10 antibody, raised against a synthetic peptide derived from the carboxyl terminus of the human c-myc protein. Myc tagging is now widely used in vector/expression systems.

2.4.15 Cell culture

Standard cell culture techniques were used for maintenance of cell lines. In general, sEnd 1 cells were cultured grown in 75cm^2 flasks in Dulbecco's Modified Eagle Medium (DMEM, Invitrogen) supplemented with 10% (v/v) Heat inactivated Fetal Bovine serum (Invitrogen), 2mM L-glutamine (Invitrogen) and 100 units penicillin G sodium and 100g streptomycin sulphate (Invitrogen) in a humidified incubator maintained at 37°C, 5% CO_2 . Cells containing the pcDNA 3.1 Hygro plasmid were cultured in the same medium as above but with an additional 500μg/ml Hygromycin (Roche) to select for cells only containing the plasmid.

Cells were passaged by washing twice with PBS followed by incubation with 1.0mL of a solution of trypsin-EDTA (Invitrogen) for 5 min at 37°C. Trypsin was then inhibited by the addition of 9.5mL of complete DMEM (with pipetting to give an even cell suspension) and cells were split by adding 0.5ml of resuspended cells to 10mls of fresh medium, giving a 1:20 split.

2.4.16 RNA extraction

Total RNA was isolated from tissue culture cells using TRIZOL Reagent (Gibco BRL) according to manufacturers instructions. The reagent is a mono-phasic solution of phenol and guanidine isothiocyanate and maintains the integrity of RNA while disrupting cells and dissolving cell components. Cells were grown to confluence in 6 well plates (3.5cm^2 wells) and subsequently lysed and harvested using 1mL of TRIZOL reagent per well. 0.2mL of chloroform was then added and the tubes shaken vigorously for 15 seconds before centrifugation at 14,000 rpm for 15 min at 2-8°C to separate the organic and aqueous phases. This extraction method results in RNA remaining exclusively in the upper aqueous phase. The aqueous phase was carefully removed and transferred to fresh eppendorf tubes and precipitated by mixing with 0.5mL isopropanol followed by centrifugation at 14,000 rpm for 10 min at 2-8°C. After washing with 75% ethanol and a final centrifugation at 7500 rpm for 5 minutes at 2-8°C, RNA pellets were resuspended in 10μL DEPC (Sigma) -treated water and heated in a 55°C water bath for 10 minutes before being stored at -20°C until required.

2.4.17 Stable transfection of sEnd 1 cells

Approximately 5μg per well of DNA is needed for successful transfection of a 6 well plate. The concentrations of double-stranded DNA, for both the N-Myc-GFRP-pcDNA 3.1 Hygro construct and the empty vector (pcDNA 3.1 Hygro) were determined from Midiprepped cultures as described earlier.

sEnd 1 cells were grown to 60-80% confluence in 6 well plates and GFRP-pcDNA 3.1 or the pcDNA 3.1 Hygro construct was transfected into sEnd 1 cells using TFX 20 Transfast transfection reagent (Promega) according to manufacturers instructions.

Briefly, 5μg DNA (GFRP-pcDNA 3.1 or pcDNA 3.1 alone) was mixed by vortexing with 1ml of media after which 22.5μl Transfast was added and the reaction mixture vortexed and incubated at RTP for 15 minutes. Media was aspirated from each of the wells of the 6 well plate and replaced with 1ml of the transfection mixture for 1 hour at 37°C. After this incubation period, 5ml of media was added to each of the wells, giving a total volume of 6mls in each well. Plates were subsequently returned to the incubator. In total, 3 wells were transfected with N-Myc GFRP-pcDNA 3.1 construct, 2 with pcDNA 3.1 empty vector and the remaining well left untransfected.

48 hours post transfection, media was replaced with media containing 500mg/ml hygromycin (Roche) to select for transfected cells. Following five days of culture in the selective medium, individual hygromycin colonies were isolated and transferred to 96 wells plates for expansion to T75 flasks.

2.4.18 Preparation of cell extracts for SDS PAGE and Western blotting

Four GFRP overexpressing and two pcDNA 3.1 mock transfected cell lines were grown to confluence in 10cm^2 petri dishes. Cells were washed with PBS and subsequently harvested into 1ml of PBS using a rubber cell scraper. Cell suspensions were centrifuged on a benchtop centrifuge to pellet the cells at 14000rpm at 4°C. Cell pellets were resuspended in RIPA buffer (see appendix) and a standard protein assay carried out to correct for protein loading, (RIPA buffer was included in the blank and standard curve at the same concentration as in the cell samples).

2.4.19 Greiss Assay

Nitrite content (used as a correlate of NO) of cell media plus/minus cytokine + LPS treatment was measured colormetrically using the Greiss Assay. 50ul of Greiss reagent A (1% sulphanilamide (w/v), 5% phosphoric acid (v/v)) and 50ul of reagent B (0.1% N-(1-naphthyl)ethylenediamine (w/v)) all from Sigma-Aldrich, were added to 100ul of media. Samples were plated in quadruplicate on a 96 well plate format alongside a blank (media alone) and a standard nitrite curve (sodium nitrite serially diluted in media in the range 10-100μM). Absorbance was read at 565 nm. The concentration of nitrite in the samples was determined by extrapolating the absorbance values from the standard curve and values corrected for protein concentration for each well.

2.4.20 Electrochemical detection of tetrahydrobiopterin

Intracellular BH_4 was measured using HPLC and electrochemical detection (Heales and Hyland 1989 and Howells and Hyland, 1987). Electrochemistry involves the study of the effect of an electric potential on a chemical compound. At a specific potential a compound can be oxidised or reduced. In an electrochemical cell, a pair of inert electrodes are placed in a solution with an electrolyte containing an analyte. A potential is applied across the electrodes resulting in either oxidation or reduction of the analyte of interest. The magnitude of the current is then related to the concentration of the analyte as means of quantification. Briefly, samples were injected onto an isocratic HPLC system with multi-channel electrochemical CoulArray detection with a 100 mm C-18 column with a running mobile phase, (50 mM sodium acetate, 5 mM citric acid, 48 μM EDTA and 0.3 mM DTE, pH 5.2) at a flow of 0.75 ml/min. The optimum potential for detection of BH_4 is +125mV. Two other sequential electrodes were set at –350mV and +700mV to reduce the BH_4 and oxidize all of the pterin within the sample respectively, allowing further selectivity and conformation of BH_4 presence. Essentially, as the analyte passes through the first electrode, the entire sample is oxidised, the analyte then passes through electrode 2, where the redox active BH_4 is reduced. The reduction leads to a loss of electrons (which can be flipped by reverse polarity and hence measureable as a current). Furthermore tetrahydrobiopterin standards were run on the HPLC to allow quantification of the peaks.

Section 2.5

Structural characterisation of lungs from *hph-1* and wild type mice

2.5.01 Structural characterisation of pulmonary hypertension

Pulmonary hypertension is characterised by structural and morphological changes to the lung vasculature and right ventricle of the heart. Structural remodelling resulting from e.g. hypoxia induced pulmonary hypertension, has been investigated in a number of clinical cases and animal models, demonstrating structural alterations that extend to the periphery of the vascular tree. Such alterations include thickening of the smooth muscle layer down the precapillary resistance vessels, with both hypertrophy (increased cell size) and hyperplasia (increased cell number) of smooth muscle cells in the blood vessel wall; proliferation, differentiation and migration of smooth muscle precursor cells (e.g pericytes and fibroblasts) into normally non muscular vessels and deposition of extracellular matrix components such as collagen and elastin (Jones and Reid 1995, Jeffery and Wanstall 2001). Furthermore, this increased muscularisation of resistance arteries and decreased compliance of the vessels leads to the development of right ventricular hypertrophy as the right heart has to work against an increased pulmonary vascular resistance.

2.5.02 Perfusion and fixing of tissues for paraffin sectioning

In order to carry out structural analysis of the pulmonary vasculature of the *hph-1* and W/T mice, airway perfusion with 10% buffered formol saline (see appendix) was performed to fix and inflate the lungs thereby maintaining cell architecture and preserving the tissue. Lungs (still attached to the heart) were perfused with 10% buffered formol saline via a cannula, as follows. Formol saline was added to a 5ml syringe attached to a clamp stand at a height of 20cm (giving a perfusion pressure of 20cm H_2O) a tube was attached to the mouth of the syringe with a tap being attached to the top to control flow (Fig 2.5.01)

Each lung was individually kept moist in PBS in a dissecting dish and subsequently a piece of suture was tied in a loose knot around the trachea. The cannula was then carefully inserted into the trachea as far as it would go without causing damage to the tissue and the suture tightened around the tube and trachea, ensuring the knot did not block the cannula. The flow control tap was opened and formal saline allowed to enter the lungs at a pressure of 20cmH_2O for a period of 5 minutes. Expansion of the lungs was viewed under a dissecting microscope. Once inflated, the tube was removed and the suture tied into a secure knot to prevent any formal saline leakage from the lungs. Perfused lungs (plus hearts) were subsequently stored in formol saline overnight.

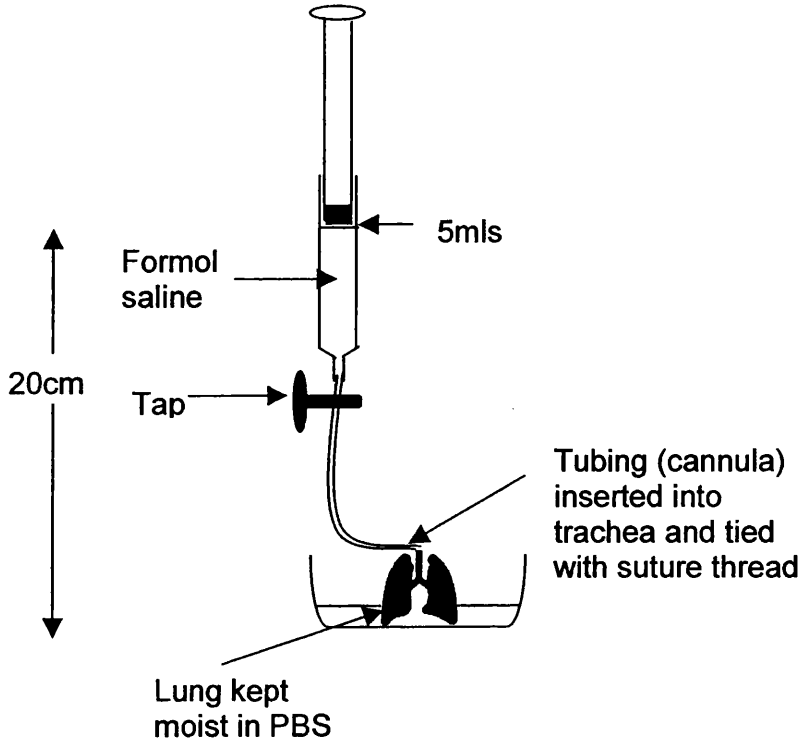

Figure 2.5.01 Set up for lung perfusion

2.5.03 Lung tissue processing

Heart lung blocs were removed from formol saline and adherent fat and excess tissue cut away. The hearts were detached from the lungs and each weighed separately. The heart was subsequently stored in 70% ethanol overnight. Lungs were dissected into the 5 constituent lobes and each lobe cut into 2-3 slices. Lung slices were stored in plastic cassettes and dehydrated in 70% ethanol for 2 hours before being processed in a Hypercentre XP enclosed tissue processor. The tissue processor gradually dehydrates the tissue by bathing it in increasing concentrations of ethanol and once dehydrated replaces the alcohol with wax via a histoclear step.

2.5.04 Embedding

Cassettes containing processed lung sections were placed alongside plastic trays of molten paraffin wax on a hot plate. Lung sections were carefully removed from the cassettes using heated forceps (to prevent wax setting) and immersed into the trays of molten wax with the cut surface facing downwards. The wax was allowed to set by placing the trays on ice blocks after which the solid paraffin wax, containing the tissue sections was removed from the plastic tray. Each wax block only contained lung sections from one animal.

2.5.05 Sectioning

Wax blocks were placed on wet ice for approximately 20 minutes before sectioning. Blocks were subsequently attached to a microtome stand and 4μm thick serial sections cut and floated on a water bath (37°C) to remove folds and finally mounted on silane coated glass slides and left to dry for at least 24 hours before immunohistochemical staining.

2.5.06 Immunohistochemistry for wax sections

Slides were placed on a hotplate at 56°C for 20-30 minutes to ensure complete adherance of tissues and subsequently dewaxed in histoclear for 5 minutes and 1 minute followed by rehydration through a descending alcohol series (100% and 70% ethanol for 2 x 30 seconds each) tap water and finally 5 minutes in 3% hydrogen peroxide solution (made up in distilled water). Slides were then autoclaved in citrate buffer (10mM citric acid (BDH) pH 6) to expose antigenic sites, cooled and washed in distilled water followed by PBS and circles drawn round the sections with a PAP waterproof pen and blocked in serum free protein blocker (DAKO) for 30 minutes. Sections were then incubated with mouse alpha smooth muscle actin monoclonal antibody (DAKO, UK) for 1 hour at RTP, washed in PBS and then treated with biotinylated goat anti mouse/rabbit antibody (DAKO Ltd.) for 30 minutes at RTP. After further washing in PBS, sections were treated with streptavidin-biotinylated horseradish peroxidase complex (Amersham, U.K.) for 30 minutes at RTP. To visualise alpha smooth muscle actin, sections were treated with 3,3'-diaminobenzinine (DAB, Sigma, U.K.) and viewed under a light microscope. The DAB reaction was stopped by immersing the slides in distilled water. Negative controls were treated in the same way with the exception that the primary antibody was omitted. Sections were counterstained with Ehrlich's haematoxylin, as described earlier.

CHAPTER 3

Design and Development of a GTP-CH1 antibody

3.01 Introduction

GTP-cyclohydrolase 1 is the first and rate-limiting enzyme in the biosynthesis of BH_4 in vertebrates and insects (Nichol *et al.*, 1985) and BH_4 levels in mammalian cells are mainly determined by GTP-CH1 activity (Auerbach *et al.* 2000). The crystal structure of GTP-CH1 from *Esherichia coli* was elucidated by Nar *et al.*, 1995, demonstrating that the enzyme exists as a decamer formed by face-to-face association of two pentamers, with the legs (formed by N-terminal pairs of monomers) of one pentamer clasping the 'body' of the other. The decamer is a toroid of subunits, with 10 equivalent active sites being located at the periphery of the toroid and each catalytic site being located at the interface of three adjacent subunits (see Figure 3.01).

There was no good specific GTP-CH1 antibody commercially available and as a result a GTP-CH1 antipeptide antibody was developed in order to provide us with tool for investigating GTP-CH1 protein expression and localisation in the porcine models described in Chapter 2.

3.02 Methods and Protocols

A new GTP-CH1 anti peptide antibody was designed by studying the crystal structure of GTP-CH1 in E.Coli elucidated by Nar *et al.*1995 (Fig 3.01) using RasMol 3.1, a package that enables the study of the macromolecular structure of proteins from a wide database. By orientating the structure, various surface exposed polypeptide chains were identified and of these, those that had a greater proportion of hydrophilic residues were selected and checked to ensure they had good cross species homology. Of all possible sequences short-listed, the

most suitable polypeptide sequence was selected and the corresponding human peptide sequence was determined on the HGMP database.

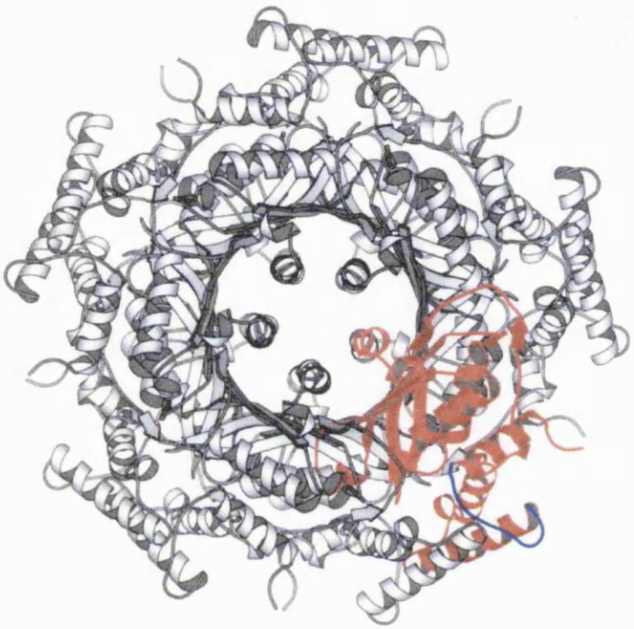

Figure 3.01 Crystal structure of GTP-CH1 with 1 monomer highlighted in red and the peptide sequence against which antibody was raised, highlighted in blue.

An N-terminal sequence CSNGFPERDPPRPGPSRPAEKPPRPEAK (amino acids 18-45) was selected, and the antigenicity of this polypeptide chain predicted by the algorithm of Hopp and Woods (1981) (Figure 3.02). The peptide was developed by Sigma Aldrich and conjugated with keyhole limpet hemocyanin (KLH), via the terminal cysteine residue. Cysteine groups on the end of the peptide form covalent bonds with the large number of cysteine residue on KLH. Pre-immune serum from 2 rabbits was collected, after which both rabbits were immunised with the conjugated peptide. Four immunisations and four bleeds

were carried out in total over a period of approximately two and a half months. During this time, the rabbit would be expected to generate specific antibodies against the GTP-CH1 peptide+KLH. The specificity of the antipeptide antibody for GTP-CH1 was tested (western blotting) after each bleed, on recombinantely expressed positive controls (kindly donated by Dr Christian Hesslinger) Two sets of serum from the two animals were obtained, 9597 and 9598 of which 9598 appeared to give rise to the lowest number of non-specific bands.

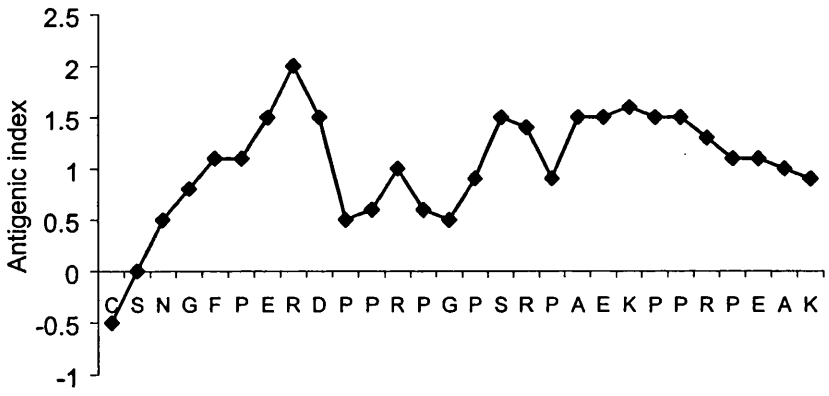

Figure 3.02 Antigenicity plot for selected amino acid sequence for GTP-CH1 antibody development. The chart displays the variation of the antigenic index as function of amino acid position. The higher the antigenic index, the more likely that the antibodies will 'see' those groups of residues

3.03 Anti peptide antibody purification

In order to improve the specificity for the GTP-CH1 antipeptide antibody 9598, 5mgs of Sigma-Aldrich produced peptide corresponding to the GTP-CH1 peptide sequence (18-45 on human sequence) was bound to 0.35g of activated thiol sepharose. Dry resin was swelled in water and washed 3 times with 100mM Tris pH 8.0, 1mM EDTA, 0.3mM NaCl. 1ml of the 5mg peptide in the same buffer was added to the resin and incubated at 4°C overnight with shaking. This process allowed the cysteine group on the peptide to disulphide bond to the thiol group on the beads. Unbound peptide solution was then removed and the resin washed once in Tris 10mM buffer and once in 100mM citric acid pH 4.5. The wash solutions were then removed and any free thiol groups remaining on the beads were blocked using 10mls 100mM citric acid pH 4.5 containing 1mM mercaptomethanol at room temperature for 2 hours.

Finally the resin was washed 3 times with phosphate buffered saline buffer pH 7.0. The resin was poured into an affinity column and 6mls of sera (9598) against the GTP-CH1 peptide was added to the affinity column and incubated at 4°C overnight with mixing. The resin was subsequently spun down and the supernatant removed. Resin was washed extensively in 6 changes of PBS buffer after which 20ul of resin (50% slurry) was removed for analysis by SDS page for the presence of bound antibody.

The mercaptoethanol in the protein-loading buffer reduces the disulphide bond between the peptide and the sepharose bead. The SDS page should separate the 2 heavy chains (50kDa each) and the 2 light chains (25kDa) of the antibody complex giving one band at

100kDa and one at 50kDa. Resin was poured into a column and the bound antibody eluted with 10 ml of glycine pH 2.0. 1ml fractions were collected into tubes containing 20ul of 1M Tris HCl pH 8.0 to neutralise it immediately. Neutral pH was confirmed by spotting onto universal indicator paper. The column was washed extensively with PBS to bring the pH back to neutral and stored in PBS containing 0.02% sodium azide at 4°C until further use. The OD_{280} of the fractions was read on a UV spectophotometer and fractions containing protein were pooled, concentrated and washed into PBS using Centricon-30 concentrators (Millipore).

3.04 Determination of the immunoreactivity of the purified antibody

The specificity of the purified antipeptide antibody for GTP-CH1 was tested on the recombinantely expressed positive controls and on particulate and soluble porcine lung homogenates from fetal, 3 day, 3H hypoxic and 14 day old animals. Briefly, 80μg of both the particulate and the soluble lung fractions were loaded along side a marker (Benchmark™ – Invitrogen) and separated by SDS-PAGE using a 12% gel. Subsequently, standard Western blotting was performed on the blot using a 1:1000 dilution of the purified antibody 9598, made up in PBST containing 5% milk (w/v) incubated overnight at 4°C and a 2 hour incubation, at RTP, of a 1:3000 dilution in PBST of HRP linked donkey-anti rabbit secondary antibody (Amersham). Immunoreactive bands were visualised using the ECL-Plus detection system (Amersham) following manufacturers instructions.

3.05 Results

Figure 3.03 shows an immunoblot showing an immunoreactive band for GTP-CH1 in all 4 recombinantely espressed positive controls using the purified antipeptide antibody 9598. Non specific bands were not present on the blot, demonstrating the specificity for the newly developed and purified antibody. Furthermore, immunoreactive bands were detectable in soluble porcine lung homogenates but not in the particulate fraction (Figure 3.04).

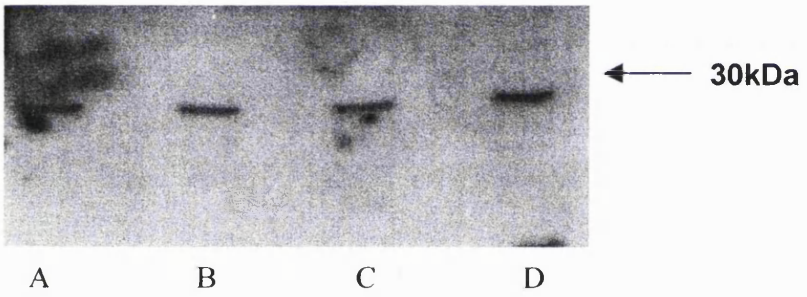

Figure 3.03 Immunoblot showing immunoreactive bands just below the 30kDa marker on 4 recombinantly expressed positive controls.

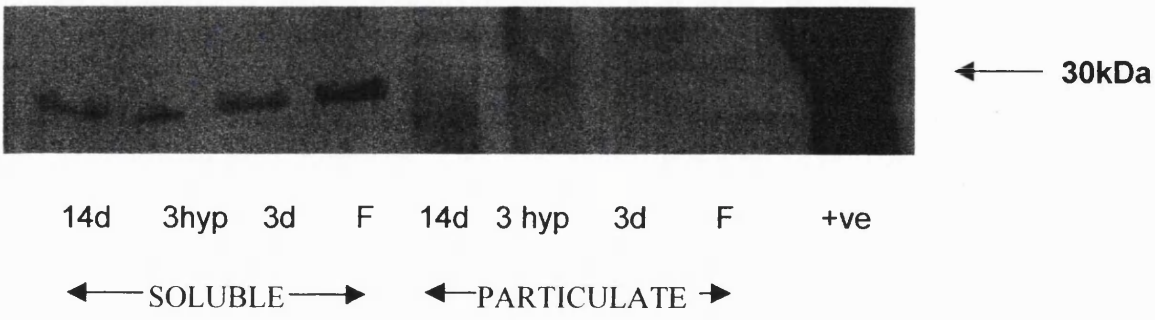

Figure 3.04 Immunoblot showing immunoreactive bands just below 30kDa in soluble fraction and but not in the particulate fraction of lung homogenates obtained from fetal (F), 3 day (3d), 3 day hypoxic (3 hyp) and 14 day old (14d) piglets.

3.06 Summary

The newly developed anti-peptide antibody for GTP-CH1, once purified, detects an immunoreactive band at the expected size of approximately 28-30kDa in both recombinantly expressed rat positive control and in soluble porcine lung homogenates. Unpurified GTP-CH1 antibody often gave rise to an extra ~60-70kDa band, is likely to correspond to the GTP-CH1 dimer. In order to minimise this dimerisation, samples should be placed on ice immediately after boiling in loading buffer. No immunoreactive bands are detectable in the particulate lung fractions, suggesting that GTP-CH1 is not membrane bound. This antibody is therefore suitable for probing for GTP-CH1 protein expression and localisation.

CHAPTER 4

Developmental regulation of tetrahydrobiopterin biosynthesis by GTP-cyclohydrolase 1 in the porcine lung

4.01 Introduction

Pulmonary vascular resistance falls rapidly after birth as the pulmonary vasculature adapts to extra-uterine life. Structural remodelling and the maturation of relaxant mechanisms are triggered by factors related to parturition and inhalation of oxygen (Haworth and Hislop 1981, Heymann 1999). Failure to adapt leads to persistent pulmonary hypertension of the newborn (PPHN) (Haworth and Hislop 1982, Gersony, 1984).

The vascular endothelium plays an important role in regulating vascular smooth muscle tone via the release of several vasoactive products, one of which is nitric oxide (NO) (Palmer *et al.*, 1987). Endothelial NO is produced from L-arginine and molecular oxygen by the catalytic activity of endothelial nitric oxide synthase (eNOS). There is increasing evidence that the NO pathway is dysfunctional in cases of PPHN, and neonates suffering from PPHN can be treated successfully with NO inhalation therapy (Kinsella *et al.*, 1992). However, the regulation of NO generation during normal adaptation and the mechanisms underlying maladaptation are unclear, particularly as eNOS itself seems to be present but its activity and functional effects are reduced. NO generation can be limited by a deficiency of an essential cofactor for NOS, tetrahydrobiopterin (BH_4), and sub optimal levels of BH_4 are likely to make NOS generate harmful superoxide radicals (O_2^{-}) (Cosentino *et al.*, 1998). The expression and activity of the enzyme GTP-cyclohydrolase 1 (GTP-CH1) is rate limiting for the generation of BH_4 (Nichol *et al.*, 1985) and the aim of the current study was to test the hypothesis that developmental regulation of GTP-CH1 and generation of BH_4 affect endothelial responses during development and that failure of the pterin pathway contributes to the failed adaptation that characterises PPHN.

Hypothesis 1:

Regulation of the GTP-CH1/BH_4 pathway and O_2^- generation affects endothelial responses in the neonatal period.

Hypothesis 2

Regulation of the GTP-CH1/BH_4 pathway and O_2^- generation affects endothelial responses in hypobaric induced pulmonary hypertension and failure of the pterin pathway contributes to the failed adaptation that characterises PPHN.

The primary aim of both studies was to try to improve the endothelium dependent relaxations in porcine pulmonary arteries (normal development and in PPHN) by supplementing isolated pulmonary arteries with BH_4 and quenching O_2^- using a SOD mimetic. Firstly, the effects of supplementation of BH_4 and SOD on the porcine pulmonary vasculature needed to be determined to elucidate whether or not these factors played a role in the vascular reactivity of the pulmonary arteries and also to determine whether there were any developmental variations or changes in the PPHN model, in response to these factors (Figure 4.01).

The second study investigated whether there was a direct correlation between any functional effects observed with BH_4 supplementation and GTP-CH1 protein levels, activity and localisation. In order to determine temporal protein expression and localisation of GTP-

CH1 in porcine lung samples, a polyclonal antibody raised against a peptide sequence of human GTP-CH1 was developed as described in chapter 3.

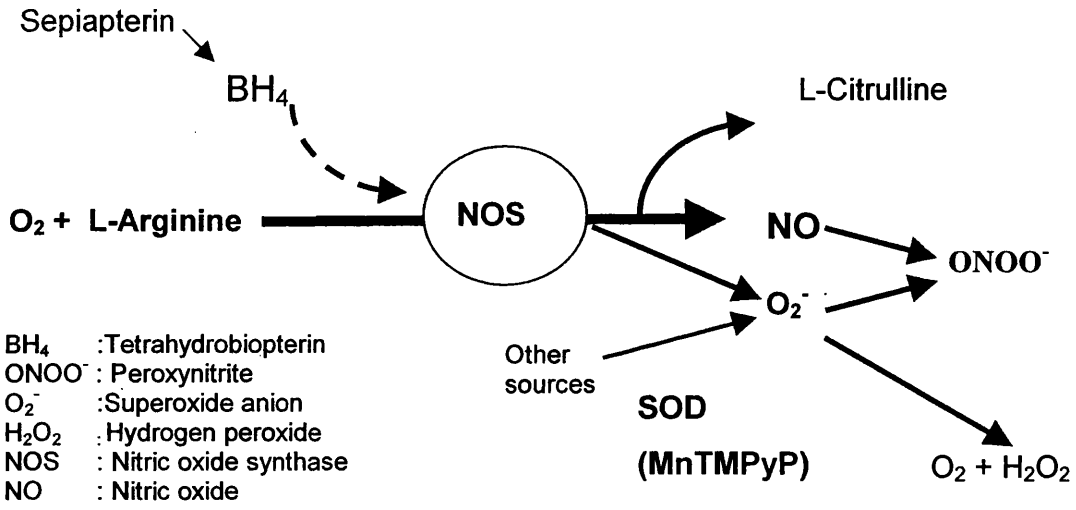

Figure 4.01 Schematic representation of study.

If GTP-CH1 expression and activity are reduced, there may be insufficient BH_4 available for efficient conversion of L-Arginine to NO and L-Citrulline, and may cause NOS to the generate O_2^-. Furthermore, hypobaric hypoxic exposure may lead to an increase in the generation of O_2^- from other sources as well as NOS. Supplementation of BH_4 (sepiapterin) and quenching of O_2^- (MnTMPyP) may reverse this effect and improve vascular reactivity.

4.02 Protocols

The functional effects of the BH_4 precursor, sepiapterin and/or the SOD mimetic, Mn(III) tetrakis (1-methyl-4-pyridyl)porphyrin pentachloride (MnTMPyP) in isolated porcine pulmonary arteries and GTP-CH1 protein expression, activity and immunolocalisation in porcine lung samples were investigated in both normal development and in a 3 day old model of PPHN. Functional studies were performed on isolated intrapulmonary arteries using standard organ chamber pharmacology. Extracted protein samples were analysed for GTP-CH1 protein expression by western blotting and activity (as described in Chapter 2). GTP-CH1 localisation was determined by immunohistochemistry using frozen sections.

Model of persistent pulmonary hypertension of the newborn

In order to mimic PPHN, newborn piglets were placed in a hypobaric chamber maintained at 50.8kPa for 3 days. The newborn piglets were delivered naturally at Camden Royal veterinary college and placed in the chamber within 20 minutes of birth. The chamber contained a heating lamp and straw bedding. The internal temperature of the chamber was 29°C. The chamber was cleaned daily for a maximum of twenty minutes. The piglets were gavage fed on modified cows milk. These piglets develop hypobaric hypoxia induced pulmonary hypertension, with right ventricular hypertrophy. Persistent right to left shunting across the foramen ovale and ductus arteriosus leads to a systemic arterial oxygen saturation of 71± 5% (Tulloh *et al.,* 1997). In the present study, right ventricular hypertrophy was confirmed by determining the ratio of left ventricle plus septum (LV + S) weight to the weight of the right ventricle (RV). In healthy 3 day old animals the ratio of LV+S/RV

approximates to 1.81 ± 0.09 whereas in the 0-3 day pulmonary hypertensive animals this is reduced to 1.37 ± 0.08. (Tulloh *et al.*, 1997). After 3 days in the chamber, piglets were killed with an overdose of pentobarbitone 100mgs/kg and the lungs removed and immersed in cold Krebs-Henseleit solution until use.

Functional studies

A minimum of five animals per age group, were studied. One or two animals of the same age were studied on each experimental day. Pulmonary arteries were carefully dissected from lung blocs and suspended in organ chambers as described in Chapter 2. The animals used were fetal (F), newborn (NB), 12-24 hours (12-24h), 3 day old (3d), 14 days old (14d), adult (approximately 3 months old) (A) and 3 day pulmonary hypertensive (3H).

Following the equilibration period and K125 challenge, a cumulative concentration response curve to 9,11-dideoxy–11α,9α epoxymethanoprostaglandin $F_{2\alpha}$ (U46619, Sigma), a thromboxane analogue, was constructed at the beginning of each experiment on one arterial ring, to determine the EC80 for U46619 for that particular animal's artery. Once determined, the EC80 of U46619 was administered to the remaining vessels and the tissues allowed to contract until a plateau had been reached. The remaining 4 vessels were then incubated for 30 minutes with the following reagents; 30μM sepiapterin (Schirks Laboratories, Switzerland), 10μM Mn(III) tetrakis (1-methyl-4-pyridyl)porphyrin pentachloride (MnTMPyP) (Calbiochem, U.K.), sepiapterin plus MnTMPyP and finally vehicle (Krebs-Henseleit alone).

Following the incubation period, a cumulative concentration response curve to acetylcholine (ACh, Sigma) was constructed in the concentration range of 1nM - 0.3mM. The ACh was then washed out for 10-15 minutes with Krebs-Henseleit and vessels allowed to return to baseline, after which the same vessels were reincubated with sepiapterin, MnTMPyP, both or neither. After the second 30-minute incubation, the EC80 for U46619 was readministered and a cumulative concentration response curve to the NO donor, sodium nitroprusside (SNP, Sigma), constructed in the range of 1nM - 3μM. Finally 10μM papaverine (phosphodiesterase inhibitor) was added to all vessels for a period of 20 minutes to allow the tissue to relax fully back down to baseline. A schematic of this protocol is shown in Fig. 4.02.

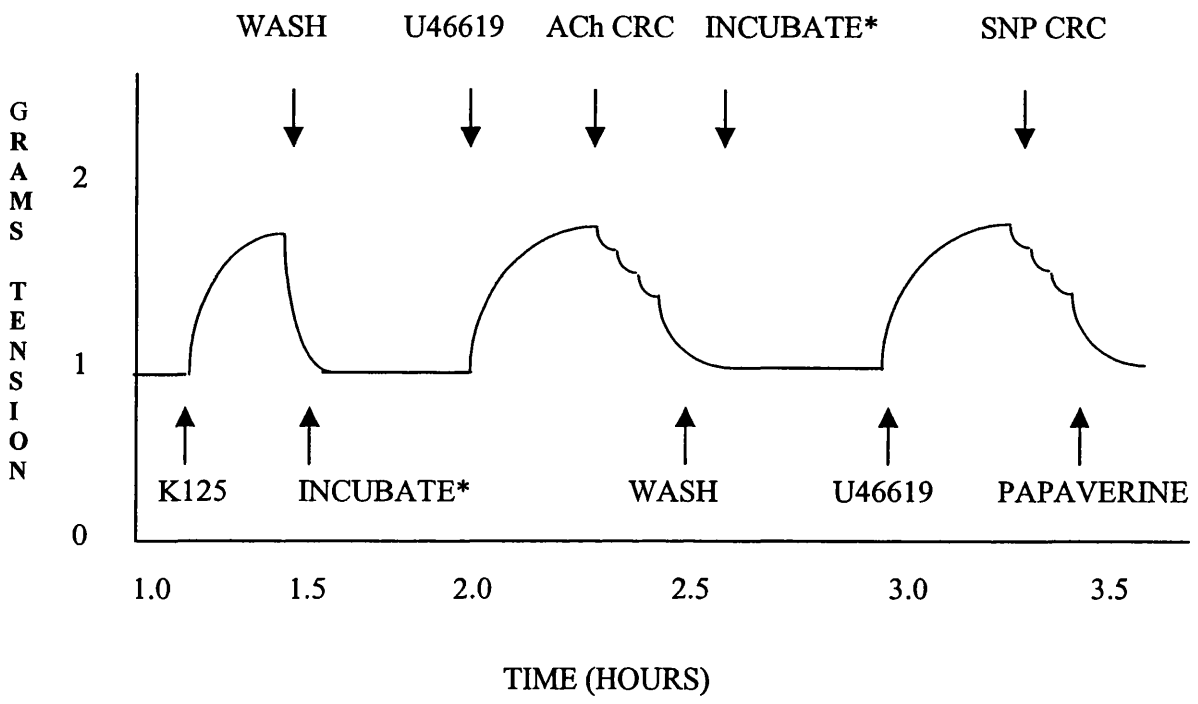

* Vessels were incubated for 30 minutes with either:

1) Sepiapterin (30μM) 2) MnTMPyP (10μM)

3) Sepiapterin + MnTMPyP 4) Control - Krebs-Henseleit

Figure 4.02 Schematic representation of organ chamber protocol

Data analysis

For all functional studies, vessels were initially contracted up to an EC80 for U46619 before constructing the appropriate concentration response curves to ACh or SNP. At the end of each experiment vessels were relaxed fully with the phosphodiesterase inhibitor, papaverine, resulting in maximal relaxation of the tissue down to baseline. For the purposes of data quantification for the relaxation studies, the precontractile U46619 response was taken to be 0% relaxation whilst the papaverine response was taken as 100%. All ACh and SNP induced relaxations mean ± SEM were calculated as a percentage of the response to papaverine. Statistical significance in concentration response curves to both ACh and SNP were determined using a Two Way ANOVA with Bonferonni post hoc test for multiple comparisons, yielding $p<0.05$ for statistically significant data sets (drug treated vs. vehicle). As a minimum of 5 experiments were conducted on 7 different groups, each group having 4 different treatments (i.e. sepiapterin, MnTMPyP, sepiapterin plus MnTMPyP and vehicle) the data have been pooled and represented as percentage maximum relaxation to ACh versus age, with the four different treatment groups.

The maximum relaxation to ACh for each experiment within each group was used and statistical significance for vehicle vs. drug treated was determined using a Two tailed paired T-test. The groups in which the concentration response curve to ACh showed statistically significant differences between vehicle and drug treatment, also showed statistical significance in maximum relaxation to ACh in the pooled data, as would be expected.

Determination of GTP-CH1 protein expression in porcine lung homogenates

In order to determine the temporal expression of GTP-CH1 protein in the healthy developing porcine lung and in hypobaric induced pulmonary hypertension, SDS-PAGE and Western blotting were carried out on porcine lung samples from F, NB, 12-24h, 3d, 14d, A and 3H. A primary GTP-CH1 anti peptide antibody (9598) was designed and developed, as described in chapter 3. Initial studies showed that GTP-CH1 was undetectable in particulate porcine lung homogenates but detectable in the soluble (cytosolic) fraction (chapter 3).

Briefly, protein samples (80μg/well) covering the entire range were resolved by electrophoresis through 12% SDS-PAGE gels, electroblotted onto PVDF membranes which were subsequently probed overnight at 4°C with a 1:1000 dilution of a primary rabbit anti GTP-CH1 antipeptide antibody followed by a secondary anti rabbit HRP conjugated antibody (Amersham). Signals were developed using ECL reagents (Amersham) and quantitated by densitometry.

Determination of GTP-CH1 localisation in porcine lung frozen sections

For immunohistochemical staining, slides covering the entire age range (F, NB, 12-24hr, 3d, 3H, 14d and A) were stained with a 1:500 dilution of the GTP-CH1 primary antibody 9598 and subsequently exposed to a 1:3000 dilution of biotinylated antirabbit secondary antibody (DAKO) and the streptavidin biotinylated horseradish peroxidase complex (ABC – Amersham). Immunoreactive staining was observed using DAB tablets (Sigma) and slides were subsequently counterstained and fixed in DPX for light microscopy.

GTP-CH1 activity measurements in porcine lung homogenates

GTP-CH1 activity was assayed by incubating lung extracts covering the entire age range (F, NB, 12-24hr, 3d, 3H, 14d and A) with GTP (0.75mM final concentration) at 37°C for 90 minutes in the dark. The reaction product was oxidised to neopterin triphosphate by acidic iodine (1 %). After reduction of excessive iodine by ascorbic acid (3 %), reaction product (neopterin triphosphate) was monitored on a plate reader with fluorescence detection. Dephosphorylation of the neopterin triphosphate by alkaline phosphatase (0.8U/200µl), and identification of neopterin by reverse HPLC was subsequently performed (Kerler *et al.*, 1989, Kerler *et al.*, 1990). Neopterin triphosphate levels correlated with neopterin levels in all cases and GTP-CH1 activities were expressed as pmol/mg/min. Dr Christian Hesslinger, University of Frankfurt, performed these studies in a blinded fashion.

4.03 Data analysis

Western blotting data for porcine lung samples

Semi-quantitative densitometric analysis of immunoreactive bands on immunoblots, was carried out using the Syngene Gene Tools data analysis package (SLS). Values obtained on each immunoblot for each age group were calculated as a percentage of 3 day values (3 day values being taken as 100%) due to the variations in absolute values between different immunoblots. One Way ANOVA was used to determine if there were any statistically significant differences between all age groups and a Bonferroni's Multiple Comparison post hoc test was used to assess for statistically significant differences between each group.

GTP-CH1 immunohistochemical staining

This technique is non-quantifiable. Localisation of protein staining was assessed visually and any obvious changes in protein localisation between different groups were noted. Nerve staining was used as a positive control and slides with poor or absent nerve staining were not analysed.

GTP-CH1 activity assays

Due to reasons discussed in the results and discussion section of this chapter, it was not feasible to perform any statistical analysis of this data.

4.04 Results

Normal development

Contractile and relaxant effects in normal porcine pulmonary arteries

Pharmacological studies performed on conduit pulmonary arteries obtained from healthy pigs, revealed an age-dependent variation in endothelium dependent relaxations to ACh, (Figures 4.04-4.06; white bars) with no significant differences in the responses to SNP (Figure 4.08a). As reported previously, responses to ACh were small at birth and increased at 3 and 14 days of age (Arrigoni *et al.*, 1999).

In vitro effects of L-sepiapterin and MnTMPyP

Contractile response

Addition of U46619 to conduit pulmonary arteries from all age groups and in 3H, caused a sustained and stable contractile response in all vessels that was unaltered by the incubation of L-sepiapterin and/or MnTMPyP (Figure 4.03).

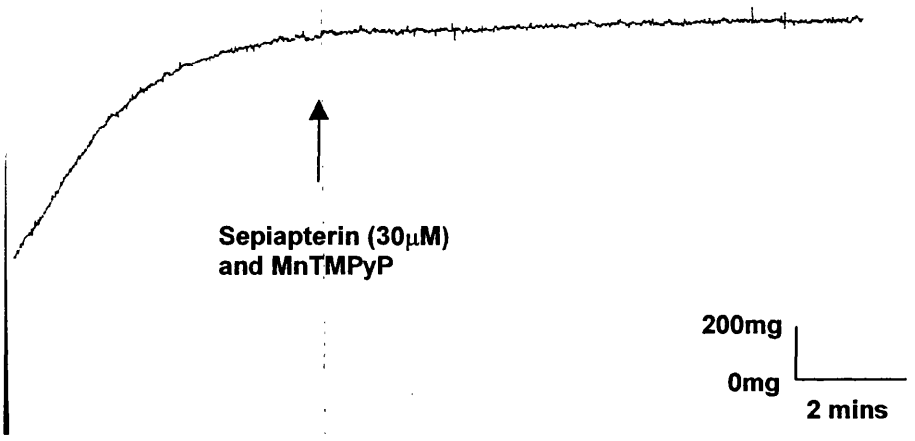

Figure 4.03 Trace of contractile response to U46619 (EC80) in a porcine pulmonary artery obtained from a 3 day old animal. Addition of sepiapterin and/or MnTMPyP had no effect on the response in all age groups studied.

Relaxant response in normal development

Neither L-sepiapterin, MnTMPyP nor a combination of the two, had any effect on the maximum endothelium dependent relaxations to ACh in F, NB, 12-24h and A vessels compared with the vehicle. However at 3 and 14 days of age, both L-sepiapterin and/or MnTMPyP, significantly enhanced the maximum endothelium dependent relaxations to ACh compared to vehicle (Figures 4.04-4.07). Results show that there is no significant difference between vessels treated with sepiapterin or MnTMPyP alone and those co incubated with sepiapterin and MnTMPyP, suggesting that these agents are working through the same mechanism. Endothelium independent relaxations to SNP reminaed unchanged between all age groups and in 3H and furthermore remained unchanged between all treated and untreated vessels from all age groups (Figures 4.08a and b).

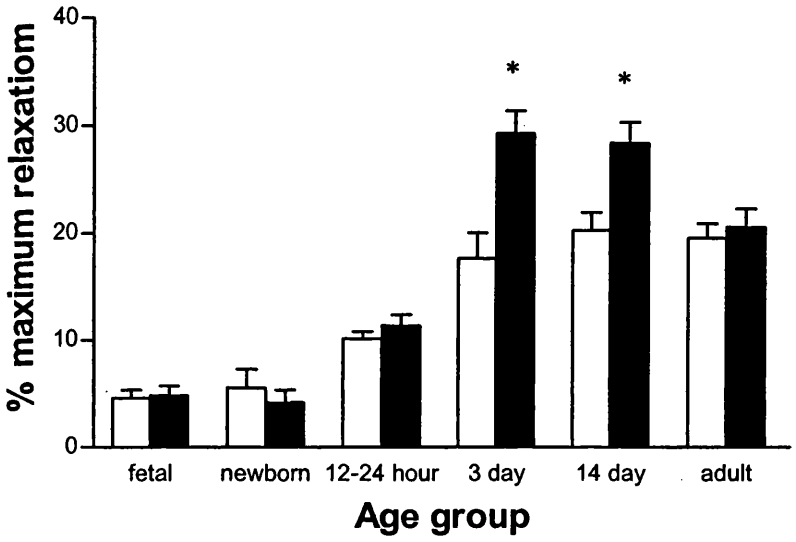

Figure 4.04 Maximum relaxation to ACh in porcine pulmonary arteries treated with sepiapterin (30μM) (■) compared to vehicle (Krebs) (□)
n≥5 values represent mean ± SEM *p<0.05 (paired t-test).

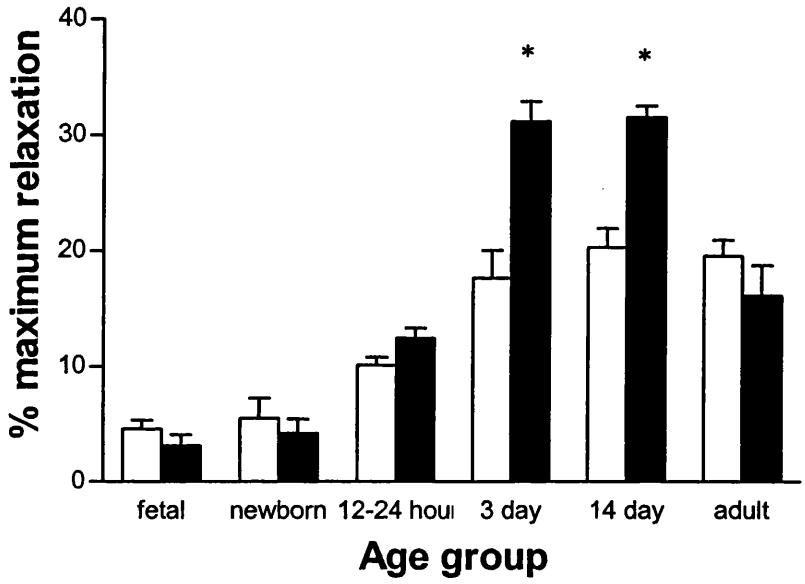

Figure 4.05 Maximum relaxation to ACh in porcine pulmonary arteries treated with MnTMPyP (10μM) (■) compared to vehicle (Krebs) (□)
n≥5; values represent mean ± SEM *p <0.05 (paired t-test)

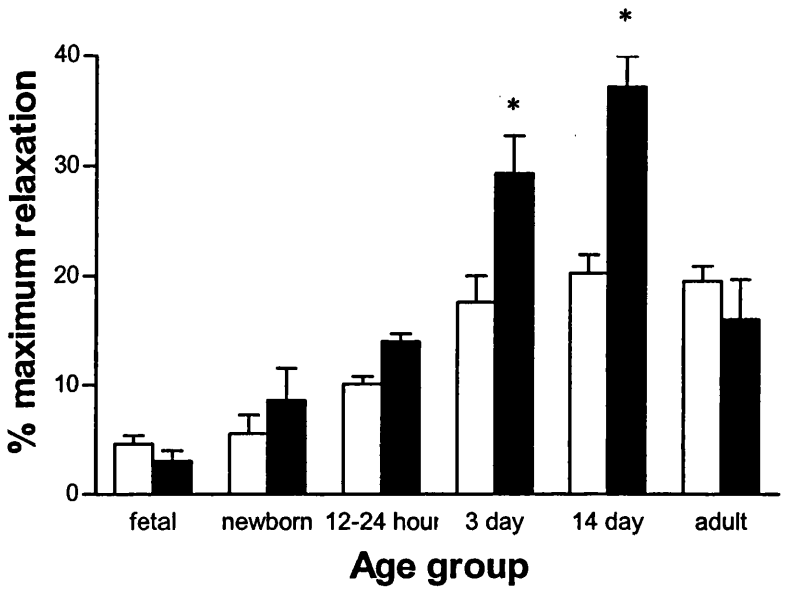

Figure 4.06 Maximum relaxation to ACh in porcine pulmonary arteries treated with a combination of sepiapterin (30μM) plus MnTMPyP (10μM) (■) compared to vehicle (Krebs) (□)
n≥5; values represent mean ± SEM *p <0.05 (paired t-test).

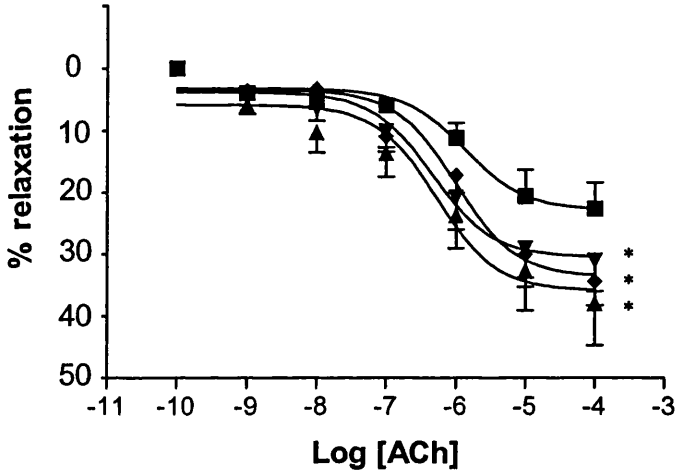

Figure 4.07 Concentration response curve to ACh in 14 day porcine pulmonary arteries treated with sepiapterin (30μM) (▼), MnTMPyP (10μM) (◆) or sepiapterin plus MnTMPyP (▲) compared to vehicle (Krebs) (■)
Values represent mean ± SEM *p <0.05 (Two way ANOVA + Bonferroni post test) n=6

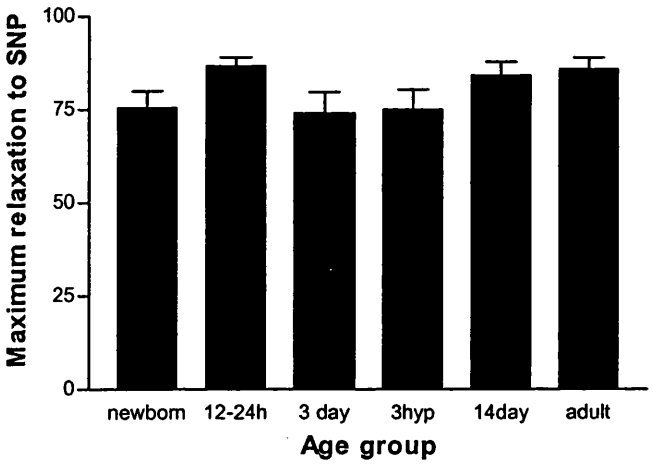

Figure 4.08 a Maximum relaxation to SNP in porcine pulmonary arteries treated with vehicle (Krebs). p=ns One Way ANOVA (with Bonferroni post hoc test) n≥5

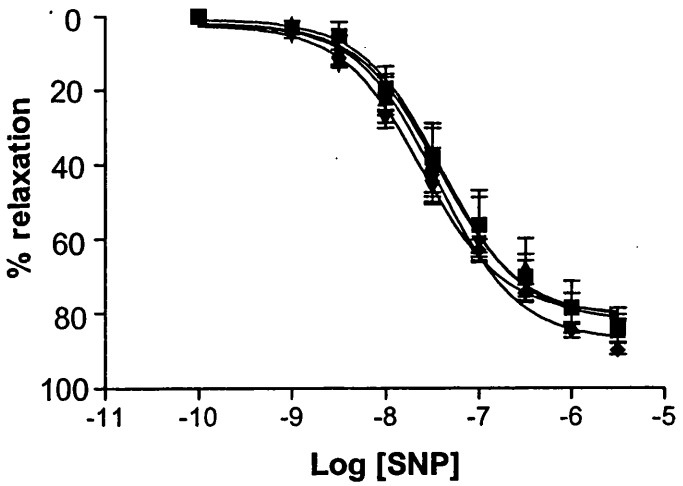

Figure 4.08b Concentration response curve to SNP in 14 day porcine pulmonary arteries treated with sepiapterin (30μM) (▲), MnTMPyP (10μM) (◆) or sepiapterin plus MnTMPyP (▼) compared to vehicle (Krebs) (■) n=6; Values represent mean ± SEM p =ns (Two way ANOVA + Bonferroni post test).

GTP-CH1 protein expression in normal development

The anti peptide antibody raised against a human GTP-CH1 $^{(17-45)}$ peptide sequence 9598, gave rise to a distinct immunoreactive band of the expected size and GTP-CH1 protein was detectable in soluble lung homogenates from all groups studied with none being detectable in particulate lung homogenates (chapter 3). In some lanes, the ~28-30 kDa band appears to be running as a doublet, which may indicate post translational modification, although further studies would be required to test this. Figures 4.09a and b show the developmental change in protein expression of GTP-CH1. GTP-CH1 expression was low in the fetus and rose immediately after birth. It remained highly expressed until 12-24 hours of age after which there was a decline at 3 and 14 day of age and finally a rise in the adult. There was no significant difference between fetal, 3 day and 14 day levels, whilst the remaining age groups were significantly higher than fetal values.

Relationship between functional data and GTP-CH1 expression in normal development

Figure 4.10 shows the percentage change versus vehicle, in the relaxation to ACh following BH_4 supplementation in porcine pulmonary arteries. By comparing this figure with Fig 4.08 it can be seen that the ages groups where GTP-CH1 expression is lowest are the same groups in which BH_4 supplementation improved the ACh relaxation i.e. 3 and 14 days of age, with the exception of fetal values. Conversely where GTP-CH1 protein expression was higher, there do not appear to be any functional effects of BH_4 supplementation.

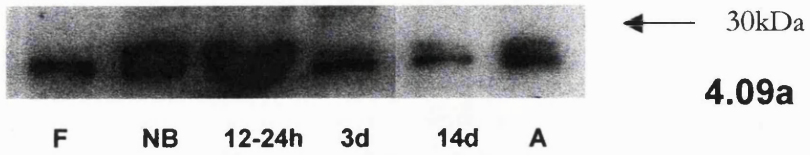

4.09a

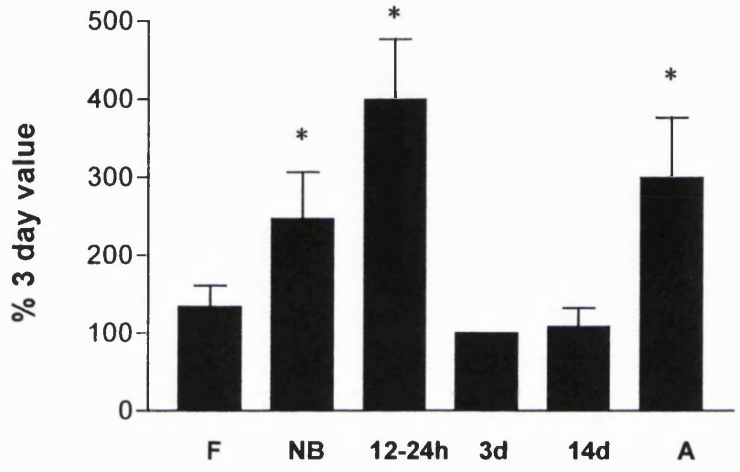

4.09b

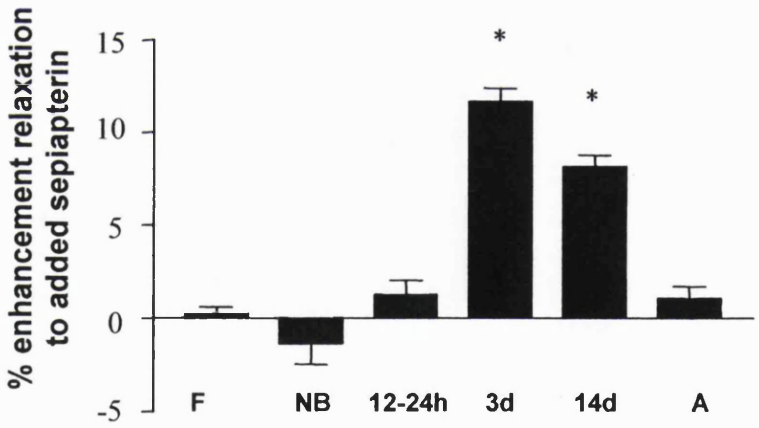

4.10

Figure 4.09a Immunoblot showing immunoreactive band below 30kDa for GTP-CH1 in all age groups F(fetal); NB (newborn); 12-24h (12-24 hours), 3d (3 day), 14d (14 day); A (Adult).

Figure 4.09b Densitometric analysis of immunoblots all values calculated as a percentage of 3-day values.
Values represent mean ± SEM. * $p < 0.05$ GTP-CH1 expression significantly different from 3 day values, One Way ANOVA with Bonferroni post hoc test.
(n = 5)

Figure 4.10 Graph illustrating developmental change in percentage enhancement of maximum relaxation to ACh over control values in sepiapterin treated vessels. ($n \geq 5$) *$p<0.05$ vs. vehicle, paired Two tailed T-test.

GTP-CH1 activity in normal development

GTP-CH1 activity results show GTP-CH1 activity (pmol/mg/min) in fetal (0.072±0.02) and newborn (0.115±0.043) vessels with very low levels detected at 12-24 hours, 3 and 14 and adult tissues. Unfortunately, the activity levels in the 12-24 hour, 3 day and 14 day and adult tissues were so close to the limit of detection, that it was not possible perform any statistical analysis of this data. The reliability of these data will be discussed later.

Immunolocalisation of GTP-CH1 in normal development

Immunohistochemical staining using the GTP-CH1 anti peptide antibody revealed that GTP-CH1 was primarily localised to the nerves, bronchial epithelial and smooth muscle cells and to the pulmonary arterial and venous smooth muscle and in some cases to the endothelial cells of the pulmonary arteries and veins. Immunolocalisation did not appear to alter with age (Figure 4.11)

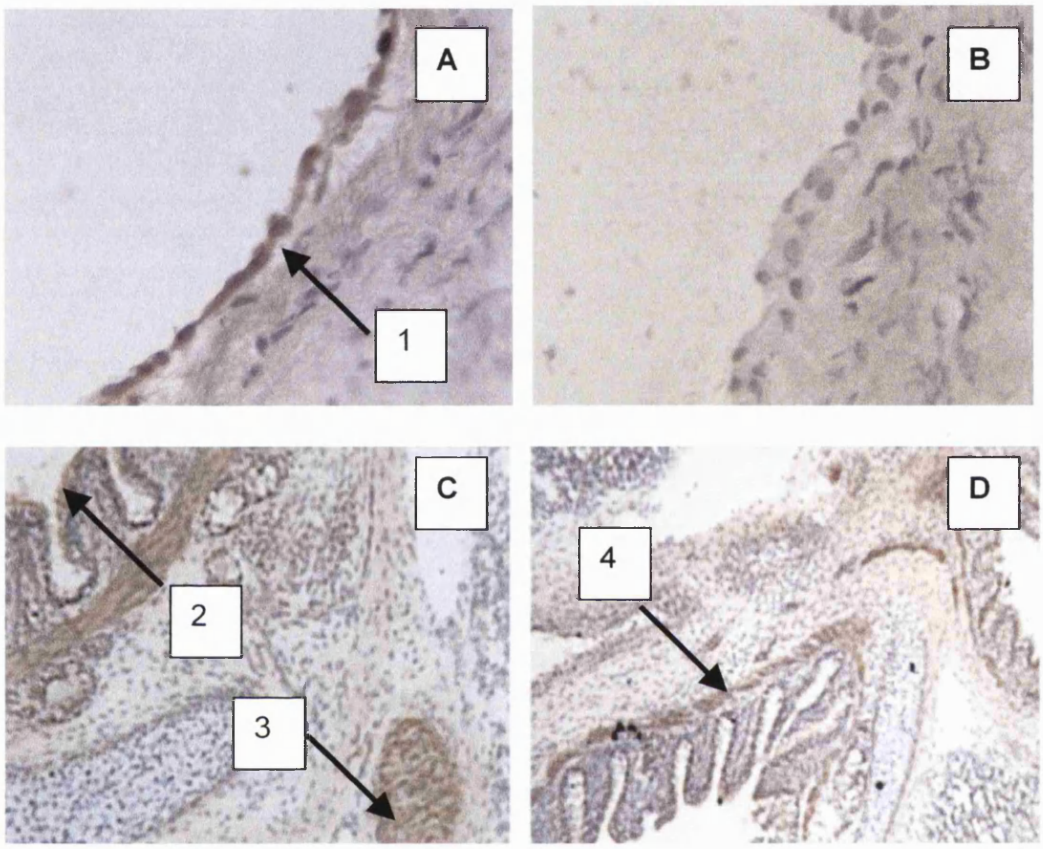

Figure 4.11 Immunohistochemical staining of porcine lung sections with the GTP-CH1 anti peptide antibody and haemotoxylin counterstaining. **A**: 12-24 hour old piglet conduit pulmonary artery endothelial cell layer (1) (x40 mag); **B**: 12-24 hour old piglet conduit pulmonary artery negative control (x40 mag); **C**: Newborn airway epithelium (2) and nerve (3) staining (x 10 mag); **D**: Newborn airway smooth muscle staining (4) (x10 mag). Counterstained with haemotoxylin.

4.06 Porcine model of PPHN

Effects of hypobaric exposure on ventricular weights

Figure 4.12 shows the RV:LV+S ratio obtained from newborn (NB), 3 day old and 3 day piglets exposed to hypobaric conditions from birth (3H). The RV:LV+S ratio is significantly higher in the 3H compared with the 3 day control, indicating right ventricular hypertrophy. The RV:LV+S ratio is not significantly different between NB and 3H, suggesting that hypobaric exposure has prevented the normal adaptation (i.e. a drop in the RV:LV+S ratio) observed in the first few days of extrauterine life. These results suggest that the animals exposed to hypobaric conditions from birth until 3 days have developed pulmonary hypertension.

Effects of hypobaric hypoxia on vascular relaxation

Pulmonary arteries from 3H piglets did not relax to the endothelium dependent vasodilator ACh when compared to the age matched control (Figure 4.13) and furthermore ACh relaxations in the 3H were not significantly different to those seen in NB animals (Figure 4.13). Vessels from NB, 3 day and 3H all relaxed fully to SNP, with no significant difference in relaxation between groups (Figure 4.14).

Effects of sepiapterin and/or MnTMPyP on vascular reactivity following hypobaric exposure

Endothelium dependent relaxations were not improved in vessels from 3H piglets after the addition of L-sepiapterin or MnTMPyP, when administered individually. However, in 3H vessels treated with L-sepiapterin plus MnTMPyP a statistically significant improvement in the relaxation to ACh was observed (Figure 4.15). Endothelium independent relaxations to SNP remained equal in all vessels regardless of treatment suggesting the effects of L-sepiapterin and MnTMPyP were endothelium dependent (Figures 4.08a and 4.16).

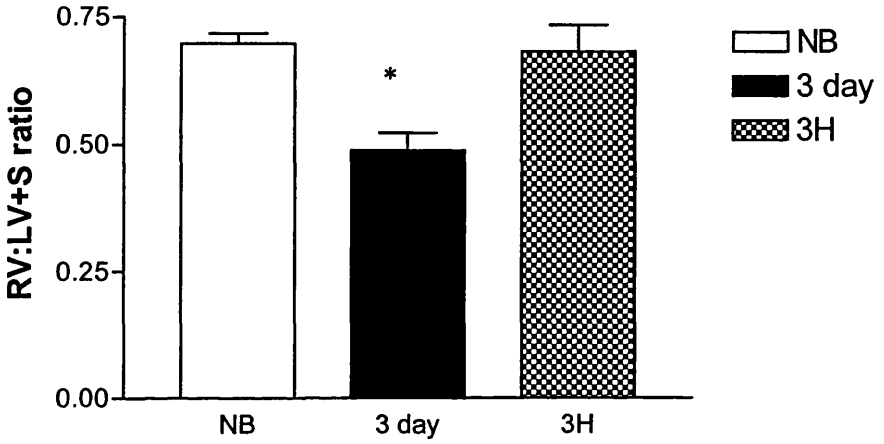

Figure 4.12 RV:LV+S ratio in NB, 3 day and 3H piglets.
*p<0.05 One Way ANOVA ; 3 day vs. 3H and NB; n=5.

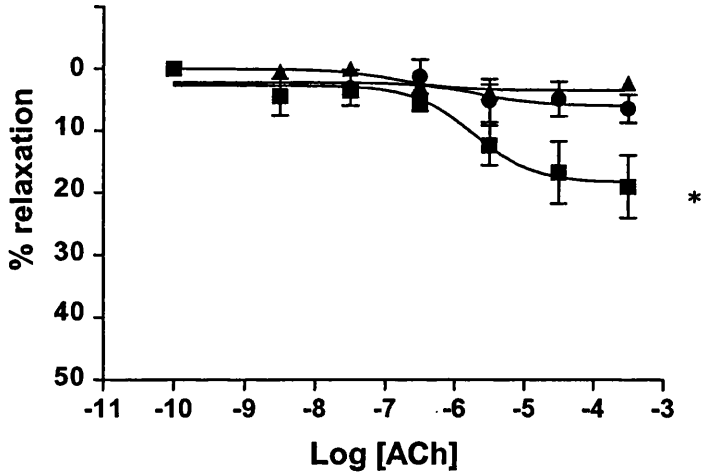

Figure 4.13 Concentration response curve to ACh in pulmonary arteries obtained from NB (●), 3 day control (■) and 3H (▲).
*p < 0.05 3H vs. 3 day control and NB vs. 3 day control, Two Way ANOVA with Bonferroni post hoc test; n=5.

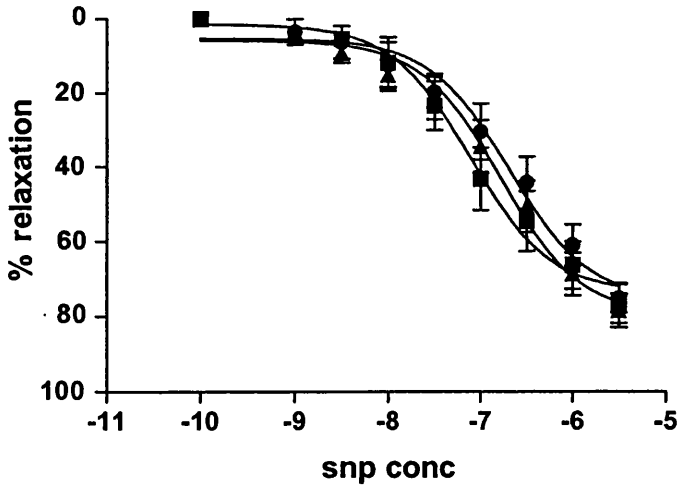

Figure 4.14 Concentration response curve to SNP in pulmonary arteries obtained from NB (●), 3 day control (■) and 3H (▲).
p=ns Two Way ANOVA with Bonferroni post hoc test; n=5.

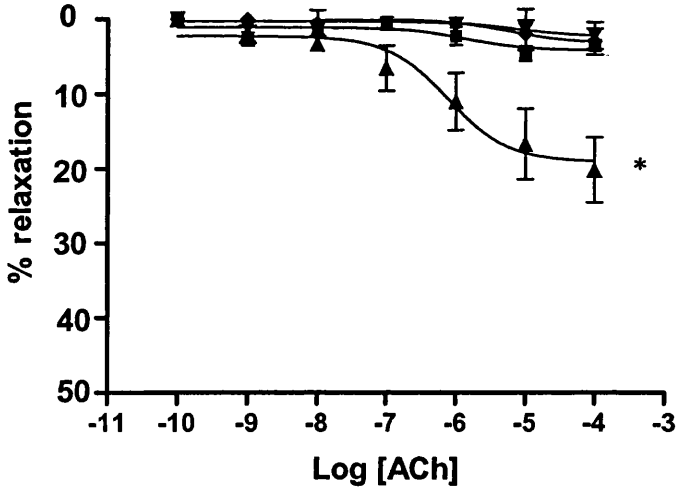

Figure 4.15 Concentration response curves to ACh in pulmonary arteries obtained from 3H piglets following treatment with 30μM sepiapterin (▼), 10μM MnTMPyP (◆) sepiapterin plus MnTMPyP (▲) or Krebs Henseleit (vehicle) (■). *p<0.0001 n=5 Two Way ANOVA with Bonferroni post hoc test n=5

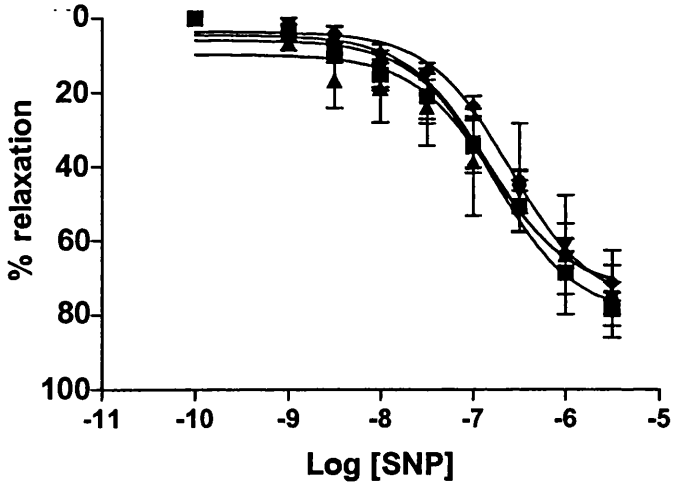

Figure 4.16 Concentration response curves to SNP in pulmonary arteries obtained from 3H following treatment with 30μM sepiapterin (▼), 10μM MnTMPyP (◆) sepiapterin plus MnTMPyP (▲) or Krebs Henseleit (vehicle) (■). p = ns Two Way ANOVA with Bonferroni post hoc test; n=5.

GTP-CH1 protein expression

There was no significant difference in GTP-CH1 protein expression between 3 day control and 3H animals (Figure 4.17a and b).

GTP-CH1 activity

GTP-CH1 activity for tissue samples fell very close to the limit of detection in the 3 day control and 3 H, and as a result it was not possible to accurately interpret or perform any statistical analysis of the data.

GTP-CH1 localisation

Immunohistochemical staining using the GTP-CH1 anti peptide antibody revealed that GTP-CH1 was primarily localised to the nerves, smooth muscle cells of the pulmonary arteries and veins and to the bronchial smooth muscle and epithelial cells of the airways (Figure 4.18). Localisation of GTP-CH1 did not appear to alter following hypobaric exposure and was consistent in all groups studied.

a)

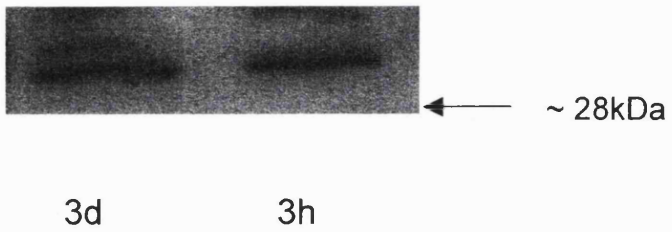

b)

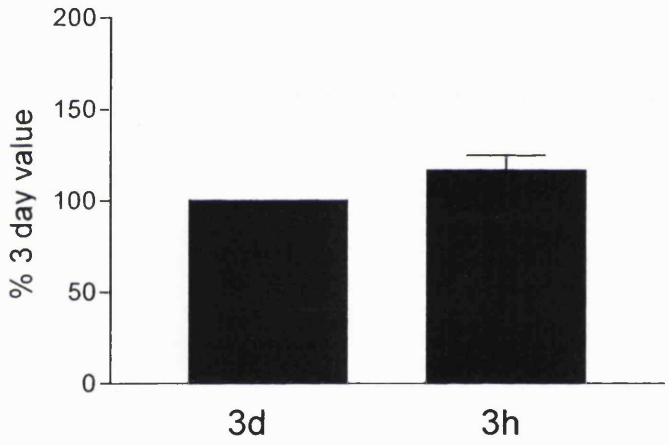

Figure 4.17 a) Immunoblot showing immunoreactive band ~28kDa for GTP-CH1 protein expression in porcine soluble lung homogenates from 3 day control and 3H piglets.

Figure 4.17 b) Densitometric analysis of immunoblots.
All values calculated mean ± SEM, as a percentage of 3 day values.
n≥5; p = ns One Way ANOVA with Bonferroni post hoc test.

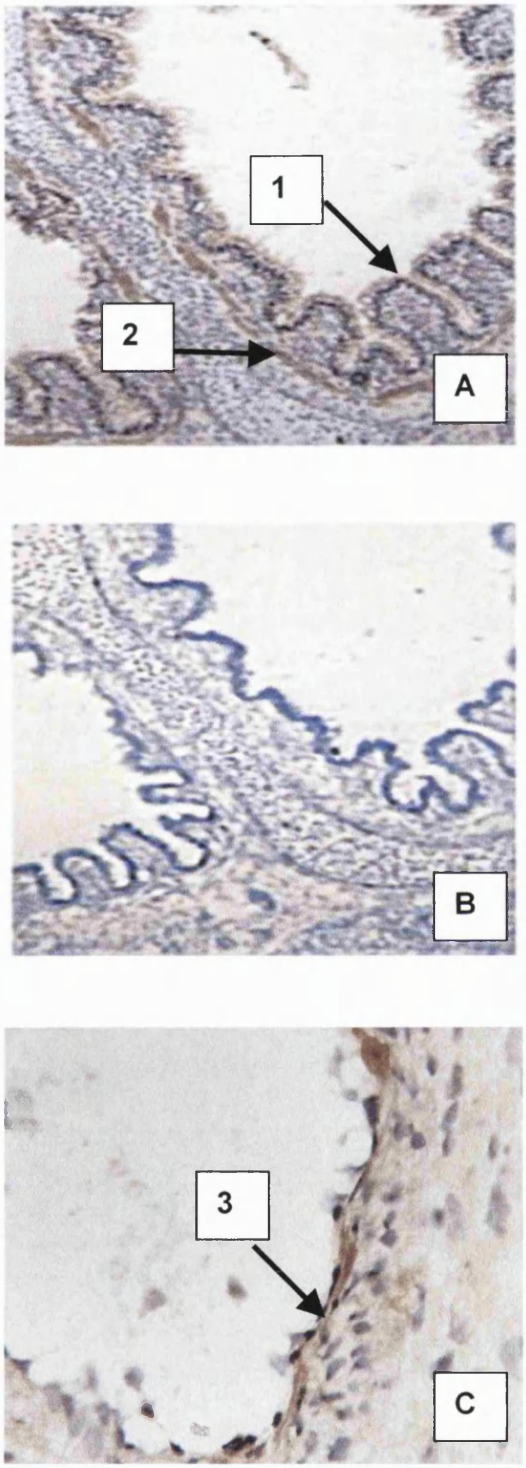

Figure 4.18 Immunohistochemical staining of porcine lung sections from 3 day pulmonary hypertensive piglets using the GTP-CH1 antipeptide antibody.
A GTP-CH1 positive staining on airway epithelium (1) and smooth muscle cells (2) (x10 mag.); **B** – negative control (x10 mag.); **C** conduit pulmonary artery endothelial cell staining (3) (x40 mag.). Counterstained with haemotoxylin.

4.07 Discussion

Normal development

There is evidence to suggest that NO is a key player in the transitional changes that occur in pulmonary blood vessels at birth and with the postnatal adaptations to air breathing that follow (Abman *et al.*, 1990). Indeed NOS inhibitors prevent adaptation to extrauterine life (Kinsella and Abman 1995). The well-characterised porcine model was used in this study to investigate BH_4 and O_2^- in the adaptation of the pulmonary vasculature to extrauterine life. Endothelium dependent relaxation of porcine conduit pulmonary arteries are low before and immediately after birth and increase thereafter, but the mechanisms responsible for these events are not fully understood. This study demonstrates developmental changes in GTP-CH1 expression and in the response of normal conduit pulmonary arteries to additional sepiapterin to increase BH_4 levels, and MnTMPyP to quench $O_2^{-\cdot}$ radicals. The data suggest that there may be a functionally significant deficiency of BH_4 contributing to the low endothelium dependent relaxation soon after birth and that altered expression of GTP-CH1 in the first few days of life may mediate these changes.

In the present study there was a clear age dependent increase in the response to ACh in the conduit pulmonary arteries, consistent with previous findings (Arrigoni *et al.*, 1999). To determine whether altered BH_4 generation and/or O_2^- contribute to these changes, L-sepiapterin was added, to generate BH_4 independently of GTP-CH1 activity and MnTMPyP to scavenge O_2^-. Fetal, newborn, 12-24 hour and adult pigs, showed no significant improvement in the maximum relaxation to ACh in the presence of L-sepiapterin and/or MnTMPyP. However, at 3 and 14 days of age, L-sepiapterin and/or MnTMPyP significantly

improved maximum relaxation to ACh. The endothelium independent relaxations to SNP remained present in all age groups, and were unaltered by either sepiapterin or MnTMPyP, suggesting that the effects caused by L-sepiapterin and MnTMPyP were endothelium dependent. These findings suggest that BH_4 becomes rate limiting for NO generation at 3 and 14 days and that there may be excess O_2^- production.

Furthermore, these studies show no apparent detrimental effect of either sepiapterin or MnTMPyP. If sepiapterin and MnTMPyP had been generating O_2^- we would have expected an attenuation of relaxation of treated tissues compared with control and/or an enhancement of the contraction to U46619 (Figure 4.02).

BH_4 is generated in a three-step process and the rate limiting step is often the expression of GTP-CH1. Immunohistochemistry confirmed that GTP-CH1 protein was confined largely to the smooth muscle of the airways, arteries and veins. In many sections, GTP-CH1 immunoreactivity also appeared to be detectable in the endothelial cells of the pulmonary arteries and veins, (consistent with a role in generating BH_4 for NOS activation) but interpretation must be cautious since layering of endothelial cells may cause this appearance. These data may suggest that biosynthesised BH_4 is transported from the smooth muscle cells into the endothelial cells where it binds to NOS, or simply that GTP-CH1 is localised to endothelial cells but is less detectable by immunohistochemistry. Indeed GTP-CH1 mRNA has been detected in isolated murine endothelial cells (see Chapter 6) and human coronary artery endothelial cells (unpublished data) and furthermore, functional effects of

BH_4 have been demonstrated in isolated porcine aortic endothelial cells (Huang *et al.*, 2000; Schmidt *et al.*, 1992).

GTP-CH1 protein was detected in soluble lung homogenates from all age groups, but was undetectable in particulate lung homogenates (chapter 3). The expression of GTP-CH1 was low in the fetus and rose immediately after birth to reach maximal levels in the 12 -24 hour samples. By 3 and 14 days of age, expression of GTP-CH1 was reduced to fetal levels and then increased again in the adult. The mechanism underlying the increase in GTP-CH1 protein expression immediately after birth is not known but there are three putative shear stress response elements in the GTP-CH1 promoter sequence. The sequence of nucleotides GGT CTC, appear at positions –796, -741 and –615 of the promoter and it is possible that the sudden increase in shear stress in the pulmonary vasculature during parturition may induce GTP-CH1 expression and the decrease in GTP-CH1 protein, that occurs at days 3 and 14, results from a reduction in shear stress following the natural adaptation to air breathing.

It is highly likely that delays between tissue acquisition and freezing rendered GTP-CH1 activity unmeasureable in the majority of samples (fetal and NB tissue were always snap frozen within minutes after death, whilst the remaining samples will have had between 1-4 hours before the tissue was frozen). This data unfortunately does not allow any conclusions to be drawn regarding the temporal changes in GTP-CH1 activity, but underlies the importance of immediate snap freezing for this type of assay.

It appears as though rate limitation of BH_4 occurs at 3 and 14 days of age, confirmed by the low GTP-CH1 protein expression and as a result, BH_4 supplementation via the BH_4 precursor L-sepiapterin significantly improves the NO mediated relaxation to ACh in these age groups. GTP-CH1 protein expression remains elevated in the remaining age groups (with the exception of the fetus) and hence the mechanism behind the low endothelium dependent relaxation in these age groups does not appear to be dependent on BH_4 and GTP-CH1 levels.

Additionally, quenching of O_2^- using the SOD mimetic MnTMPyP significantly improved the endothelium dependent relaxations in 3 and 14 day old animals but not in the remaining age groups. As stated earlier, suboptimal concentrations of BH_4 may turn NOS into a generator of O_2^- (Cosentino *et al.,* 1998). As GTP-CH1 protein was lowest in 3 and 14 day animals, it may be possible that low levels of endogenous BH_4 turn NOS into a generator of O_2^- hence MnTMPyP inactivates these harmful anions and restores the endothelium dependent relaxations.

Together, these data suggest that low GTP-CH1 expression at days 3 and 14 renders NOS inefficient and that supplementation with exogenous BH_4 improves endothelium dependent relaxation. The finding that MnTMPyP also improves endothelium dependent relaxation in these vessels and that the effects of sepiapterin and MnTMPyP are not additive is consistent with enhanced $O_2^{-\cdot}$ generation contributing to the effects of BH_4 deficiency. In isolated enzyme systems BH_4 deficient NOS may generate $O_2^{-\cdot}$ and furthermore several recent *in vivo* studies have demonstrated the importance of BH_4 for NOS dimerisation and

endothelial function, and these may explain the effects we have seen (Vasquez Vivar *et al.*, 1999, Cosentino *et al.*, 2001, Cai *et al.*,2002, Ozaki *et al.*, 2002).

Although it is clear that the relaxation at days 3 and 14 can be enhanced by supplementing BH_4, it is also evident that the very low degree of relaxation seen in newborn animals is not because BH_4 supply is rate limiting. However, the inconsistency in these data is that GTP-CH1 protein expression is low in the fetus yet BH_4 supplementation or MnTMPyP did not appear to improve endothelium dependent relaxations. Furthermore, relaxation was enhanced above adult levels in the 3-14 day old animals when BH_4 was added, yet in the adult animals, BH_4 does not appear to be rate limiting for NO mediated relaxation. These effects may be explained by considering eNOS. Although eNOS protein is expressed in the fetus (Hislop *et al.*, 1997), eNOS activity is lowest in the fetus increasing immediately after birth to maximal levels in 1,3 and 14 day old animals and finally decreasing in adulthood (Arrigoni *et al.*, 2002). Thus the supranormal relaxation seen at days 3 and 14 on adding sepiapterin probably reflects the high level of eNOS activity and relatively low GTP-CH1 expression at these ages. Conversely, the low eNOS activity in the fetus may furthermore explain the absence of any effects of sepiapterin (despite the low levels of GTP-CH1 protein) in the vasculature in the fetal vessels.

Hypobaric induced pulmonary hypertension

The study demonstrates that supplementation of BH_4 (sepiapterin) or SOD (MnTMPyP) individually, have no effect on vessels obtained from 3H piglets and did not restore the endothelium dependent relaxation to ACh. However, supplementing BH_4 and SOD in combination, significantly increased endothelium dependent relaxations in the pulmonary arteries of the 3H piglet. This is the first time that an intervention has been shown to enhance endothelium dependent relaxation in this animal model. However the mechanism of this effect is not clear since was no significant difference between the expression or localisation of GTP-CH1 in the 3H compared with the 3 day control animal.

The present study confirmed previous findings that piglets maintained at low atmospheric pressure 50.8kPa (and hence low oxygen ~10%) from birth, develop pulmonary hypertension characterised structurally by right ventricular hypertrophy (Haworth and Hislop, 1981; Tulloh *et al.*, 1997) (Figure 4.12). Endothelium dependent relaxations to ACh were absent in unsupplemented vessels (vehicle) obtained from 3H animals when compared to their age matched controls, and were similar to relaxations observed in NB animals, consistent with published findings (Tulloh *et al.*, 1997, Arrigoni *et al.*, 1999) whilst endothelium independent relaxations to SNP remained intact and unaltered between the 3H and the 3 day control piglets.

By examining the literature, it is likely that in the porcine model of pulmonary hypertension used in this study, eNOS protein and activity are decreased following hypobaric exposure, resulting in endothelial dysfunction thereby explaining the lack of relaxation to ACh in

isolated pulmonary arteries (Hislop *et al.*, 1997, Fike *et al.,* 1998). The reasoning behind this reduction in NOS activity/expression may possibly occur as a result of either decreased cofactor availability e.g. L-arginine or BH_4, increased catabolism of NO by O_2^- or increased endogenous inhibition of NOS. Indeed, one explanation could be the observed reduction in the activity of dimethylarginine dimethylaminohydroxylase (DDAH II) (Arrigoni *et al.*,2003). DDAH is an endogenous inhibitor of asymmetric dimethylarginine (ADMA), which in itself is an endogenous NOS inhibitor. Furthermore increased levels of ADMA have been measured in infants with PPHN (Pierce *et al.*, 2000).

Unlike the control 3 day old piglet, 3H piglets showed no improvement of ACh mediated relaxation to either sepiapterin or MnTMPyP when added individually, yet demonstrated a significant enhancement of ACh mediated relaxation when added together. Alongside these findings, GTP-CH1 protein expression appeared unaltered between the 3 day control and 3H piglets, indicating that GTP-CH1 does not appear to be affected by hypobaric exposure, and furthermore the localisation of GTP-CH1, as determined by immunohistochemistry, appeared unaffected by hypobaric exposure.

Thus, the explanation as to why MnTMPyP and sepiapterin, when administered together, resulted in a significant improvement in the endothelium dependent relaxations appears complex. Tsutsui *et al.*, (1996) demonstrated similar findings to those obtained in the present study following investigations on isolated canine middle cerebral arteries where addition of sepiapterin or SOD alone did not improve endothelium dependent relaxations (in fact sepiapterin attenuated these relaxations), yet when administered in combination,

significantly improved vascular reactivity, concluding that increased availability of BH_4 (following sepiapterin administration) may stimulate the production of NO, provided that the activity of superoxide dismutase in the surrounding environment is high enough to prevent auto oxidation of BH_4 and inactivation of NO by O_2^-. Therefore one possible explanation of the effects seen in this study are that the potential increase in O_2^- in arteries following hypobaric exposure, may have generated sufficient O_2^- to inactivate NO, outweighing any beneficial effects of sepiapterin administration alone, and perhaps causing auto oxidation of generated BH_4, yet when administered in combination with MnTMPyP, inactivation of the excess O_2^- would allow NO mediated vasodilatation to prevail.

A second explanation could be that the effects observed are occurring via the vasodilatory effects of H_2O_2 generated following dismutation of O_2^-. Indeed this mechanism has been proposed in explaining the effects of BH_4 deficiency in vascular reactivity in the *hph-1* mouse (Cosentino *et al.*, 2000). However, in order to confirm this, the experiments would have to be repeated in the presence of catalase, a scavenger of H_2O_2 and we would expect the vasodilatation seen following sepiapterin and MnTMPyP addition, in 3H animals, to be reversed.

A final mechanism could be that sepiapterin and MnTMPyP are working through some as yet unknown mechanism when administered in combination, independent of the NO/BH_4 pathway.

4.08 Summary

Developmental regulation of GTP-CH1 occurs during the neonatal period in the pulmonary vasculature and this results in a functionally significant limitation of BH_4. One mechanism by which this deficiency may affect endothelial function is that eNOS may be unable to form a stable dimer and/or may generate harmful $O_2^{-\cdot}$ radicals causing endothelial dysfunction. GTP-CH1 protein expression and localisation appear unaffected in a porcine model of PPHN, although BH_4 and SOD supplementation together, appear to restore endothelial function.

It remains to be determined whether the developmental changes in GTP-CH1 also alter NO generation in other tissues and whether this may be functionally important in certain types of developmental pulmonary hypertensive disorders.

CHAPTER 5

Structural characterisation of the pulmonary vasculature of the hph-1 mouse

5.01 Introduction

A chemical mutation induced by N-ethyl-N'-nitrosourea, resulting in a 90% deficiency in GTP-CH1 activity and a 50% reduction in BH_4 levels has been induced in a laboratory mouse termed the hyperphenylalaninemic or *hph-1* mouse mutant (McDonald and Bode 1988). Other than hyperphenylalanemia, these mice show increased neonatal mortality but can grow to adulthood and breed successfully. Lifespan studies have not been conducted on these mice and mainly the neurological phenotype resulting from this mutation has been extensively studied. It would be predicted that the mutation in the *hph-1* mice would potentially reduce eNOS activity (as a result of reduced BH_4) and would, in theory, reduce basal and stimulated NO release. We therefore decided to establish the effects of this mutation on the pulmonary vasculature and the aim of the current study was to investigate whether the deficiency of BH_4 resulting from reduced GTP-CH1 activity would contribute to the development of pulmonary hypertension in the *hph-1* mouse (Figure 5.01).

Hypothesis

Hph-1 mice display the structural characteristics of a pulmonary hypertensive phenotype.

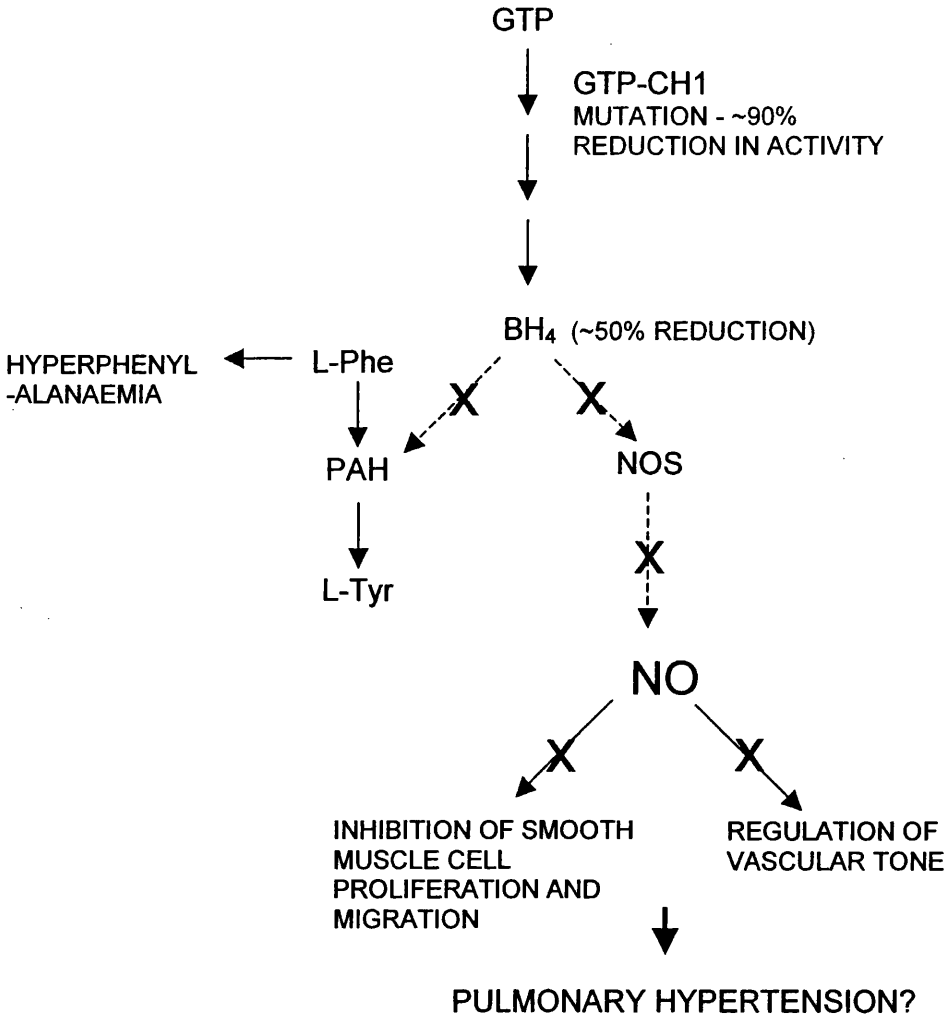

Figure 5.01 Schematic representation of study. Reduced GTP-CH1 activity in the *hph-1* mouse may result in reduced basal and stimulated NO release which may in turn lead to smooth muscle cell proliferation and migration and prevent normal regulation of vascular tone, leading to pulmonary hypertension.

5.02 Methods and Protocols

Dissection of heart and lungs from *Hph-1* and C57BL/6 W/T mice

Six wild type C57BL/6 X CBA and six *hph-1*, 12 week old, sex-matched (4 female, 2 male) mice were supplied by Dr Simon Heales (Institute of Neurology, Queen's Square, London) Hearts and lungs were carefully dissected from mice killed by cervical dislocation, ensuring that the trachea remained attached to the lungs, and placed in chilled PBS. Any other tissue e.g. kidneys, spleen, liver etc were snap frozen in liquid nitrogen incase of future requirement. The age, sex and weight of all animals used were additionally recorded.

Heart weight measurements

Immediately after death, the hearts and lungs were removed *en bloc* and immersed in chilled phosphate buffered saline. To assess ventricular hypertrophy in the *hph-1* versus wild type C57BL/6 mice, the atria were removed at the plane of the atrial-ventricular valves. The right ventricle (RV) was subsequently dissected from the left ventricle plus septum (LV + S). The RV and LV + S were then weighed and the RV/LV+S ratio calculated.

Measurement of alpha smooth muscle actin labelled thickness of pulmonary arteries.

4μm paraffin sections slides were immunostained with mouse alpha smooth muscle actin monoclonal antibody (1:3000) (DAKO, UK) (as described in Chapter 2). Positive staining was visualised using DAB (Sigma) and slides were subsequently counterstained and fixed for light microscopy.

Structural analysis

Using a light microscope (Magnification x 40; Zeiss Axioskop2, U.K.) approximately 10 arteries per animal each at the level of the alveolar ducts (AD), respiratory bronchiole (RB) and terminal bronchiole (TB) were identified anatomically (correct identification confirmed by vessel size) and the images captured and transferred to the data acquisition system Open Lab Software v3.04 (Improvision, Coventry, U.K.). The total extèrnal area (from the outer smooth muscle wall) of the artery and the luminal area were measured and the arterial wall area calculated by subtracting luminal area from the total external area. Arterial wall area was then expressed as a percentage of the total external area.

In addition to measuring percentage wall areas, extension of muscle into normally non-muscularised arteries was assessed in both *hph-1* and wild type groups. Arteries at the level of alveoli were identified using a light microscope (magnification x 40) and classified by circumferential staining with alpha actin as either non muscular (NM), partially muscular (PM) < 75% brown staining or fully muscular (M) >75% brown staining.

5.03 Data analysis

Body weights, corrected and uncorrected (for body weight) lung and heart weights, percentage wall area, percentage of muscular arteries and lumen areas have been expressed as mean ± SEM. Two-tailed unpaired t-tests were used to test for statistically significant differences between *hph-1* and C57BL/6.

5.04 Results

Table 5.01 summarises the body weights, total heart weights and total lung weights for the *hph-1* and the C57BL/6 X CBA wild type mice. The animals were age and sex matched (n=6) and the C57BL/6 X CBA mice were significantly heavier than the *hph-1* mice, whilst the corrected heart weight and corrected and absolute lung weights were greater in the *hph-1* mice.

Parameter	***Hph-1*** **(Mean±SEM)**	**C57BL/6 X CBA** **(Mean±SEM)**
Body weight (g)	23.13±1.51*	28.47±2.12
Absolute heart weight/g	0.14±0.01	0.13±0.01
Heart weight (g)/body weight	0.01±0.0005*	0.005±0.00008
Absolute lung weight/g	0.47±0.07*	0.37±0.04
Lung weight (g)/body weight	0.02±0.004*	0.013±0.0009

Table 5.01 Body, heart and lung weights for *hph-1* and C57BL/6 X CBA wild type mice. n=6 *p<0.05 vs. C57BL/6 X CBA mice. Two tailed unpaired t-test

Results show that there was no significant difference between the left ventricular weights of *hph-1* and C57BL/6 X CBA mice (Figure 5.02), but there was a significant difference between right ventricular absolute weights and also when expressed as ratio of RV: LV+S (Figures 5.02 and 5.03).

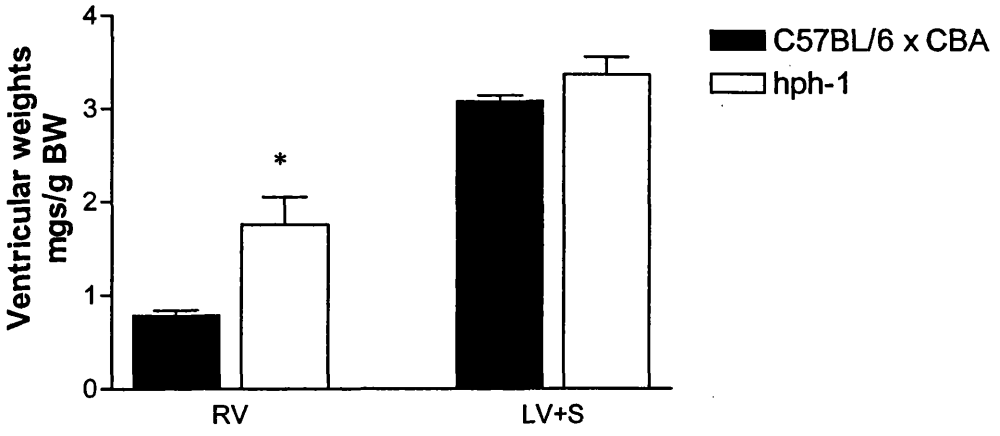

Figure 5.02 Corrected ventricular weights for C57BL/6 X CBA and *hph-1* mice.
*p=0.0083. RV weights *hph-1* vs C57BL/6 X CBA; n=6.

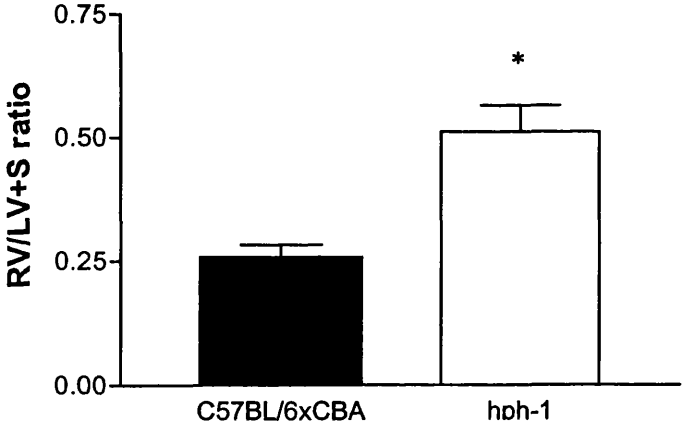

Figure 5.03 Right ventricular (RV) : Left ventricular (LV) plus septum (S) ratio for C57BL/6 and *hph-1* mice.
*p=0.0015, C57BL/6 X CBA vs *hph-1*; n=6

Alpha actin immunostained lung sections obtained from both *hph-1* and C57BL/6 X CBA mice were studied using a light microscope (x40 magnification; Zeiss Axioskop2, UK) and resistance arteries at the level of the alveolar duct (AD), respiratory bronchiole (RB) and terminal bronchiole (TB) (See Figure 1.01) were identified anatomically. In order to confirm that vessels were correctly identified, the mean lumen areas and derived lumen diameters were calculated and have been expressed graphically in figures 5.04a and b. The lumen areas of vessels at the level of the AD typically fell around 1000μm^2 and that for the RB 1400μm^2 and the TB around 2000μm^2 and there were no significant differences in lumen area at each level (AD, RB, TB) between the *hph-1* and the C57BL/6 X CBA mice; lumen diameters were derived from the areas giving the mean lumen diameter of vessels associated with the AD of 30μm, RB of 40μm and TB of 50μm, and again there was no significant different in lumen diameter between the C57BL/6 X CBA and *hph-1* at all three levels.

Percentage wall area was subsequently assessed, by measuring the area of alpha smooth muscle actin staining in each of the resistance vessels. Figure 5.05a illustrates that the percentage wall area in all vessels from *hph-1* mice is greater than in C57BL/6 X CBA mice, with a highly significant difference in the vessels associated with the AD (Figure 5.05 a and b).

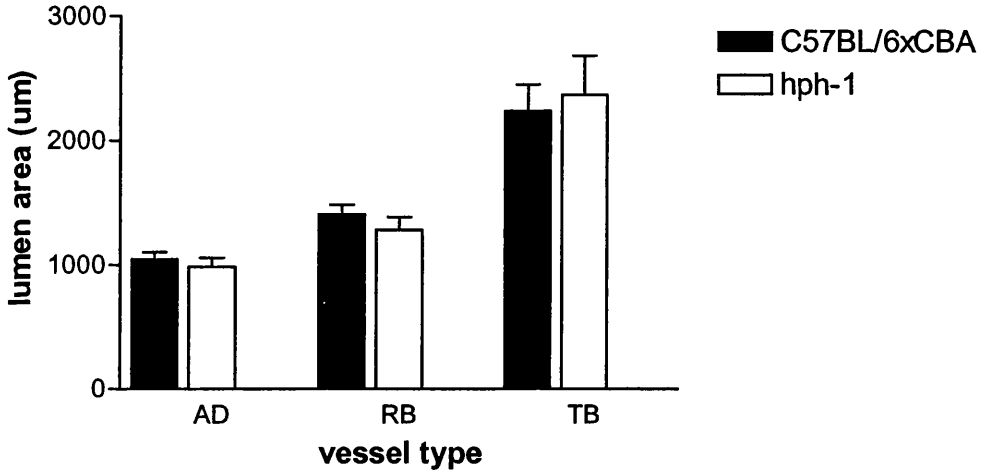

Figure 5.04a Lumen areas for resistance arteries at the level of the AD (alveolar duct), RB (respiratory bronchiole) and TB (terminal bronchiole) in hph-1 and C57BL/6 mice. p=ns, *hph-1* vs. C57BL/6 X CBA; n=6.

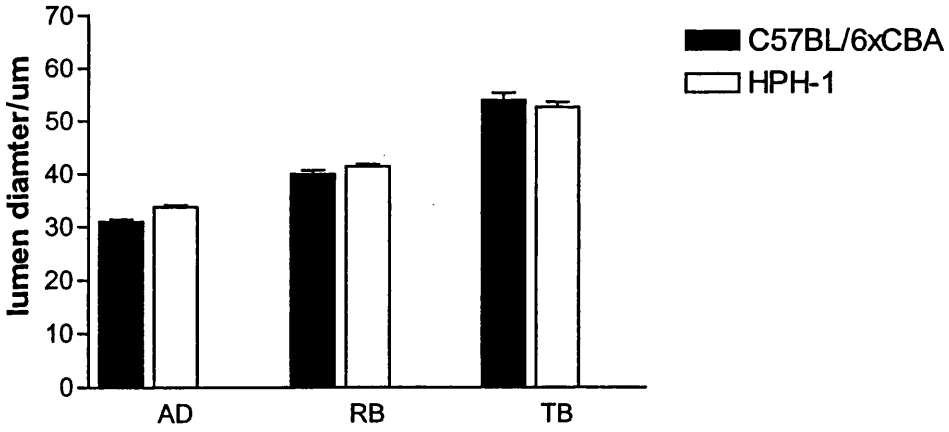

Figure 5.04b Derived lumen diameters for resistance arteries at the level of the AD (alveolar duct), RB (respiratory bronchiole) and TB (terminal bronchiole) in C57BL/6 and *hph-1* mice. P=ns, *hph-1* vs. C57BL/6 X CBA; n=6.

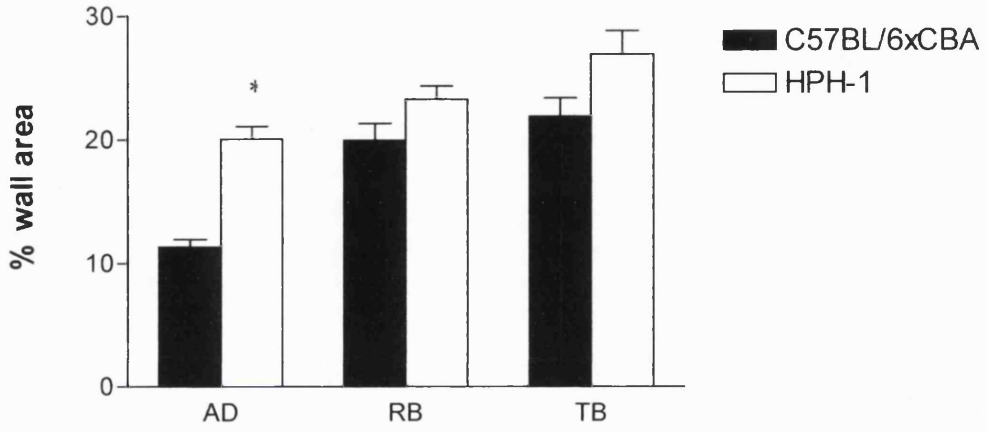

Figure 5.05a Percentage wall area of resistance arteries at the level of the AD,RB and TB in C57BL/6 and *hph-1* mice.
*p=0.0021 *hph-1* vs. C57BL/6 X CBA.

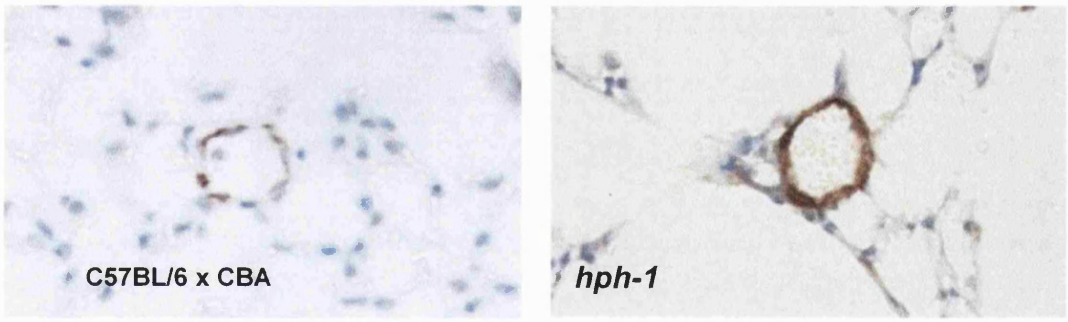

Figure 5.05b Alpha actin smooth muscle staining on lung sections from C57BL/6xCBA and *hph-1* mice (X40 magnification). Both images show an artery associated with an AD and it can be seen that the smooth muscle area is greater in the *hph-1* compared to the C57BL/6xCBA.

Finally, figure 5.06 illustrates the relative proportions of pre-capillary arteries, identified using standard light microscopy, at the level of the alveoli that were either non muscular (no actin staining), partially muscular (<75% circumferential actin staining) or fully muscular (100% actin circumferential staining). There were a significantly lower proportion of non-muscular vessels in the *hph-1* compared with the C57BL/6 X CBA mice, and a significantly higher proportion of partially muscular and fully muscular vessels in the *hph-1* mice compared with the C57BL/6 X CBA.

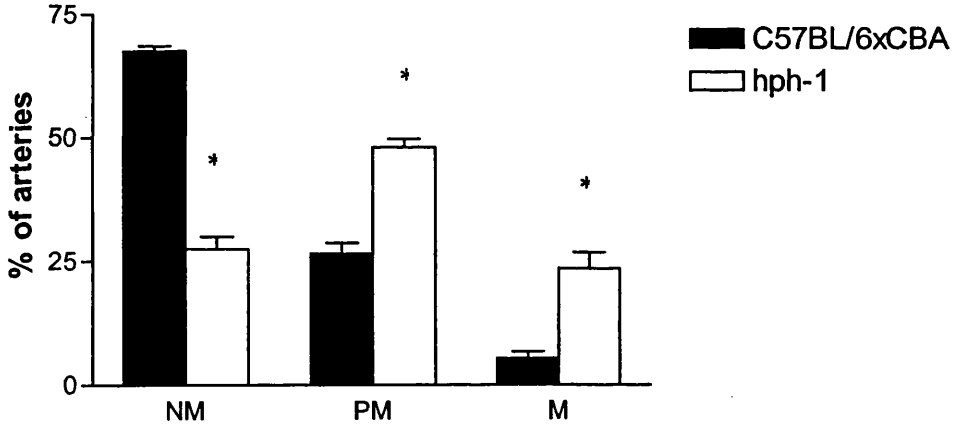

Figure 5.06 Percentage of arteries at the level of the alveoli that are non muscular (NM), partially muscular (PM) or fully muscular (M) in C57BL/6 and *hph-1* mice. *p= <0.0001 (NM), 0.0037 (PM) and 0.0062 (M) *hph-1* vs. C57BL/6 X CBA; n=6

5.05 Discussion

The results from this chapter indicate that mice deficient in GTP-CH1/BH_4 develop pulmonary hypertension. All three structural characteristics of pulmonary hypertension (i.e. right ventricular hypertrophy, increased smooth muscle wall area of resistance arteries and extension of muscle into normally non muscular arteries) are present in the *hph-1* mice when compared with the wild type C57BL/6 X CBA. These results are somewhat surprising as NOS has a much higher affinity for BH_4 than the aromatic amino acid hydroxylases and hence it would not be expected that the partial deficiency in BH_4 present in *hph-1* mice would be sufficient enough to affect NOS activity in these animals. However impairment of the NO/cGMP pathway has been documented in cerebellar slices from the *hph-1* mouse (Brand *et al.*, 1996) and furthermore there is evidence to suggest decreased binding of BH_4 to brain NOS in the *hph-1* mice *in vivo* (Brand *et al.*, 1995). Canevari *et al.*, (1999) more recently, demonstrated diminished NO synthesis (evaluated by measuring cGMP levels) in the brains of *hph-1* mice and showed that acute peripheral BH_4 administration significantly elevated cGMP levels in *hph-1* mice but not in the wild type animals.

This deficiency of BH_4 may render eNOS inefficient and hence contribute towards the development of pulmonary hypertension. Although the results obtained from studying the structure of the pulmonary vasculature and the hearts of the *hph-1* mice and the C57BL/6 X CBA wild types are all indicative of a structural pulmonary hypertensive phenotype, *in vivo* haemodynamic measurements will be necessary to confirm these findings. It would be expected that heart rate and right ventricular pressures would also be elevated in the *hph-1* mice compared to the C57BL/6 X CBA.

Table 5.01 summarises body, heart and lung weights. The body weights of the C57BL/6 X CBA mice were significantly higher (p = 0.0005) than the *hph-1* mice whilst corrected heart weights (p=<0.0001) and corrected (p=0.0006) and absolute (p=0.0153) lung weights were significantly higher in the *hph-1* mice compared to the C57BL/6 X CBA wild type. Cosentino *et al.*, (2001) found no significant difference in body weights between 8 week old *hph-1* and C57BL/6 X CBA mice and whether a difference occurs after 8 weeks of age is yet to be determined, although it may be possible that variations in animal colonies and husbandry may account for these inconsistent findings. The increase in heart weight may be due to right ventricular hypertrophy and it seems that overall the *hph-1* mice have larger lungs compared to the wild type C57BL/6 X CBA.

By examining figures 5.02 and 5.03 it can be seen clearly that the *hph-1* mice only develop right ventricular hypertrophy (as determined by the RV: LV + S ratio) but not left ventricular hypertrophy, signifying pulmonary hypertension but not systemic hypertension. This detection of right ventricular hypertrophy, but absence of left ventricular hypertrophy in the *hph-1* mouse has now recently also been confirmed by an independent group (Channon, personal communication). There is evidence in the literature demonstrating increased sensitivity of the pulmonary vasculature to changes in NOS activity when compared with the systemic vasculature in a canine (Cases *et al.*, 2001) and porcine model (Licker *et al.*, 1998) and that inhibition of NOS results in an often profound increase in pulmonary arterial pressure (Fineman *et al.*, 1991; van Gelderen *et al.*, 1993). Taken together these studies suggest that the potential dysfunction of eNOS resulting from BH_4 deficiency in the *hph-1* mouse only affects the pulmonary vasculature and that there may be other

compensatory mechanisms within the systemic vasculature to overcome the deleterious effects of NO reduction.

Abnormal pulmonary vasoconstriction and vascular remodelling occurring in response to a variety of stimuli (e.g. hypoxia) are the characteristics of pulmonary hypertension leading to increased pulmonary vascular resistance and elevated pulmonary artery pressure. Abnormal vasoconstriction becomes progressively less important and vascular remodelling becomes more important as the disease advances (Reeves *et al.*, 1986). The endothelium plays a vital role in pulmonary vascular remodelling via the release of a number of vasoactive mediators including NO and PGI_2 which are known to have antimitogenic and antiproliferative effects on pulmonary artery smooth muscle cells (Thomae *et al.*, 1995, Wharton *et al.*, 2000), indeed pulmonary hypertension is associated with impaired production of NO and PGI_2. NO and PGI_2 have also been reported to inhibit the production of growth factors including ET-1 from endothelial and smooth muscle cells (Wort *et al.*, 2000, Kourembanas *et al.*, 1993). It is known that basal release of NO contributes to the normally low pulmonary vascular tone in normoxia and impaired NO production reduces the ability of the pulmonary vasculature to relax and favours the occurrence of excessive pulmonary vasoconstriction and, along with the loss of antiproliferative and antimitogenic effects, may contribute to the development of increased pulmonary vascular resistance.

The *hph-1* mice studied have an increased smooth muscle wall area (Figure 5.05) with no apparent change in lumen area or diameter[5], at all three levels of arteries studied, compared

[5] Lumen diameter has been derived from lumen area and assumes the vessel is perfectly circular.

to the C57BL/6 X CBA wild types (Figure 5.04a and b) and furthermore the extension of muscle into normally non muscularised pre-capillary arteries was significantly higher in the *hph-1* mice compared to the C57BL/6 X CBA wild types (Figure 5.06). These structural changes are likely to lead to a number of physiological effects. The increase in smooth muscle wall in the resistance arteries and extension of muscle into normally non-muscularised precapillary arteries, will result in augmented increases in wall tension in response to contractile stimuli. In remodelled vessels there is an increase in the wall to lumen ratio (which has been observed in the *hph-1* mice) which means that any active contraction of the smooth muscle will cause a greater increase in vascular resistance than that caused by the same level of contraction induced in a normal unremodelled vessel (with lower wall to lumen ratio) in response to a vasoconstrictor (Folkow 1971). Furthermore, increased muscularisation during remodelling often causes narrowing of the lumen area (although this has not been observed in this study) and even if this narrowing is very small, the effect on increasing pulmonary vascular resistance will be large, predicted mathematically by Poiseuille's Law which states that resistance to the steady laminar flow of fluid along a straight cylindrical tube is proportional to the tube length, fluid viscosity and inversely proportional to the tube radius raised to the fourth power.

To date, only one study has been performed on the *hph-1* mice directly investigating the effects of BH_4 deficiency on eNOS in the vasculature. Cosentino *et al.*, (2001) measured intracellular BH_4 levels and constitutive NOS activity in isolated aortas and these were significantly lower in the aortas of the *hph-1* mice vs. wild type, with the NOS activity being restored in the presence of exogenous BH_4 to levels comparable to wild type mice.

Functionally the aortas contracted to noradrenaline to the same extent in both the *hph-1* and the C57BL/6 X CBA but relaxations to ACh were greater in the *hph-1* mice compared with the C57BL/6 X CBA an effect concluded to result, in part, from H_2O_2 mediated relaxation in the *hph-1* mice, (occurring as a result of BH_4 deficient eNOS generating O_2^- and subsequent conversion to H_2O_2 and O_2 by endogenous SOD).

Overall, the results in this chapter have shown a correlation between BH_4 availability and structural remodelling of the pulmonary vasculature and right ventricle consistent with that occurring in the pathological state of pulmonary hypertension. It appears as though the mutation leading to a marked decrease in GTP-CH1 activity and hence BH_4 availability renders eNOS inefficient and this limits both basal and stimulated NO release. This may, in turn, lead to increased smooth muscle cell proliferation and migration and furthermore promote the production of growth factors including ET-1, which would further contribute towards structural remodelling seen. Inefficient eNOS may also generate harmful O_2^- which in turn may increase the catabolism of any NO released thereby creating a vicious circle causing further remodelling as a result of limited NO. Overall these structural effects have the effect of increasing pulmonary vascular resistance, which in turn causes right ventricular hypertrophy. The evidence in the literature, that the lung is more sensitive to changes in NOS activity supports the apparent absence of any effect in the systemic vasculature (although further studies on the systemic vasculature are necessary to confirm this).

In conclusion, it appears that the GTP-CH1/BH_4 pathway is important in the regulation of pulmonary vascular tone and that a deficiency of BH_4 (as observed in the *hph-1* mouse mutant) results in a structural pulmonary hypertensive phenotype.

CHAPTER 6

Regulation of GTP-cyclohydrolase 1 by GTP-cyclohydrolase 1 feedback regulatory protein

6.01 Introduction

Previous chapters identify that loss of BH_4 is likely to be associated with pulmonary hypertension but that GTP-CH1 expression is normal, at least in the porcine model. An alternative cause of deficient BH_4, may be changes in the GTP-CH1 feedback regulatory protein (GFRP). GTP-CH1 forms a complex with GFRP, the activity of which is regulated by the relative concentrations of BH_4 or phenylalanine, where BH_4 promotes the formation of the inhibitory complex (thereby limiting BH_4 biosynthesis) and phenylalanine promotes the formation of a stimulatory complex, upregulating BH_4 synthesis (Harada *et al.*, 1993). Deficiency of BH_4 has been implicated as a mechanism of NOS dysfunction in a wide range of disease states but whether GFRP can regulate NO production *in vivo*, is not known and it may be possible that alterations in the expression of GFRP may be implicated in BH_4 availability *in vivo*. The aim of the present study was to investigate whether BH_4 and NO production from both eNOS and iNOS could be regulated in an endothelial cell line in culture, by stably overexpressing GFRP.

Hypothesis

GFRP over expression will reduce intracellular BH_4 levels and nitrite production from sEnd 1 cells both pre and post cytokine + LPS treatment.

Figure 6.01 represents the predicted system resulting from over expression of GFRP. Essentially, the system predicts that GFRP in excess will result in GFRP and GTP-CH1 forming a predominantly inhibitory complex, thereby limiting BH_4 biosynthesis and hence reducing or preventing the activation of NOS. The two outcomes to be measured will be

NO generation (a correlate of nitrite (NO_2^-) production) from eNOS (basal) and NO generation from iNOS (post cytokine + LPS treatment). It would be predicted that this GFRP over expressing cell line would effectively be a model of BH_4 deficiency and that intracellular BH_4 levels and released NO levels should be diminished in these cell lines compared with the mock transfected control lines.

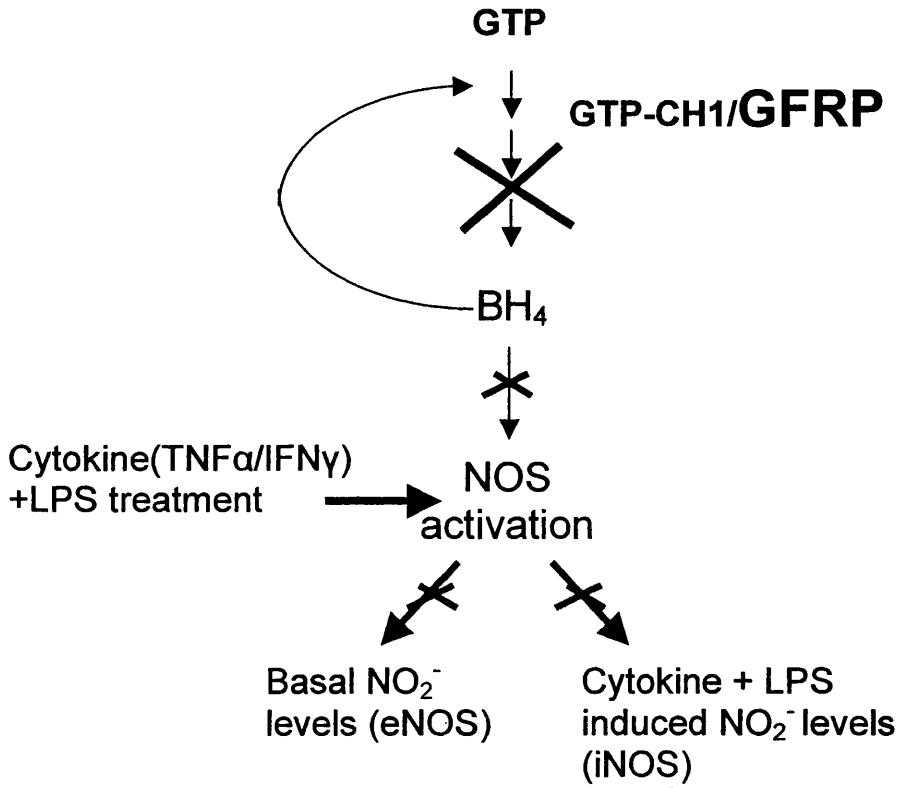

Figure 6.01 Predicted schematic representation of study, over expression of GFRP should limit BH_4 biosynthesis and hence NOS activation.

6.02 Methods and protocols

The human protein sequence of GFRP was analysed using the HGMP database and showed 95% sequence homology with the murine GFRP sequence (figure 6.02). Given this information, we would predict that human GFRP would have the same physiological effects as murine GFRP.

```
Human: 1   MPYLLISTQIRMEVGPTMVGDEQSDPELMQHLGASKRRALGNNFYEYYVDDPPRIVLDKL
           MPYLLISTQIRMEVGPTMVGDE SDPELMQHLGASKR  LGNNFYEYYV+DPPRIVLDKL
Mouse: 1   MPYLLISTQIRMEVGPTMVGDEHSDPELMQHLGASKRSVLGNNFYEYYVNDPPRIVLDKL

Human: 61  ERRGFRVLSMTGVGQTLVWCLHKE 84
           E +GFRVLSMTGVGQTLVWCLHKE
Mouse: 61  ECKGFRVLSMTGVGQTLVWCLHKE 84
```

Figure 6.02 Amino acid sequence alignment for human GFRP and murine GFRP showing 95% sequence homology.

Chapter 2 describes in detail all materials and methods used in this study. Briefly, human GFRP cDNA was synthesized and amplified by PCR with an N-Myc residue and ligated with the hygromycin resistant mammalian expression vector pcDNA 3.1 Hygro. This construct was then transfected into the murine endothelial cell line sEnd 1 (donated by Dr E Wagner, Institute of Molecular Pathology, Vienna) (Williams *et al.*, 1988). The negative controls used in this study were mock-transfected empty vector cells (i.e. pcDNA 3.1 Hygro vector without GFRP insert). Successfully transfected cells (both GFRP and mock transfected) were selected using Hygromycin B supplemented cell culture medium. Individual colonies were selected and presence of the N-Myc GFRP insert in transfected cells confirmed by western blotting using the 9E10 anti Myc antibody.

NO_2^- production was measured from cells basally (as a correlate of NO generated by eNOS) and following cytokine + LPS treatment (as a correlate of NO generated by iNOS) using the Greiss assay, and intracellular BH_4 levels were measured using HPLC and electrochemical detection. In addition, the expression of iNOS message and protein in mock transfected and GFRP transfected cells lines pre and post cytokine + LPS treatment were measured using SDS-PAGE, Western blotting and PCR.

iNOS induction – cytokine+LPS treatment

Cells were treated with a cocktail of cytokines + LPS in order to induce iNOS expression. GFRP and mock-transfected cells were grown in quadruplicate in 24 well plates until 70-80% confluent. Media was removed from each well, the cells washed with two washes of PBS and replaced either with fresh media containing 10ng/ml Tumour Necrosis Factor α (TNF α), 100U/ml (R&D systems) Interferon gamma γ (IFN γ) (R&D systems) and 5μg/ml Lipopolysaccaride (LPS) (Sigma) in order to induce iNOS, or unsupplemented medium. After 20 hours incubation, 100μl of media from both treated and untreated wells, was transferred to a clear 96 well plate. Adherant cells were lysed with RIPA buffer (appendix) and total cellular protein determined in order to control for cell number using a standard protein assay.

Detection of GTP-CH1 and GFRP pre and post cytokine + LPS treatment in untransfected sEnd 1 cells.

To assess the effects of cytokine + LPS treatment on GTP-CH1 and GFRP message in sEnd 1 cells, PCR amplification was performed on cDNA prepared from RNA extracted from sEnd 1 cells pre and post cytokine + LPS treatment using oligonucleotide primers designed in the murine GTP-CH1 [Forward: GCTGCTTACTCGTCCATTCT] [Reverse: CGCATTACCATGCACATGTG] (94°C 10 secs; 56°C 10 secs; 72°C 30secs) and GFRP [Forward:ATAGTCCTGGACAAGCTGGAAT],[Reverse:GGGAGTTGACAATTTGGA AAGA] sequences (HGMP database), (94°C 10 secs; 60°C; 72°C 30 secs). Bands were visualised using a UV transillumintor.

Expression of Myc tagged protein in GFRP over expressing cell lines

In order to establish that Myc-tagged protein was detectable in cell lines that were transfected with the N-Myc-GFRP pcDNA 3.1 construct and that mock transfected pcDNA 3.1 control sEnd 1 cells did not contain any Myc protein, standard SDS-PAGE and Western blotting were performed. Briefly, 15μg of protein per well, for each cell line (4 GFRP and 2 mock transfected) was loaded onto a 12.5% SDS-PAGE gel. Following transfer to a nitrocellulose membrane and blocking in 5% milk in PBST, membranes were incubated for 2 hours at RTP with the primary antibody, anti N-myc antibody 9E10 (1:1000 in PBST). Following subsequent washing, a 1 hour incubation at RTP using the secondary antibody HRP-linked anti mouse antibody (1:3000 in PBST) (Amersham) was performed and signals were developed using ECL Plus (Amersham).

Analysis of the effects of GFRP over expression on NO production

GFRP and mock transfected sEnd 1 cells were grown in quadruplicate in 24 well plates until 70-80%confluent. Media was removed from each well and replaced either with fresh media containing cytokines and LPS in order to induce iNOS, or unsupplemented medium. After 20 hours incubation, the media was again removed. Adherant cells were lysed with RIPA buffer and total cellular protein determined in order to control for cell number. Total nitrite content of cell media plus/minus cytokine + LPS treatment was measured colormetrically using the Greiss Assay as described in chapter 2.

Measurement of iNOS protein expression

2 GFRP lines and 2 mock-transfected lines were grown to 70-80%confluence in 10cm^2 petri dishes and treated with either cytokine + LPS or unsupplemented media. Cells were subsequently washed, resuspended in RIPA buffer and assayed for protein content. Standard SDS-PAGE and Western blotting using an iNOS primary antibody (1:1000 dilution in PBST) (Insight) and donkey anti rabbit secondary antibody (1:3000 dilution in PBST) (Insight) were performed and iNOS immunoreactivity visualised using the ECL plus detection system.

Determination of INOS message in GFRP over expressing and mock-transfected cell lines

In order to demonstrate that clonal selection had not resulted in the selection of cell lines with low levels iNOS messenger RNA, PCR amplification was performed. First strand cDNA synthesis was performed on RNA extracted (Trizol) from cell pellets harvested in PBS from 10cm^2 petri dishes plus/minus cytokine + LPS treatment, from both GFRP over expressing and mock transfected cell lines. Subsequent PCR amplification using 2 oligonucleotide primers complementary to the murine iNOS sequence (HGMP) [forward CAC CTT GGA GTT CAC CCA GT], [reverse ACC ACT CGT ACT TGG GAT GC] (94°C,10secs; 60°C, 10 secs; 72°C 30 secs) was performed. To correct for loading, PCR amplification was performed on the same samples using 2 oligonucleotide primers complementary to the murine alpha actin sequence (HGMP) [forward CTG ACA GAG GCA CCA CTG AA], [reverse CAT CTC CAG AGT CCA GCA CA] (94°C,10secs; 56°C, 10 secs; 72°C 30 secs). Samples were loaded onto a 2% (w/v) agarose gel and bands were visualised using a UV transilluminator.

Analysis of BH_4 levels in GFRP over expressing and mock transfected cells

GFRP over expressing and mock transfected cell lines were grown to 70-80% confluence in 75cm^2 flasks and each cell line treated with cytokines plus LPS or unsupplemented media. Cells were washed and harvested in 200μl of PBS and 20 μl of the suspension removed for protein assay. The remaining 180 μl was centrifuged at maximum speed for 5 minutes at 4°C and the pellet resuspended in an extraction buffer containing 0.1M perchloric acid (BDH), 6.5mM dithioerythritol (Sigma) and 2.5mM DETAPAC (iron chelator) (Sigma) and centrifuged at maximum speed for 5 minutes at 4°C and the supernatent loaded straight (due to the labile nature of BH_4) onto the HPLC coupled to an electrochemical detector for analysis of BH_4 (as described in chapter 2).

6.03 Data analysis

Greiss assays

Nitrite production from cell lines both basally and post cytokine + LPS treatment was measured using the Greiss assay were calculated as a percentage of the mixed population of pcDNA 3.1 mock transfected cells (pcDNA 1) for each experiment. The mean±SEM for all experiments (n=5) on each cell line was subsequently calculated. Statistical significant differences in nitrite levels between GFRP and mock transfected sEnd 1 cells both basally and post cytokine + LPS treatment were determined using an unpaired Two tailed T-test.

Analysis of BH_4 measurements

Intracellular BH_4 levels from GFRP overexpressing and mock-transfected cells were determined using electrochemical detection. Values were corrected for protein yielding mean±SEM values of pmol/mg protein. Statistical analysis was performed using an unpaired two tailed T-test to compare basal and cytokine + LPS treated levels of BH_4 for each individual cell line and to compare basal and cytokine + LPS treated levels of BH_4 between cell lines (i.e. GFRP overexpressing vs. mock transfected control).

6.04 Results

In the following results pcDNA 1 corresponds to a mixed population of mock transfected control cells, pcDNA 2 corresponds to a single colony of mock transfected cells and B1, C1, C5 and C12 all correspond to GFRP-Myc transfected cell lines.

Cloning of GFRP

As described in chapter 2, GFRP was initially cloned into pCR2.1-TOPO and this was used as a template for the subsequent PCR amplification and ligation into pcDNA 3.1 Hygro. Both GFRP inserts (i.e. in pCR2.1-TOPO and pcDNA 3.1 Hygro vector) when sequenced, shared at least 99.6% homology with the published human GFRP sequence, demonstrating that cloning had been successful.

Effects of cytokine + LPS treatment on GTP-CH1 and GFRP in sEnd 1 cells

PRC amplification of cDNA extracted from untransfected sEnd 1 cells pre and post cytokine + LPS treatment gave rise to the gel image depicted in Figure 6.03. GTP-CH1 and GFRP are expressed basally in sEnd1 cells and cytokine + LPS treatment increased GTP-CH1 levels and decreased GFRP levels.

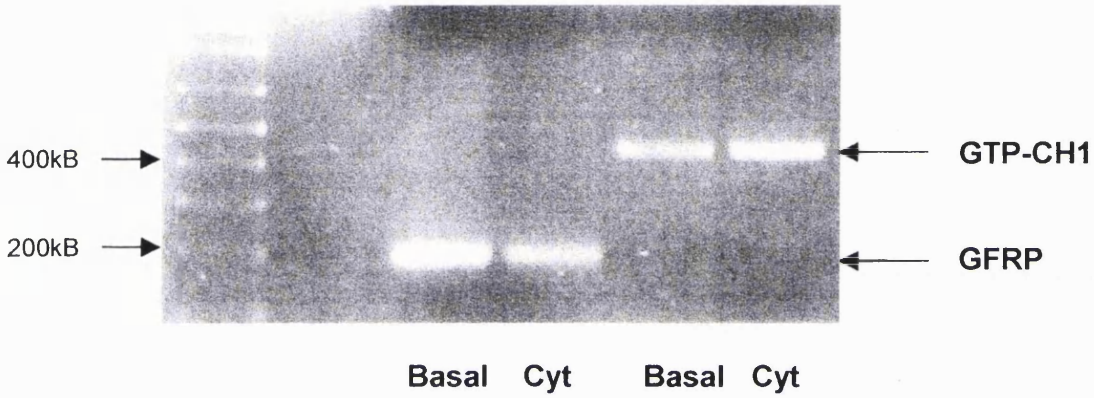

Figure 6.03 – Gel image of PCR products following PCR amplification of cDNA extracted from untransfected sEnd 1 cells (pre (basal) and post (cyt) cytokine + LPS treatment) using either GTP-CH1 or GFRP oligonucleotide primers.

Transfection of sEnd 1 cells

Successful transfection of either the N-Myc-GFRP-pcDNA 3.1 Hygro construct or the empty vector (pcDNA 3.1 Hygro) control into sEnd 1 cells and subsequent selection for five days using 500μg/ml Hygromycin supplemented media, resulted in cell death of all untransfected cells and survival of transfected cells which formed colonies over a period of 2-3 days. These colonies were then picked and expanded and all appeared to replicate at equal rates (i.e. GFRP over expression did not appear to significantly alter cell division). Confirmation of Myc protein expression in all predicted GFRP transfected cell lines was demonstrated by western blotting using the Myc antibody (Figure 6.04) The band at approximately 12 kDa corresponds to the GFRP protein (~9.5kDa) plus the Myc tag, (~1-2kDa). No immunoreactive band was detectable in the mock transfected and untransfected cells. It can be seen that there is clonal variation in the amount of MycTagged protein present in the cells, where the highest protein expression appears to be in B1> C12> C1 > C5.

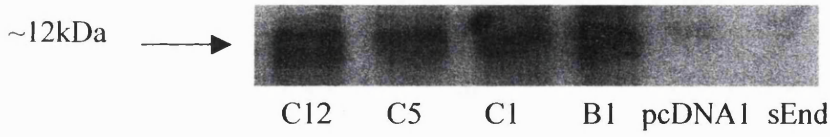

Figure 6.04 Representative immunoblot showing immunoreactive band at approximately 12kDa corresponding to Myc + GFRP. B1, C1, C5 and C12 correspond to GFRP over expressing cell lines whilst pcDNA corresponds to a mock transfected cell line and sEnd 1 corresponds to the native untransfected cell line.

Measurement of nitrite basally and post cytokine + LPS treatment

Cytokine + LPS treatment resulted in an increase in nitrite levels in all cell lines, with nitrite levels in mock transfected cells, typically reaching 5 μM (basally) and 40μM (post cytokine + LPS treatment), consistent with published findings (Leiper *et al.*, 2002). By studying figure 6.05, it can be seen that there is no significant difference in basal (pre cytokine + LPS) nitrite levels in all 6 cell lines studied. Interestingly Figure 6.05 illustrates a statistically significant reduction in nitrite production post cytokine + LPS treatment, in the GFRP overexpressing cell lines compared with the mock-transfected cell lines. Values have been calculated as a percentage of the nitrite production in the mock-transfected mixed colony population.

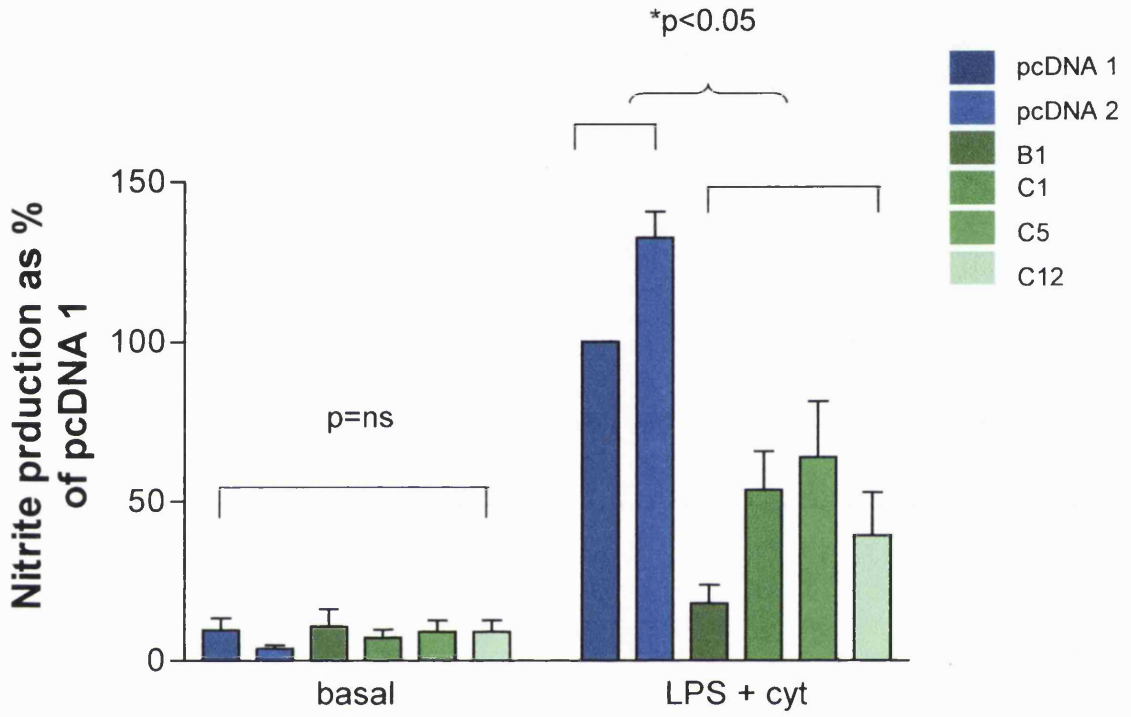

Figure 6.05 Nitrite production from GFRP over expressing and mock transfected cells as measured by Greiss assay, both basally and post cytokine + LPS treatment. *p<0.05 One Way ANOVA with Tukey Kramer post hoc test; n=5. Nitrite values are significantly higher in mock transfected control cells (blue bars) compared to GFRP over expressing cells (green bars) post cyrokine + LPS treatment.

iNOS protein expression

Western blotting for iNOS was performed on cell homogenates from cell lines B1 and C12 (GFRP overexpressing) and pcDNA 1 and pcDNA 2 (mock transfected) pre and post cytokine + LPS treatment. The immunoblot shown in figure 6.06 shows no detectable iNOS protein in all cell lysates without cytokine + LPS treatment, as would be expected, but detectable iNOS protein in lysates obtained post cytokine + LPS treatment. iNOS protein expression is much lower in both GFRP (very low levels in B1 following longer autoradiogram exposure) cell lysates post cytokine + LPS treatment compared with the mock-transfected lines.

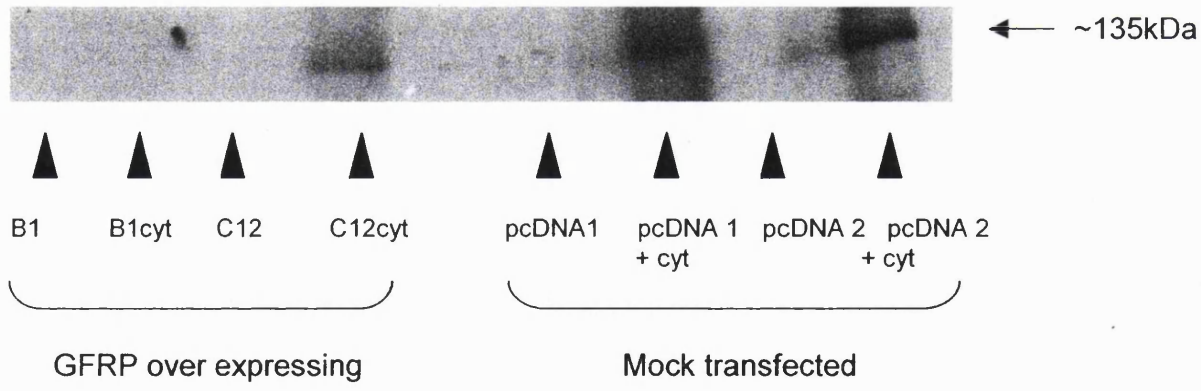

Figure 6.06 Immunoblot showing immunoreactive bands corresponding to iNOS. Bands are only detectable in cells treated with cytokine + LPS (cyt) and protein expression is reduced in B1 and C12 compared with pcDNA 1 and pcDNA 2 (n=2).

iNOS mRNA measurements

It was essential to check that iNOS messenger RNA was present in equal concentrations in the both GFRP over expressing and the mock transfected, as it may have been possible that clonal selection resulted in cell lines with reduced iNOS message being chosen. RNA was extracted from cells B1,C5, C12, pcDNA 1 and pcDNA 2 cells pre and post cytokine + LPS treatment using Trizol reagent. cDNA prepared (using RT beads) from extracted RNA was subsequently PCR amplified using iNOS and alpha actin primers (described in the earlier protocol section). Figure 6.07 shows a gel image illustrating the presence of iNOS message in all 5 cell lines post cytokine + LPS treatment with none being detactable in untreated cells. Alpha actin bands are present in all PCR reactions and there were no obvious differences in loading.

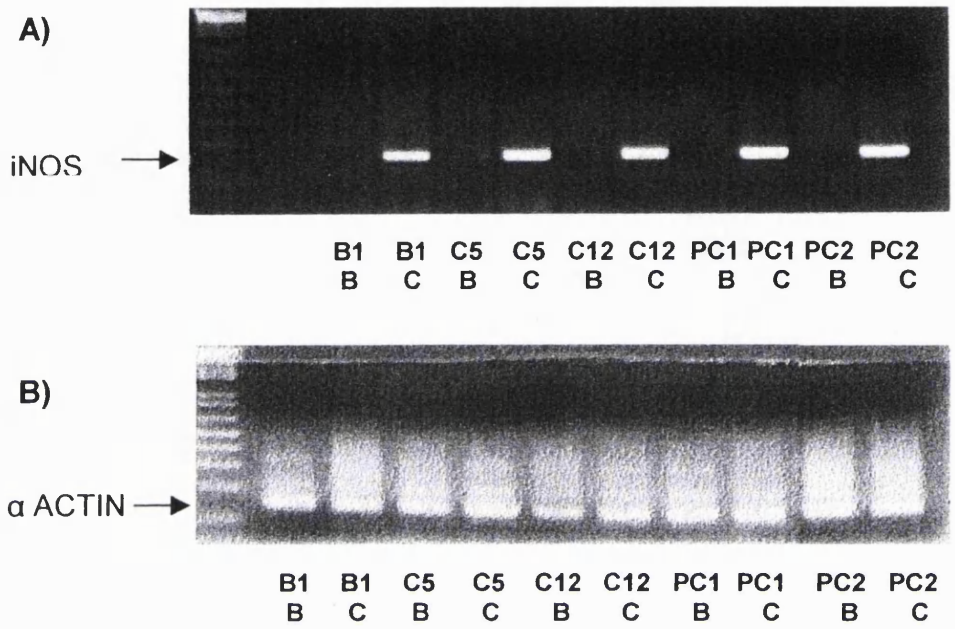

Figure 6.07 Gel image of showing products obtained following PCR amplification using A) iNOS oligonucleotide primers and B) alpha actin oligonucleotide primers on cDNA extracted from 3 GFRP over expressing cell lines (B1, C5 and C12) and 2 mock transfected control lines (pc1 and pc2), with (C) and without (B) cytokine + LPS treatment (n=2).

BH_4 measurements

To investigate the effects of GFRP over expression on intracellular BH_4 levels, BH_4 was extracted from 2 GFRP over expressing (B1 and C12) and two mock transfected control (pcDNA 1 and pcDNA 2) cells, basally and following cytokine+LPS treatment. Figure 6.08 illustrates an increase in nitrite levels (and hence successful iNOS induction) following cytokine + LPS stimulation. Figure 6.09a depicts a typical trace as measured by electrochemical detection on the HPLC, where BH_4 elutes at approximately 6.5 minutes. Figure 6.09b illustrates the data obtained from the cell lysates, showing a trend towards an increase in intracellular BH_4 levels following cytokine+LPS stimulation in all cell lines studied, although the difference was not statistically significant. There is no significant difference in intracellular BH_4 levels in GFRP overexpressing compared to mock transfected cells both with and without cytokine+LPS treatment.

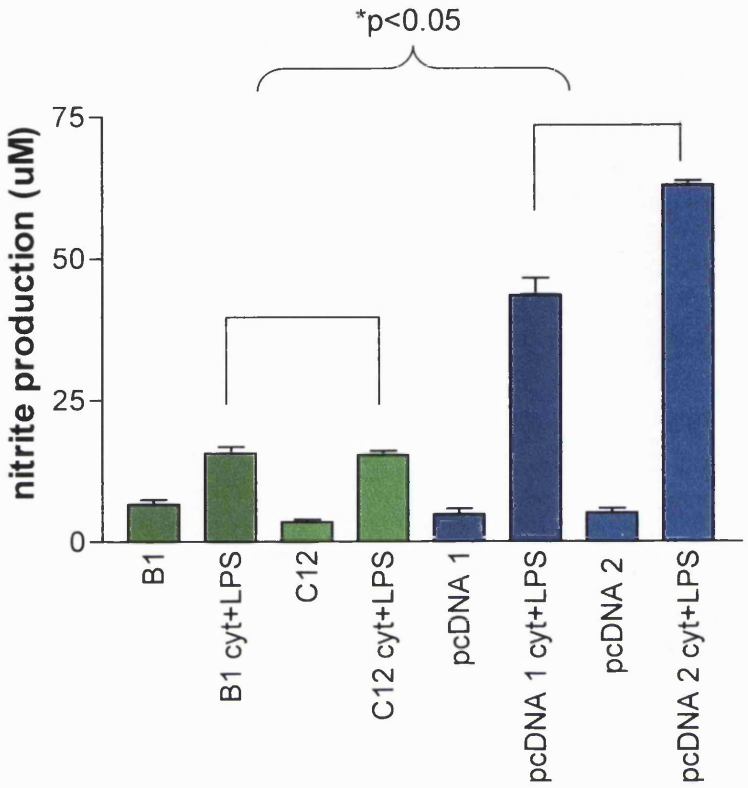

[6]**Figure 6.08** Nitrite production in GFRP over expressing (B1, C12) and mock transfected (pcDNA 1 and 2) cells with and without cytokine+LPS treatment. *p<0.05 Two tailed unpaired T-test (GFRP over expressing (green bars) vs. mock transfected control cells (blue bars) post cytokine+LPS treatment) n=3

[6] C12 cells were treated with cytokines+LPS on a different day compared with B1, pcDNA 1 and pcDNA 2, due to reduced confluency on the first day of treatment. This may explain the discrepancy with Figure 6.05, where nitrite levels are lower in B1 compared to C12 following cytokine+LPS stimulation.

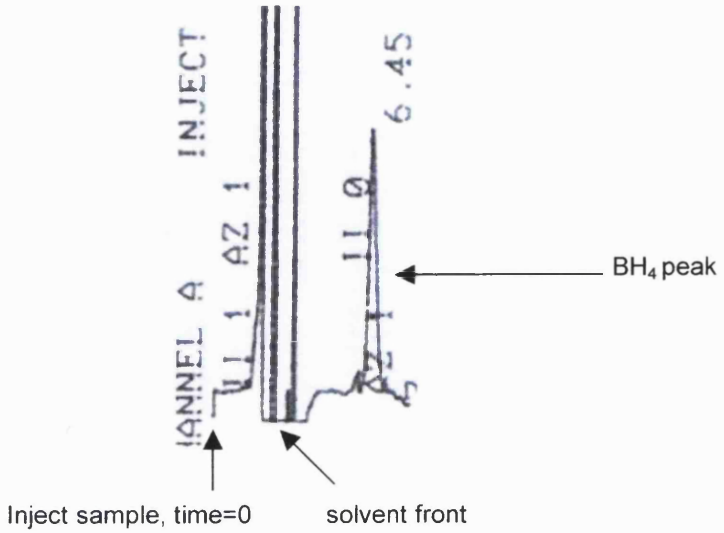

Figure 6.09a Typical trace obtained from cell lysates depicting a distinct BH_4 peak at 6.45 minutes as measured by HPLC using electrochemical detection.

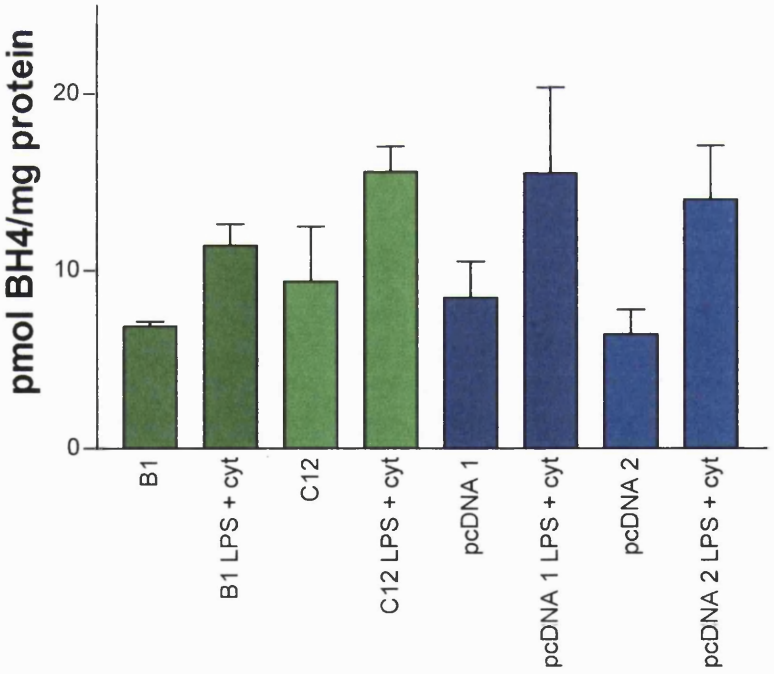

Figure 6.09b Intracellular BH_4 levels in GFRP overexpressing cells (green bars) and mock transfected control cells (blue bars) with and without cytokine+LPS treatment. (p<ns One Way ANOVA with Tukey Kramer post test) n=3

6.05 Discussion

This chapter has provided preliminary evidence that GFRP over expression has the ability to alter nitrite generation following cytokine+LPS stimulation, when over expressed in an endothelial cell line (sEnd 1). These studies demonstrate, for the first time, that over expression of GFRP attenuates iNOS mediated nitrite release but has no apparent effect on eNOS derived NO (figure 6.05). Moreover, GFRP transfection levels appear to correlate with this attenuation i.e. cell lines B1 and C12 showed the greatest expression of Myc-tagged protein and also had the greatest effect diminishing NO production post cytokine + LPS treatment (Figs 6.04 and 6.05).

Intracellular BH_4 levels appear to increase following cytokine + LPS stimulation (consistent with published findings) as shown in figure 6.09b. Surprisingly, the intracellular BH_4 levels both basally and following cytokine+LPS stimulation, do not appear to be significantly different between GFRP over expressing and mock transfected control cells.

The most salient finding of this study is that GFRP over expression appears to affect iNOS protein. iNOS protein was greatly decreased in cell lysates obtained from GFRP over expressing cell lines (B1 and C12) compared with mock transfected control cell lines (Figure 6.06) post cytokine + LPS treatment, even though iNOS mRNA was present in all cell lines studied (Fig 6.07a). Once again, the transfection level of Myc tagged protein correlated with the reduction in iNOS protein.

Immunostimulants such as IFN γ, LPS and TNF α have been known to not only induce iNOS but also stimulate pterin synthesis in mammalian cells by potentiating the activity of GTP-CH1 (Nathan 1992; Werner *et al.*, 1998, Werner *et al.*, 1993). A study performed in rat hepatocytes, showed that pre-treatment with an NO donor increased NO production in cells following cytokine stimulation, an effect proposed to occur as a result of elevated BH_4 via suppression of GFRP (Park *et al.*, 2002). It is therefore apparent that the GTP-CH1/GFRP/BH_4 pathway is regulated by cytokines in such a way so as to maximise BH_4 availability for iNOS activation. Indeed figure 6.03 demonstrates the effect of cytokine + LPS stimulation on GTP-CH1 and GFRP in sEnd 1 cells, showing an increase in GTP-CH1 expression and decrease in GFRP expression post cytokine + LPS treatment, consistent with published findings.

In studies in rats treated with LPS, significant elevations have been shown to occur in both plasma biopterin levels alongside a 20 fold elevation in nitrite levels. Moreover, pre-treatment with the GTP-CH1 inhibitor, DAHP, reversed this effect (Gross *et al.*, 1996). Hence, pharmacological GTP-CH1 inhibition has demonstrated functional effects on nitrite production and biopterin levels *in vivo*. It would therefore be predicted that in a GFRP over expressing cell line, this normal increase in BH_4 biosynthesis following cytokine + LPS stimulation would be inhibited, thereby attenuating iNOS generated nitrite. Indeed, figures 6.05 and 6.08 depict this clearly.

The apparent lack of effect on eNOS mediated nitrite release should be treated with caution as nitrite generated by eNOS falls close to the limit of detection of the Greiss assay and hence this may explain the lack of any observed effect of GFRP over expression on eNOS generated nitrite. A more stringent analysis of eNOS generated NO would be to use the more sensitive chemiluminescence assay. The method is based upon the chemiluminescent reaction between NO and the luminol (5-amino-2,3-dihydro-1,4-phthalazinedione)-H_2O_2 system with a limit of detection falling close to 100fM (Kikuchi *et al.*, 1996). This would give a more definitive answer as to whether or not GFRP over expression affects NO generation from eNOS in sEnd 1 cells. However, the effects of GFRP over expression may be iNOS specific if we consider the dependency of the different NOS dimers on BH_4 levels.

There are several lines of evidence to suggest that of all three NOS dimers, iNOS is the least stable and that BH_4 availability seems to be more important for iNOS dimer formation and stabilisation compared with eNOS and nNOS (Venema *et al.*, 1997; Panda *et al.*, 2002; Aoyagi *et al.*, 2001). BH_4 is believed to interact with residues in both subunits of the NOS dimer and also hydrogen bonds to the active site heme. This dimerisation activates NOS in a number of ways including creating high affinity binding sites for L-arginine and allowing electron transfer from the reductase domain flavins to the oxygenase domain heme (Crane *et al.*, 1998; Raman *et al.*, 1998; Panda *et al.*, 2001). Dimerisation of purified heme-containing iNOS monomer is promoted by BH_4 and the stability of the iNOS dimer is enhanced by the bound pterin cofactor. However, BH_4 is not an absolute requirement for dimerisation of all three isoforms of recombinantly overexpressed NOS (Ghosh *et al.*, 1997) although observed BH_4 independent activity of purified NOS could be attributed to substoichiometric

quantities which remain bound to the enzyme after purification (Mayer *et al.*, 1991). A thorough and systematic study conducted by Panda *et al.*, (2002) demonstrated that iNOS dimers were the least stable, and most susceptible to trypsin proteolysis compared to eNOS and furthermore that BH_4 best promoted recoveries of iNOS dimers following urea dissociation and trypsin proteolysis. The three isoforms of NOS thus differ markedly in their strengths and BH_4 requirements, despite their general structural similarity and, as a result, these features may provide the basis for control and regulation of each isoform dependent on their biological environment.

We would predict the mechanism via which GFRP over expression limits iNOS mediated nitrite generation would be by limiting BH_4 availability, as a result of the formation of a predominantly inhibitory complex with GTP-CH1. However, the intracellular BH_4 levels measured pre and post cytokine+LPS treatment in the cell lines studied in this chapter, show no significant difference between GFRP overexpressing and mock transfected control cells. This result is somewhat surprising as there is a consistent attenuation of iNOS mediated nitrite release in the GFRP over expressing cell lines, which correlate with the transfection level. At this stage it is only possible to speculate the reasoning behind this apparent lack of effect on intracellular BH_4 levels in GFRP over expressing cells.

It is possible that the mechanism via which GFRP over expression attenuates iNOS generated nitrite production is via limitation of BH_4 availability for stable iNOS dimerisation following cytokine stimulation. The window during which iNOS is rapidly synthesized may be in the first few hours following cytokine + LPS treatment, and hence

BH_4 levels at this time point may be critical. BH_4 levels in the GFRP over expressing cell lines may not have increased immediately following cytokine + LPS treatment and hence may have only reached suboptimal levels for full iNOS dimerisation. The BH_4 values measured in these cell lines were after a 20 hour cytokine + LPS incubation period, by which time, BH_4 levels in GFRP over expressing cells may have increased to the same level as the mock transfected control cells. It is therefore essential to conduct a time course study on these cells, investigating the BH_4 and nitrite levels at hourly time points following cytokine+LPS treatment, rather than at just one arbitrary time point.

GFRP over expression also may be resulting in sequestration of free intracellular BH_4 thereby reducing BH_4 availability for iNOS activation and hence, although total intracellular BH_4 levels measured would be unchanged, the proportion available for NOS dimerisation may be significantly reduced. Furthermore, GFRP over expression may be inhibiting iNOS mediated nitrite release by some, as yet, unknown mechanism. Further studies are essential to determine, what effects, if any, GFRP over expression is having on the BH_4 levels for NOS activation.

In summary, this chapter has demonstrated a potential functional significance of GFRP over expression in endothelial cells. GFRP over expression appears to affect the NOS pathway although further studies will be required to test this directly and fully characterise these cells in order to confirm the initial findings presented in this chapter. If the findings in this chapter are correct, it may suggest that GFRP over expression may have a specific

inhibitory effect on iNOS, and this in itself could lead to potential therapies for the treatment of inflammatory diseases, such as sepsis.

CHAPTER 7

General discussion

Deficiency of BH_4, an essential cofactor for NOS, is believed to be associated with the pathogenesis of vascular endothelial dysfunction in a variety of disease states and suboptimal levels of BH_4 may be associated with the generation of O_2^- from NOS (Katusic 2001).

Pulmonary hypertension and persistent pulmonary hypertension of the newborn (PPHN) are associated with endothelial dysfunction and impairment of the NO pathway (Jeffery and Wanstall 2001; Adnot 1995; Abman 1999) and it may be possible that increased O_2^- levels generated from dysfunctional NOS may contribute towards this endothelial dysfunction. Furthermore, the GFRP/GTP-CH1 regulatory complex can regulate BH_4 levels, but little data exists regarding the functional effects or clinical implications of GFRP levels *in vivo*.

The work presented in this thesis supports a role of BH_4 and SOD in pulmonary vascular reactivity in the neonatal period and additionally demonstrates the importance of GTP-CH1 levels in the development of pulmonary hypertension. Furthermore a physiological effect of GFRP over expression in endothelial cells has been demonstrated.

Hypercholesterolaemia, hypertension and smoking are all associated with endothelial dysfunction and it is likely that loss of NO biological activity and/or biosynthesis is a central mechanism behind this endothelial dysfunction (Katusic 2001) and there is also evidence that acute administration of BH_4 is able to restore endothelial dysfunction in a number of diseases (Stroes *et al.*, 1997; Ueda *et al.*, 2000; Tiefenbacher *et al.*, 2000). The high capacity of the endothelium to synthesize BH_4 is likely to reflect an important role for this pterin in the regulation of endothelial function (Tsutsui *et al.*, 1996). The role of the GTP-CH1/BH_4 pathway in pulmonary hypertension and in PPHN is currently unknown and one

the aims of this thesis was to try and restore endothelial dysfunction in a model of PPHN and to try and establish whether the GTP-CH1/BH_4 pathway is implicated in the development of PPHN and additionally whether a mutation in GTP-CH1 from birth could contribute towards development of pulmonary hypertension. The studies within this thesis have given an insight into how the regulation of BH_4 by GTP-CH1 and/or GFRP may affect NO generation in a number of systems.

Chapter 3 describes the development of an antipeptide antibody, raised against a conserved surface exposed hydrophilic sequence of GTP-CH1, which was subsequently used to assess the localisation and protein expression of GTP-CH1 in porcine lung samples. This method of utilizing the crystal structure to select an antigenic surface exposed conserved peptide sequence currently appears to be the best method for the development of a GTP-CH1 antibody, as GTP-CH1 antibodies developed by other groups using randomly selected sequences have proven to be far less specific.

The first hypothesis to be tested investigated whether or not sepiapterin and/or MnTMPyP administration could improve endothelium dependent relaxations during the neonatal period and in the adult porcine lung and whether any effects seen could be explained by a developmental regulation of GTP-CH1. This study was loosely based on previous findings that i)BH_4 supplementation using the precursor sepiapterin, when co-administered with SOD improved endothelium dependent relaxations in mature isolated canine middle cerebral arteries (Tsutsui *et al.*, 1996) ii) that catabolism of NO by its reaction with O_2^- may

lead to endothelial dysfunction and iii) suboptimal BH_4 levels may be associated with increased O_2^- generation (Cosentino *et al.*, 1998; Cosentino and Luscher 1999).

Chapter 4 demonstrates a developmental change in GTP-CH1 protein expression, which correlates temporally with the functional effects of supplemented BH_4 in that BH_4 supplementation using the BH_4 precursor sepiapterin resulted in a statistically significant improvement in ACh mediated relaxations in isolated porcine pulmonary arteries at 3 and 14 days of age but not in any other age groups studied (fetal, newborn, 12-24hour and adult) and alongside these functional effects, GTP-CH1 protein expression was low at 3 and 14 days of age. Following MnTMPyP supplementation both alone and in the presence of sepiapterin, ACh relaxations were improved in both 3 and 14 day old animals but not in the other age groups studied. The lack of any additive effect of both agents, suggested that sepiapterin and MnTMPyP were working through the same mechanism and furthermore that reduced BH_4 may lead to increased O_2^- generation. This study has also for the first time shown the localisation of GTP-CH1 protein in porcine lung sections. Immunohistochemistry revealed that GTP-CH1 was predominantly localised to nerves, arterial, pulmonary venous and bronchial smooth muscle and airway epithelial cells and was unchanged developmentally.

The second hypothesis focused on whether there was a change in GTP-CH1 expression in a porcine model of PPHN and whether sepiapterin and/or MnTMPyP administration could reverse the profound endothelial dysfunction seen in the porcine model of PPHN (hypobaric exposure in newborn piglets for 3 days (3H)). This study was based on the previous studies in which BH_4 supplementation restored endothelial dysfunction in a variety

of disease states (Stroes *et al.*, 1997; Ueda *et al.*, 2000; Tiefenbacher *et al.*, 2000). Unlike the 3 day control animals, supplementation of BH_4 and SOD individually, did not improve vascular reactivity, yet significantly improved ACh mediated relaxations when added together in 3H. GTP-CH1 protein expression and localisation were unaffected by hypobaric exposure compared to the age matched control. It therefore appears unlikely that GTP-CH1 contributes to the marked endothelial dysfunction observed in isolated vessels from 3day old animals with PPHN, but does provide evidence that ACh mediated relaxations can be improved by the co incubation of sepiapterin and MnTMPyP, an effect previously unobserved in this animal model. The possible mechanisms via which these two agents in combination may be eliciting an effect are discussed in greater detail in Chapter 4. Further studies investigating the mechanisms via which these agents may be acting when used in combination could lead to alternative therapies for the treatment of PPHN.

Although GTP-CH1 protein expression and localisation appeared unaffected by hypobaric exposure, we decided to investigate the effects of a 90% reduction in the activity of GTP-CH1 from birth, on the pulmonary vasculature of adult *hph-1* mice. The study described in Chapter 5 demonstrates, for the first time, that the *hph-1* mouse model of GTP-CH1 deficiency displays a structural phenotype for pulmonary hypertension, and although haemodynamic measurements are essential to confirm this finding, the right ventricular hypertrophy observed in the *hph-1* mice has now been confirmed by an independent group (Channon and colleagues).

The implications of this finding are that previously undiagnosed pulmonary hypertension may exist in patients where a mutation in the GTP-CH1 gene already exists, e.g Dopa responsive dystonia sufferers, and furthermore may point towards the importance of GTP-CH1/BH_4 in the lung. By tying together chapters 4,5 and 6, a change in the expression of GFRP may also have implications in the progression of the development of pulmonary hypertension and may explain the link between BH_4 availability and endothelial dysfunction. An interesting future study arising from these findings would also be to cross a GTP-CH1 over expressing mouse (recently developed by Channon and colleagues) with an *hph-1* mouse, where we would expect a potential reversal of the pulmonary hypertensive phenotype.

Finally, the role of GFRP over expression in an endothelial cell line was investigated. Few studies have shown any functional effect of this protein and hence we developed a GFRP over expressing cell line. Chapter 6 has only given a brief characterisation of these cell lines but the functional effects observed so far seem to suggest that GFRP over expression attenuates cytokine + LPS stimulated nitrite generation from iNOS possibly as a result of reducing BH_4 availability for stable dimerisation and full activity of iNOS. This findings may have a number of potential therapeutic implications as excess GFRP may have the ability to behave as a BH_4 biosynthesis inhibitor and hence may be able to reduce NO generation in situations where it may have adverse effects (e.g. sepsis). Furthermore, an increase in endogenous GFRP levels may contribute towards the progression of a number of disease states where a reduction in BH_4 levels may be implicated.

In summary, the main findings of this thesis are:

- GTP-CH1 protein expression alters developmentally in the porcine lung and largely correlates with a functional effect of supplemented BH_4, seen at 3 and 14 days of age.
- SOD supplementation improves vascular reactivity to ACh in isolated porcine pulmonary arteries at 3 and 14 days of age.
- BH_4 and SOD supplementation together improve the relaxation response to ACh in the 3 day porcine model of PPHN.
- GTP-CH1 protein expression is unchanged by hypobaric exposure for 3 days when compared to the age matched control.
- GTP-CH1 protein is localised to the nerves, bronchial smooth muscle, epithelial cells and venous and arterial smooth muscle and GTP-CH1 mRNA is detectable in isolated endothelial cells (sEnd 1). Localisation of GTP-CH1 appears unchanged with age or following hypobaric exposure.
- The GTP-CH1 mouse mutant, *hph-1*, displays the structural characteristics of a pulmonary hypertensive animal.
- GFRP over expression attenuates iNOS mediated nitrite release from sEnd 1 cells.

CHAPTER 8

Future work

8.01 Introduction

In order to answer some of the questions raised in the results chapters of this thesis and to confirm preliminary findings, the following future studies have been suggested.

8.02 Future studies in porcine developmental and PPHN models

Functional studies in porcine pulmonary arteries

For complete characterisation of the role of the BH_4/GTP-CH1 pathway in the developing pulmonary vasculature and in PPHN, other pharmacological reagents acting upon different parts of the *de novo* and salvage (Figure 1.05) would need to be used.

As sepiapterin works by being converted to BH_4 via the salvage pathway, it would be useful to confirm the effects of sepiapterin by using a blocker of this pathway. Methoxyacetylserotonin (MAS) is an inhibitor of both the salvage and *de novo* pathways and we would predict a reversal of the effects seen in the age groups where sepiapterin improved ACh mediated relaxations i.e. 3 and 14 day old animals.

Superoxide measurements in porcine pulmonary arteries

In order to investigate O_2^- levels and whether there is a temporal change or a change following hypobaric exposure, the reactive dye dihydroethidine could be used to visualise O_2^- .This would allow us to compare O_2^- levels in tissues from 3H versus 3 day control. Additionally, SOD levels could be investigated using antibodies raised against SOD, as endogenous SOD levels may explain the differences observed in the response to MnTMPyP.

GTP-CH1 protein expression in porcine pulmonary arteries

GTP-CH1 protein expression as measured by Western blotting, was performed on soluble protein fractions extracted from the cardiac lobe. The advantage of using the cardiac lobe is that a large amount of protein can be easily extracted and furthermore the relative proportions of airways, arteries and veins should remain constant with age and following hypobaric exposure. However, in order to conclusively prove that the developmental changes observed in GTP-CH1 and the apparent lack of effect after 3 days exposure to hypobaric conditions occurred in the pulmonary arteries themselves, (and hence correspond with the functional studies) the experiments should be repeated using protein extracted from isolated pulmonary arteries.

BH_4 measurements in porcine pulmonary arteries

To confirm that the functional effects observed following sepiapterin supplementation are as a direct result of reduced GTP-CH1 expression and hence reduced BH_4 levels, it would be useful to measure BH_4 using electrochemical detection from isolated pulmonary arteries.

8.03 *Hph-1* characterisation studies

Assessment of collagen and elastin

One further parameter, which would have been interesting to investigate in the *hph-1* characterisation studies, would have been a study of the relative amounts of collagen and elastin in the vessel walls, although due to time restrictions this has not been possible. Deposition of collagen in the media and adventitia, another effect associated with pulmonary vascular remodelling, results in decreased compliance of the vessels (Tozzi *et al.*, 1994) and this results in the right heart working against an increased lung resistance leading to the development of right ventricular hypertrophy. We would therefore expect greater amounts of collagen and elastin in the vessel walls from the *hph-1* mice compared to the wild type C57BL/6 X CBA, given the other structural findings. This measurements could be made following staining of paraffin wax sections using Van Gieson's staining techniques.

Evidence of developmental changes

A second interesting investigation would be to look for developmental changes i.e. do the *hph-1* mice show a pulmonary hypertensive phenotype from birth or does it occur later in life and furthermore lifespan studies would tell us whether this mutation results in premature death.

Systemic hypertension measurements

Although there was no observed left ventricular hypertrophy, it would be useful to perform alpha actin staining on vessels from systemic organs e.g. the kidneys, to elucidate whether or not there was any evidence of systemic hypertension. Haemodynamic measurements would give information about any changes in systemic arterial pressures in the *hph-1* compared to the C57BL/6 wild types.

Gender differences

Studying a greater number of animals would also be interesting to elucidate whether or not there are any gender differences, e.g. in the extent of right ventricular hypertrophy and smooth muscle wall area of resistance vessels. Although pooling male and female data sets lead to the conclusion that the *hph-1* mice displayed a pulmonary hypertensive phenotype, this pooling may have masked a gender difference.

BH_4 levels in the lung

A comparison of BH_4 levels in the lungs of *hph-1* vs. wild type would further support the role of GTP-CH1/BH_4 availability and the observed pulmonary hypertensive phenotype. Unfortunately, these measurements are complicated by the fact that the lungs need to be completely cleared of blood, before BH_4 can be extracted and run on the HPLC.

8.04 GFRP over expression studies

Chapter 6 has given an insight into possible mechanisms of the actions of GFRP on NO generation. However, although the results presented within this chapter suggest that GFRP over expression attenuates iNOS mediated nitrite release following cytokine + LPS stimulation and iNOS protein expression, further studies will be needed to confirm these findings to fully elucidate the effects of GFRP over expression on the BH_4/NO pathway in sEnd 1 endothelial cells.

BH_4 measurements

Although the results presented in Chapter 6 suggest that there is no change in intracellular BH_4 measurements, it is likely that the method used is not reflecting the amount of BH_4 available for iNOS activation following cytokine + LPS treatment. As suggested in the discussion of Chapter 6, time course experiments may be needed to demonstrate effects of GFRP over expression on BH_4 levels.

Reversal of the effects of GFRP over expression

An interesting study to determine whether or not the effects of GFRP over expression on iNOS can be reversed would be to supplement cells with excess BH_4. It would be expected that there would be a restoration of nitrite production following cytokine + LPS treatment and furthermore, an increase in iNOS protein expression in the GFRP over expressing cells, comparable to the mock transfected control cells.

Northern blotting for iNOS

Although iNOS mRNA has been shown to be present to the same extent in both GFRP over expressing and mock transfected control cells using PCR, northern blotting for iNOS would provide a more quantitative method of analysing iNOS mRNA levels.

Western and northern blotting for eNOS

To determine the effects of GFRP overexpression on eNOS protein, western and northern blotting should be employed. If the results presented in Chapter 6 are correct (i.e.GFRP over expression did not affect eNOS mediated nitrite release) we would expect there to be no change in eNOS protein expression between GFRP over expressing and mock transfected control cells, and furthermore, there should be no change in eNOS mRNA levels between all cell lines studied.

Investigation of the effects of GFRP over expression on iNOS dimer formation

The observed reduction of iNOS protein in GFRP over expressing cells could be due to either reduced cytokine + LPS induction or increased iNOS degradation possibly secondary to a failure of dimer formation. Pulse chase experiments would allow us to track iNOS dimer formation/degradation. We would expect that BH_4 deficiency as a result of GFRP over expression would either reduce the rate of protein synthesis during the 'pulse' and/or increase the rate of degradation during the 'chase' compared to the control cells.

GTP-CH1 activity measurements

GTP-CH1 activity would be predicted to be lower in the GFRP overexpressing cell lines compared with the control lines. GTP-CH1 activity would be measured as described in chapter 2.

Reversal of GFRP inhibition with BH_4 supplementation

It would be predicted that adding BH_4 in excess could reverse the effects of GFRP over expression on iNOS mediated nitrite release, following cytokine treatment.

GFRP over expressing mouse

If the preliminary data in Chapter 6 proves to be correct, a future longer-term study would be to develop a GFRP over expressing mouse, using the construct developed in Chapter 6. We would predict that this mouse model would demonstrate less iNOS activity following cytokine+LPS treatment and hence may be a sepsis resistant model. Furthermore, this mouse would demonstrate the effects of GFRP over expression on the pulmonary vasculature i.e. does GFRP over expression in vivo, result in the development of pulmonary hypertension?

Appendix

Krebs-Henseleit solution:

Stock solution A (20X) – all dissolved in distilled H_20 (dH_20)

2.38M NaCl (BDH) – to give final conc. 119mM

94mM KCl (BDH) – to give final conc. 4.7mM

20mM $MgSO_4$ $7H_2O$ (BDH) – to give final conc. 1mM

Stock solution B (20X) – all dissolved in dH_20

500mM $NaHCO_3$ (BDH – to give final conc. 25mM

24mM KH_2PO_4 (BDH) – to give final conc. 1.2mM

$CaCl_2$ (1M stock) – dissolved in dH_20

11g $CaCl_2$ (BDH) in 100ml dH_20

Working solution - made up to 2L in dH_20

100ml each solution A and B

11mM (4g) Glucose (BDH)

2.5mM (5ml of 1M stock) $CaCl_2$

Bubble with 95% O_2/5% CO_2 for 20 minutes

Resolving Gel

Volume of Bis acrylamide solution added determines final percentage of gel.

30% Bis-Acrylamide (BioRad) – e.g. for 12.5% gel in a final volume of 10ml
(12.5/30) x 10 = 4.2mls

0.375M Tris (pH 8.8) (BDH)
0.1% v/v Sodium dodecyl sulphate (SDS) (Sigma Aldrich)
0.1% v/v ammonium persulphate (APS) (Sigma-Aldrich)
~ 0.05% v/v N,N,N', N-Tetramethylethylenediamine (TEMED) – (Sigma-Aldrich)
dH_20 to make up to final volume

For 12.5% resolving gel – 10mls final volume

30% Bis-Acrylamide	4.2mls
Tris (pH 8.8) - 3M stock made up in dH_20	1.25mls
SDS (10% w/v stock made up in dH_20)	100µl
APS (10% w/v stock made up in dH_20)	100µl
TEMED	5µl
dH_20 (to make up to 10mls)	4.35mls

Stacking gel

To make final volume 1ml:

17% v/v 30% Bis-Acrylamide	0.17ml
130mM Tris (pH 6.8) – 1M stock made up in dH_20	0.13ml
SDS (10% w/v stock made up in dH_20)	0.01ml
APS (10% w/v stock made up in dH_20)	0.01ml
TEMED	0.001ml
dH_20 (to make up to final volume)	0.68ml

Sample loading buffer

(1 x stock) - make up into 10mls

80mM Tris (w/v) (BDH)

5% (v/v) β-mercaptoethanol (BDH)

0.02% Bromophenol blue (w/v)

10% glycerol (v/v)

2% SDS (w/v)

pH to 6.8 with HCl

Blotting solution

	To make 1L in dH_20	
130mM SDS (Sigma)	SDS	0.37g
50mM Tris (Sigma)	Tris	5.8g
40mM Glycine (Sigma)	Glycine	2.9g
20% (v/v) methanol (BDH)	methanol	200ml

Running buffer

	To make 1L in dH_20	
250mM Tris	Tris	30g
1.9M Glycine	Glycine	144g
1% v/v SDS (10% stock solution)	10% SDS	100ml

RIPA buffer

1 % (v/v) Phosphate buffered saline (Sigma)

IGEPAL (v/v) (Sigma) 1%

Na-deoxycholate (Sigma) 0.5%

EDTA (Sigma) 1 mM

PMSF (Sigma) 1 mM

1 tablet protease inhibitor in 10ml PBS (Roche) containing aprotinin, leupeptin, pepstatin

10% Neutral buffered Formol Saline

A. 0.33M NaH_2PO_4 (BDH) - 40g in 1 litre buffer salts (10x stock)

B. 0.55M Na_2HPO_4 (BDH) - 65g in 1 litre (20x stock)

To make 1 litre 10% buffered formol saline:

100 ml solution A

50 ml solution B

Make up to 1 litre with dH_2O

10% v/v (100 ml) 40% formaldehyde (Sigma)

References

ABMAN SH.

Pediatr Rev. 1999 Nov;20(11):e103-9

Abnormal vasoreactivity in the pathophysiology of persistent pulmonary hypertension of the newborn.

ABMAN SH, CHATFIELD BA, RODMAN DM, HALL SL, MCMURTRY IF.

Am J Physiol. 1991 Apr; 260(4 Pt 1): L280-5

Maturational changes in endothelium-derived relaxing factor activity of ovine pulmonary arteries in vitro.

ABMAN SH, CHATFIELD BA, HALL SL, MCMURTRY IF.

Am J Physiol. 1990 Dec; 259(6 Pt 2): H1921-7

Role of endothelium-derived relaxing factor during transition of pulmonary circulation at birth.

ACHAN V, TRAN CT, ARRIGONI F, WHITLEY GS, LEIPER JM, VALLANCE P.

Circ Res 2002 Apr 19;90(7):764-9

all-trans-Retinoic acid increases nitric oxide synthesis by endothelial cells: a role for the induction of dimethylarginine dimethylaminohydrolase.

ADNOT S, RAFFESTIN B, EDDAHIBI S

Respir Physiol 1995 Aug;101(2):109-20

NO in the lung.

ADNOT S, RAFFESTIN B, EDDAHIBI S, BRAQUET P, CHABRIER PE.

J Clin Invest. 1991 Jan;87(1):155-62

Loss of endothelium-dependent relaxant activity in the pulmonary circulation of rats exposed to chronic hypoxia.

ALDERTON WK, COOPER CE, KNOWLES RG.

Biochem J. 2001 Aug 1;357(Pt 3):593-615

Nitric oxide synthases: structure, function and inhibition.

AOYAGI M, ARVAI AS, GHOSH S, STUEHR DJ, TAINER JA, GETZOFF ED

Biochemistry 2001 Oct 30;40(43):12826-32

Structures of tetrahydrobiopterin binding-site mutants of inducible nitric oxide synthase oxygenase dimer and implicated roles of Trp457.

ARRIGONI FI, VALLANCE P, HAWORTH SG, LEIPER JM.

Circulation 2003 Mar 4;107(8):1195-201

Metabolism of asymmetric dimethylarginines is regulated in the lung developmentally and with pulmonary hypertension induced by hypobaric hypoxia.

ARRIGONI FI, HISLOP AA, POLLOCK JS, HAWORTH SG, MITCHELL JA.

Life Sci. 2002 Feb 22;70(14):1609-20.

Birth upregulates nitric oxide synthase activity in the porcine lung.

ARRIGONI FI, HISLOP AA, HAWORTH SG, MITCHELL JA.

Newborn intrapulmonary veins are more reactive than arteries in normal and hypertensive piglets.

Am J Physiol. 1999 Nov;277(5 Pt 1):L887-92

AUERBACH G, HERRMANN A, BRACHER A, BADER G, GUTLICH M, FISCHER M, NEUKAMM M, GARRIDO-FRANCO M, RICHARDSON J, NAR H, HUBER R, BACHER A.

Proc Natl Acad Sci U S A. 2000 Dec 5;97(25):13567-72.

Zinc plays a key role in human and bacterial GTP cyclohydrolase I.

BAGI Z, KOLLER A

J Vasc Res 2003 Jan-Feb;40(1):47-57

Lack of nitric oxide mediation of flow-dependent arteriolar dilation in type I diabetes is restored by sepiapterin.

BALLIGAND JL, KELLY RA, MARSDEN PA, SMITH TW, MICHEL T.

Proc Natl Acad Sci U S A. 1993 Jan 1; 90(1):347-51

Control of cardiac muscle cell function by an endogenous nitric oxide signaling system.

BARBACANNE MA, SOUCHARD JP, DARBLADE B, ILIOU JP, NEPVEU F, PIPY B, BAYARD F, ARNAL JF

Free Radic Biol Med. 2000 Sep 1;29(5):388-96

Detection of superoxide anion released extracellularly by endothelial cells using cytochrome c reduction, ESR, fluorescence and lucigenin-enhanced chemiluminescence techniques.

BECKMAN JS, BECKMAN TW, CHEN J, MARSHALL PA, FREEMAN BA.

Proc Natl Acad Sci U S A. 1990 Feb;87(4):1620-4

Apparent hydroxyl radical production by peroxynitrite: implications for endothelial injury from nitric oxide and superoxide.

BECKMAN JS, KOPPENOL WH

Am J Physiol. 1996 Nov;271(5 Pt 1):C1424-37

Nitric oxide, superoxide, and peroxynitrite: the good, the bad, and ugly.

BEC N, GORREN AC, VOELKER C, MAYER B, LANGE R

J Biol Chem 1998 May 29; 273(22): 13502-8

Reaction of neuronal nitric-oxide synthase with oxygen at low temperature. Evidence for reductive activation of the oxy-ferrous complex by tetrahydrobiopterin.

BERKENBOSCH JW, BARIBEAU J, PERREAULT T

Am J Physiol Lung Cell Mol Physiol 2000 Feb;278(2):L276-83

Decreased synthesis and vasodilation to nitric oxide in piglets with hypoxia-induced pulmonary hypertension.

BHAGAT K, HINGORANI AD, PALACIOS M, CHARLES IG, VALLANCE P. (A)

Cardiovasc Res. 1999 Mar;41(3):754-64

Cytokine-induced venodilatation in humans in vivo: eNOS masquerading as iNOS.

BHAGAT K, VALLANCE P (B)

Curr Opin Nephrol Hypertens 1999 Jan;8(1): 89-96

Effects of cytokines on nitric oxide pathways in human vasculature.

BRADFORD MM.

Anal Biochem. 1976 May 7; 72:248-54.

A rapid and sensitive method for the quantitation of microgram quantities of protein utilizing the principle of protein-dye binding.

BRAND MP, BRIDDON A, LAND JM, CLARK JB, HEALES SJ

Brain Res 1996 Sep 30;735(1):169-72

Impairment of the nitric oxide/cyclic GMP pathway in cerebellar slices prepared from the *hph-1* mouse.

BRAND MP, HEALES SJ, LAND JM, CLARK JB.

J Inherit Metab Dis 1995;18(1):33-9

Tetrahydrobiopterin deficiency and brain nitric oxide synthase in the hph1 mouse.

BREDT DS, HWANG PM, GLATT CE, LOWENSTEIN C, REED RR, SNYDER SH.

Nature. 1991 Jun 27; 351(6329): 714-8

Cloned and expressed nitric oxide synthase structurally resembles cytochrome P-450 reductase.

CAI S, ALP NJ, MCDONALD D, SMITH I, KAY J, CANEVARI L, HEALES S, CHANNON KM.

GTP cyclohydrolase I gene transfer augments intracellular tetrahydrobiopterin in human endothelial cells: effects on nitric oxide synthase activity, protein levels and dimerisation. Cardiovasc Res. 2002 Sep; 55(4):838-49.

CANALS S, CASAREJOS MJ, DE BERNARDO S, RODRIGUEZ-MARTIN E, MENA MA.

J Neurochem. 2001 Dec;79(6):1183-95

Glutathione depletion switches nitric oxide neurotrophic effects to cell death in midbrain cultures: implications for Parkinson's disease.

CANEVARI L, LAND JM, CLARK JB, HEALES SJ

J Neurochem 1999 Dec;73(6):2563-8

Stimulation of the brain NO/cyclic GMP pathway by peripheral administration of tetrahydrobiopterin in the *hph-1* mouse.

CARVILLE C, RAFFESTIN B, EDDAHIBI S, BLOUQUIT Y, ADNOT S

J Cardiovasc Pharmacol 1993 Dec;22(6):889-96

Loss of endothelium-dependent relaxation in proximal pulmonary arteries from rats exposed to chronic hypoxia: effects of in vivo and in vitro supplementation with L-arginine.

CASES A, HAAS J, BURNETT JC, ROMERO JC

Am J Physiol Regul Integr Comp Physiol 2001 Jan; 280(1): R143-8

Hemodynamic and renal effects of acute and progressive nitric oxide synthesis inhibition in anesthetized dogs.

CHO HJ, XIE QW, CALAYCAY J, MUMFORD RA, SWIDEREK KM, LEE TD, NATHAN C

J Exp Med 1992 Aug 1; 176(2): 599-604

Calmodulin is a subunit of nitric oxide synthase from macrophages.

CHOWIENCZYK PJ, WATTS GF, COCKCROFT JR, BRETT SE, RITTER JM

Lancet. 1994 Jul 30; 344(8918): 305-6

Sex differences in endothelial function in normal and hypercholesterolaemic subjects.

COSENTINO F, SILL JC, KATUSIC ZS.

Hypertension. 1994 Feb; 23(2):229-35

Role of superoxide anions in the mediation of endothelium-dependent contractions.

COSENTINO F, PATTON S, D'USCIO LV, WERNER ER, WERNER-FELMAYER G, MOREAU P, MALINSKI T, LUSCHER TF

J Clin Invest. 1998 Apr 1; 101(7): 1530-7

Tetrahydrobiopterin alters superoxide and nitric oxide release in prehypertensive rats.

COSENTINO F, LUSCHER TF.

Cardiovasc Res. 1999 Aug 1; 43(2): 274-8.

Tetrahydrobiopterin and endothelial nitric oxide synthase activity.

COSENTINO F, BARKER JE, BRAND MP, HEALES SJ, WERNER ER, TIPPINS JR, WEST N, CHANNON KM, VOLPE M, LUSCHER TF.

Arterioscler Thromb Vasc Biol. 2001 Apr;21(4):496-502.

Reactive oxygen species mediate endothelium-dependent relaxations in tetrahydrobiopterin-deficient mice.

CRANE BR, ARVAI AS, GHOSH DK, WU C, GETZOFF ED, STUEHR DJ, TAINER JA

Science 1998 Mar 27;279(5359):2121-6

Structure of nitric oxide synthase oxygenase dimer with pterin and substrate.

CREAGER MA, GALLAGHER SJ, GIRERD XJ, COLEMAN SM, DZAU VJ, COOKE JP.

J Clin Invest. 1992 Oct;90(4):1248-53

L-arginine improves endothelium-dependent vasodilation in hypercholesterolemic humans.

EDDAHIBI S, ADNOT S, CARVILLE C, BLOUQUIT Y, RAFFESTIN B

Am J Physiol 1992 Aug;263(2 Pt 1):L194-200

L-arginine restores endothelium-dependent relaxation in pulmonary circulation of chronically hypoxic rats.

FIKE CD, KAPLOWITZ MR, THOMAS CJ, NELIN LD.

Am J Physiol. 1998 Apr;274(4 Pt 1):L517-26

Chronic hypoxia decreases nitric oxide production and endothelial nitric oxide synthase in newborn pig lungs.

FIKE CD, KAPLOWITZ MR

J Appl Physiol 1996 Nov;81(5):2078-87

Chronic hypoxia alters nitric oxide-dependent pulmonary vascular responses in lungs of newborn pigs.

FIKE CD, KAPLOWITZ MR.

J Appl Physiol 1994 Dec;77(6):2853-62

Effect of chronic hypoxia on pulmonary vascular pressures in isolated lungs of newborn pigs.

FINEMAN JR, HEYMANN MA, SOIFER SJ

Am J Physiol 1991 Apr; 260(4 Pt 2): H1299-306

N omega-nitro-L-arginine attenuates endothelium-dependent pulmonary vasodilation in lambs.

FORSTERMANN U, CLOSS EI, POLLOCK JS, NAKANE M, SCHWARZ P, GATH I, KLEINERT H.

Nitric oxide synthase isozymes. Characterization, purification, molecular cloning, and functions.

Hypertension. 1994 Jun;23(6 Pt 2):1121-31.

FRIDOVICH I.

Superoxide radical: an endogenous toxicant.

Annu Rev Pharmacol Toxicol. 1983;23:239-57

FOLKOW B.

Clin Sci 1971 Jul;41(1):1-12

The haemodynamic consequences of adaptive structural changes of the resistance vessels in hypertension.

FUKUDA Y, TERAGAWA H, MATSUDA K, YAMAGATA T, MATSUURA H, CHAYAMA K

Tetrahydrobiopterin restores endothelial function of coronary arteries in patients with hypercholesterolaemia.

Heart 2002 Mar;87(3):264-9

FURCHGOTT RF.

Annu Rev Pharmacol Toxicol. 1984;24:175-97

The role of endothelium in the responses of vascular smooth muscle to drugs.

FURCHGOTT RF, ZAWADZKI JV.

Nature. 1980 Nov 27;288(5789):373-6.

The obligatory role of endothelial cells in the relaxation of arterial smooth muscle by acetylcholine.

GARDNER PR, NGUYEN DD, WHITE CW

Arch Biochem Biophys 1996 Jan 1;325(1):20-8

Superoxide scavenging by Mn(II/III) tetrakis (1-methyl-4-pyridyl) porphyrin in mammalian cells.

GARG UC, HASSID A

Clin Invest 1989 May;83(5):1774-7

Nitric oxide-generating vasodilators and 8-bromo-cyclic guanosine monophosphate inhibit mitogenesis and proliferation of cultured rat vascular smooth muscle cells.

GERSONY W.M.

Clin. Perinatol (1984) 11: 517-524

Neonatal pulmonary hypertension: pathophysiology, classification and etiology.

GESIERICH A, NIROOMAND F, TIEFENBACHER CP

Role of human GTP cyclohydrolase I and its regulatory protein in tetrahydrobiopterin metabolism.

Basic Res Cardiol. 2003 Mar;98(2):69-75

GHANAYEM NS, GORDON JB.

Respir Res. 2001;2(3):139-44.

Modulation of pulmonary vasomotor tone in the fetus and neonate.

GHOSH DK, WU C, PITTERS E, MOLONEY M, WERNER ER, MAYER B, STUEHR DJ.

Biochemistry 1997 Sep 2;36(35):10609-19

Characterization of the inducible nitric oxide synthase oxygenase domain identifies a 49 amino acid segment required for subunit dimerization and tetrahydrobiopterin interaction.

GIOVANELLI J, CAMPOS KL, KAUFMAN S

Proc Natl Acad Sci U S A. 1991 Aug 15; 88(16): 7091-5

Tetrahydrobiopterin, a cofactor for rat cerebellar nitric oxide synthase, does not function as a reactant in the oxygenation of arginine.

GORREN AC, MAYER B.

1998 Jul;63(7):734-43. Biochemistry (Mosc).

The versatile and complex enzymology of nitric oxide synthase.

GORREN AC, LIST BM, SCHRAMMEL A, PITTERS E, HEMMENS B, WERNER ER, SCHMIDT K, MAYER B.

Biochemistry. 1996 Dec 24;35(51):16735-45

Tetrahydrobiopterin-free neuronal nitric oxide synthase: evidence for two identical highly anticooperative pteridine binding sites.

GRIENDLING KK, SORESCU D, USHIO-FUKAI M.

NAD(P)H oxidase: role in cardiovascular biology and disease.

Circ Res. 2000 Mar 17;86(5):494-501. Review

GROSS S.S, JONES, C., HATTORI, Y,AND RAMAN C.S.

Tetrahydrobiopterin: An essential cofactor of nitric oxide synthase with an elusive role.

In: Nitric Oxide Biology and Pathobiology. San Diego, CA: Academic, 2000 p. 167-187

GROSS, S.S., MADERA, A., PARK, K.H., AND LEVI, R

In Methods in Nitric Oxide Research 1996. Ed. Martin Feelisch and Jonathan Stamler. John Wiley and Sons Ltd.

GROSS SS, LEVI R.

J Biol Chem. 1992 Dec 25;267(36):25722-9

Tetrahydrobiopterin synthesis. An absolute requirement for cytokine-induced nitric oxide generation by vascular smooth muscle.

GROSS SS, JAFFE EA, LEVI R, KILBOURN RG.

Biochem Biophys Res Commun. 1991 Aug 15;178(3):823-9

Cytokine-activated endothelial cells express an isotype of nitric oxide synthase which is tetrahydrobiopterin-dependent, calmodulin-independent and inhibited by arginine analogs with a rank-order of potency characteristic of activated macrophages.

GUTLICH M, ZIEGLER I, WITTER K, HEMMENS B, HULTNER L, MCDONALD JD, WERNER T, RODL W, BACHER A

Molecular characterization of *HPH-1*: a mouse mutant deficient in GTP cyclohydrolase I activity.

Biochem Biophys Res Commun 1994 Sep 30;203(3):1675-81

GUZIK TJ, WEST NE, BLACK E, MCDONALD D, RATNATUNGA C, PILLAI R, CHANNON KM

Circ Res. 2000 May 12;86(9):E85-90

Vascular superoxide production by NAD(P)H oxidase: association with endothelial dysfunction and clinical risk factors.

HARADA T, KAGAMIYAMA H, HATAKEYAMA K.

Science. 1993 Jun 4;260(5113):1507-10

Feedback regulation mechanisms for the control of GTP cyclohydrolase activity.

HAWORTH S.G. AND HISLOP A.A

Cardiovasc Res. 1981 Feb;15(2):108-19

Adaptation of the pulmonary circulation to extra-uterine life in the pig and its relevance to the human infant.

HAY D.W., LUTTMANN MA, HUBBARD WC, UNDEM BJ

Br. J Pharmacol. 1993 Nov: 110(3):1175-83

Endothelin receptor subtypes in human and guinea pig pulmonary tissues.

HAWORTH SG AND HISLOP AA.

Cardiovascular Research. 1981; 15(2):108-19.

Adaptation of the pulmonary circulation to extra-uterine life in the pig and its relevance to the human infant.

HAWORTH SG, HISLOP AA

Effect of hypoxia on adaptation of the pulmonary circulation to extra-uterine life in the pig.

Cardiovasc Res 1982 Jun;16(6):293-303

HEALES S, HYLAND K

Determination of quinonoid dihydrobiopterin by high-performance liquid chromatography and electrochemical detection.

J Chromatogr. 1989 Sep 29; 494:77-85.

HEATH D

The rat is a poor animal model for the study of human pulmonary hypertension.

Cardioscience 1992 Mar;3(1):1-6

HESSLINGER C, KREMMER E, HULTNER L, UEFFING M, ZIEGLER I.

Phosphorylation of GTP cyclohydrolase I and modulation of its activity in rodent mast cells.

J Biol Chem. 1998; 273(34): 21616-22.

HEYMANN MA.

Eur J Obstet Gynecol Reprod Biol. 1999 Jun;84(2):127-32.

Control of the pulmonary circulation in the fetus and during the transitional period to air breathing.

HISLOP AA, SPRINGALL DR, OLIVEIRA H, POLLOCK JS, POLAK JM, HAWORTH SG.

Arch Dis Child Fetal Neonatal Ed. 1997 Jul; 77(1): F16-22

Endothelial nitric oxide synthase in hypoxic newborn porcine pulmonary vessels

HISLOP A, REID L

Changes in the pulmonary arteries of the rat during recovery from hypoxia-induced pulmonary hypertension.

Br J Exp Pathol 1977 Dec; 58(6): 653-62

HISLOP A, REID L

New findings in pulmonary arteries of rats with hypoxia-induced pulmonary hypertension.

Br J Exp Pathol 1976 Oct; 57(5):542-54

HOPP, T.P. AND WOODS, K.R.

Prediction of protein antigenic determinants from amino acid sequences.

Proc Natl Acad Sci 86:152-156(1981)

HOSHIGA M, HATAKEYAMA K, KAGAMIYAMA H

Adv Exp Med Biol. 1993; 338:223-6

Tissue distribution of tetrahydrobiopterin generating enzymes.

HOWELLS DW, HYLAND K

Clin Chim Acta. 1987 Jul 30; 167(1): 23-30.

Direct analysis of tetrahydrobiopterin in cerebrospinal fluid by high-performance liquid chromatography with redox electrochemistry: prevention of autoxidation during storage and analysis.

HUANG PL, HUANG Z, MASHIMO H, BLOCH KD, MOSKOWITZ MA, BEVAN JA, FISHMAN MC.

Nature. 1995 Sep 21; 377(6546): 239-42.

Hypertension in mice lacking the gene for endothelial nitric oxide synthase.

HUANG A, VITA JA, VENEMA RC, KEANEY JF JR

J Biol Chem 2000 Jun 9; 275(23): 17399-406

Ascorbic acid enhances endothelial nitric-oxide synthase activity by increasing intracellular tetrahydrobiopterin.

HYLAND K AND BOLA F

Abstract: Biol Chem Hoppe Seyler 370: 387 (1989)

Tetrahydrobiopterin and biogenic amine status of the *hph-1* mouse mutant

HYLAND K, GUNASEKERA RS, ENGLE T, ARNOLD LA

J Neurochem 1996 Aug;67(2):752-9

Tetrahydrobiopterin and biogenic amine metabolism in the *hph-1* mouse.

HWANG O, BAKER H, GROSS S, JOH TH.

Synapse. 1998 Feb; 28(2): 140-53.

Localization of GTP cyclohydrolase in monoaminergic but not nitric oxide-producing cells.

HWANG O, CHOI HJ, PARK SY.

Neuroreport. 1999 Nov 26; 10(17): 3611-4.

Up-regulation of GTP cyclohydrolase I and tetrahydrobiopterin by calcium influx.

IGNARRO LJ, BUGA GM, WOOD KS, BYRNS RE, CHAUDHURI G.

Proc Natl Acad Sci U S A. 1987 Dec; 84(24): 9265-9

Endothelium-derived relaxing factor produced and released from artery and vein is nitric oxide.

IGNARRO LJ, HARBISON RG, WOOD KS, KADOWITZ PJ.

J Pharmacol Exp Ther. 1986 Jun; 237(3): 893-900.

Activation of purified soluble guanylate cyclase by endothelium-derived relaxing factor from intrapulmonary artery and vein: stimulation by acetylcholine, bradykinin and arachidonic acid.

ISAACSON TC, HAMPL V, WEIR EK, NELSON DP, ARCHER SL

J Appl Physiol 1994 Feb; 76(2): 933-40

Increased endothelium-derived NO in hypertensive pulmonary circulation of chronically hypoxic rats.

JANSSENS SP, BLOCH KD, NONG Z, GERARD RD, ZOLDHELYI P, COLLEN D.

J Clin Invest. 1996 Jul 15; 98(2): 317-24.

Adenoviral-mediated transfer of the human endothelial nitric oxide synthase gene reduces acute hypoxic pulmonary vasoconstriction in rats.

JEFFERY T AND WANSTALL J

Pharmacology and Therapeutics 2001 (1-20)

Pulmonary vascular remodelling: a target for therpeutic intervention in pulmonary hypertension.

JONES RC, REID L.

Vasculature remodelling in clinical and experimental pulmonary hypertensions

In: Pulmonary Vascular remodelling ed. Bishop JE, Reeves JT and Laurent GJ

London: Portland 1995: 47-116

KATUSIC, Z

Am J physiol Heart Circ Physiol 2001 281: H981-H986

Vascular endothelial dysfunction: does tetrahydrobiopterin play a role?

KATUSIC, Z., STELTER, A., MILSTEIN, S

Arterioscler Thomb Vasc Biol 1998; 18:27-32

Cytokines stimulate GTP cyclohydrolase 1 gene expression in cultured human umbilical vein endothelial cells

KAUFMAN, S

J Biol. Chem. 239, 332-338 1963

The structure of the primary oxidation product formed from tetrahydropteridines during phenylalanine hydroxylation.

KERLER F, SCHWARZKOPF B, KATZENMAIER G, LE VAN Q, SCHMID C, ZIEGLER I, BACHER A

Biochim Biophys Acta. 1989; 990(1):15-7

Biosynthesis of tetrahydrobiopterin: a sensitive assay of 6-pyruvoyltetrahydropterin synthase using [2'-3H]dihydroneopterin 3'-triphosphate as substrate.

KERLER F, HULTNER L, ZIEGLER I, KATZENMAIER G, BACHER A

J Cell Physiol. 1990; 142(2):268-71

Analysis of the tetrahydrobiopterin synthesizing system during maturation of murine reticulocytes.

KIKUCHI K, NAGANO T, BECKMAN J.

Determination of Nitric Oxide by chemiluminscence in the reaction with luminol and hydrogen peroxide.

In Methods in Nitric Oxide Research. Ed. Martin Feelisch and Jonathan Stamler. 1996. John Wiley & Sons Ltd.

KINOSHITA H, MILSTIEN S, WAMBI C, KATUSIC ZS.

Am J Physiol. 1997 Aug;273(2 Pt 2):H718-24

Inhibition of tetrahydrobiopterin biosynthesis impairs endothelium-dependent relaxations in canine basilar artery.

KINOSHITA H, KATUSIC ZS

Am J Physiol 1996 Aug; 271(2 Pt 2):H738-43

Exogenous tetrahydrobiopterin causes endothelium-dependent contractions in isolated canine basilar artery.

KINSELLA JP, NEISH SR, SHAFFER E, ABMAN SH.

Lancet. 1992 Oct 3;340(8823):819-20.

Low-dose inhalation nitric oxide in persistent pulmonary hypertension of the newborn.

KINSELLA JP, ABMAN SH.

J Pediatr. 1995 Jun; 126(6): 853-64.

Recent developments in the pathophysiology and treatment of persistent pulmonary hypertension of the newborn.

KIRA Y, SATO EF, INOUE M.

Arch Biochem Biophys. 2002 Mar 1; 399(1): 96-102.

Association of Cu,Zn-type superoxide dismutase with mitochondria and peroxisomes.

KNOWLES RG, MONCADA S.

Biochem J. 1994 Mar 1; 298 (Pt 2): 249-58.

Nitric oxide synthases in mammals.

KOUREMBANAS S, MCQUILLAN LP, LEUNG GK, FALLER DV

J Clin Invest 1993 Jul;92(1):99-104

Nitric oxide regulates the expression of vasoconstrictors and growth factors by vascular endothelium under both normoxia and hypoxia.

KWON NS, NATHAN CF, STUEHR DJ.

J Biol Chem. 1989 Dec 5; 264(34):20496-501.

Reduced biopterin as a cofactor in the generation of nitrogen oxides by murine macrophages.

LAMAS S, MARSDEN PA, LI GK, TEMPST P, MICHEL T.

Proc Natl Acad Sci U S A. 1992 Jul 15;89(14):6348-52

Endothelial nitric oxide synthase: molecular cloning and characterization of a distinct constitutive enzyme isoform.

LEIPER J, MURRAY-RUST J, MCDONALD N, VALLANCE P

Proc Natl Acad Sci U S A 2002 Oct 15;99(21):13527-32

S-nitrosylation of dimethylarginine dimethylaminohydrolase regulates enzyme activity: further interactions between nitric oxide synthase and dimethylarginine dimethylaminohydrolase.

LEIPER J, VALLANCE P.

Cardiovasc Res. 1999 Aug 15; 43(3): 542-8.

Biological significance of endogenous methylarginines that inhibit nitric oxide synthases.

LICKER M, BOUSSAIRI H, HOHN L, MOREL DR.

Acta Physiol Scand 1998 Aug; 163(4):339-48

Role of nitric oxide in the regulation of regional blood flow and metabolism in anaesthetized pigs.

LINDNER M, HAAS D, MAYATEPEK E, ZSCHOCKE J, BURGARD P.

Mol Genet Metab 2001 May;73(1):104-6

Tetrahydrobiopterin responsiveness in phenylketonuria differs between patients with the same genotype.

LIU SF, HISLOP AA, HAWORTH SG, BARNES PJ.

Br J Pharmacol. 1992 Jun; 106(2):324-30

Developmental changes in endothelium-dependent pulmonary vasodilatation in pigs.

LIU, Q AND GROSS SS

Methods enzymol 268: 311-324 (1996)

Binding sites of nitric oxide synthases

LOWENSTEIN CJ, GLATT CS, BREDT DS, SNYDER SH.

Proc Natl Acad Sci U S A. 1992 Aug 1; 89(15): 6711-5

Cloned and expressed macrophage nitric oxide synthase contrasts with the brain enzyme.

LUSCHER TF, BOULANGER CM, DOHI Y, YANG ZH.

Hypertension. 1992 Feb;19(2):117-30.

Endothelium-derived contracting factors.

MACKENZIE A, FILIPPINI S, MARTIN W

Effects of superoxide dismutase mimetics on the activity of nitric oxide in rat aorta.

Br J Pharmacol 1999 Jul; 127(5):1159-6

MACKENZIE, A AND MARTIN, W

British Journal of Pharmacology (1998) 124, 719-728

Loss of endothelium derived nitric oxide in rabbit aorta by oxidant stress: restoration by superoxide dismutase mimetics

MAEDA T, HAENO S, ODA K, MORI D, ICHINOSE H, NAGATSU T, SUZUKI T

Brain Dev 2000 Sep; 22 Suppl 1:S50-3

Studies on the genotype-phenotype relation in the *hph-1* mouse mutant deficient in guanosine triphosphate (GTP) cyclohydrolase I activity.

MAITA N, OKADA K, HATAKEYAMA K, HAKOSHIMA T

Crystal structure of the stimulatory complex of GTP cyclohydrolase I and its feedback regulatory protein GFRP.

Proc Natl Acad Sci U S A. 2002 Feb 5; 99(3): p1212

MARINOS RS, ZHANG W, WU G, KELLY KA, MEININGER CJ

Am J Physiol Heart Circ Physiol 2001 Aug; 281(2): H482-9

Tetrahydrobiopterin levels regulate endothelial cell proliferation.

MAYER B, JOHN M, HEINZEL B, WERNER ER, WACHTER H, SCHULTZ G, BOHME E

FEBS Lett 1991 Aug 19; 288(1-2): 187-91

Brain nitric oxide synthase is a biopterin- and flavin-containing multi-functional oxido-reductase.

MCDONALD JD, BODE VC.

Pediatric Research 1988; 23: 63-67

Hyperphenyalaninemia in the *hph-1* mouse mutant.

MCDONALD JD, COTTON RGH, JENNINGS I, LEDLEY FD, WOO SLC, BODE VC

J Neurochem 1988; 50:655-657

Biochemical defect of the *hph-1* mouse mutant is a deficiency in GTP cyclohydrolase I activity.

MCQUESTON JA, KINSELLA JP, IVY DD, MCMURTRY IF, ABMAN SH.

Am J Physiol. 1995 Jan;268(1 Pt 2):H288-94

Chronic pulmonary hypertension in utero impairs endothelium-dependent vasodilation.

MEININGER CJ, MARINOS RS, HATAKEYAMA K, MARTINEZ-ZAGUILAN R, ROJAS JD, KELLY KA, WU G.

Biochem J. 2000 Jul 1;349(Pt 1):353-6

Impaired nitric oxide production in coronary endothelial cells of the spontaneously diabetic BB rat is due to tetrahydrobiopterin deficiency.

MILSTIEN S, KATUSIC Z.

Oxidation of tetrahydrobiopterin by peroxynitrite: implications for vascular endothelial function.

Biochem Biophys Res Commun. 1999 Oct 5; 263(3): 681-4.

MILSTIEN S, JAFFE H, KOWLESSUR D, BONNER TI

Purification and cloning of the GTP cyclohydrolase I feedback regulatory protein, GFRP.

J Biol Chem. 1996 Aug 16; 271(33): 19743-51.

MITCHELL JA, SHENG H, FORSTERMANN U, MURAD F.

Br J Pharmacol. 1991 Oct; 104(2):289-91

Characterization of nitric oxide synthases in non-adrenergic non-cholinergic nerve containing tissue from the rat anococcygeus muscle.

MOHAZZAB KM, KAMINSKI PM, WOLIN MS.

Am J Physiol. 1994 Jun;266(6 Pt 2):H2568-72

NADH oxidoreductase is a major source of superoxide anion in bovine coronary artery endothelium.

MONCADA S, PALMER RM, HIGGS EA

Pharmacol Rev 1991 Jun; 43(2): 109-42

Nitric oxide: physiology, pathophysiology, and pharmacology.

MORRELL NW AND WILKINS MR

Clinical Medicine (2001) Vol 1, No 2: 138-145

Genetic and molecular mechanisms of pulmonary hypertension

MULLER, STEINBERGER, TOPKA

Mutations of GCH1 in Dopa Responsive dystonia

J. Neural Transm (2002) 109:321-328

MUNTAU AC, ROSCHINGER W, HABICH M, DEMMELMAIR H, HOFFMANN B, SOMMERHOFF CP, ROSCHER AA.

Tetrahydrobiopterin as an alternative treatment for mild phenylketonuria.

N Engl J Med. 2002 Dec 26; 347(26):2122-32

MURAMATSU M, TYLER RC, RODMAN DM, MCMURTRY IF.

J Appl Physiol 1996 Apr; 80(4): 1336-44

Thapsigargin stimulates increased NO activity in hypoxic hypertensive rat lungs and pulmonary arteries.

MURATA T, YAMAWAKI H, HORI M, SATO K, OZAKI H, KARAKI H

Eur J Pharmacol 2001 Jun 1; 421(1):45-53

Hypoxia impairs endothelium-dependent relaxation in organ cultured pulmonary artery.

NAKANE H, MILLER FJ JR, FARACI FM, TOYODA K, HEISTAD DD.

Hypertension. 2000 Feb; 35(2): 595-601

Gene transfer of endothelial nitric oxide synthase reduces angiotensin II-induced endothelial dysfunction.

NAR H, HUBER R, MEINING W, SCHMID C, WEINKAUF S, BACHER A.

Structure. 1995 May 15;3(5):459-66

Atomic structure of GTP cyclohydrolase I.

NATHAN C

FASEB J 1992 Sep; 6(12): 3051-64

Nitric oxide as a secretory product of mammalian cells.

NATHAN C, XIE QW

J Biol Chem 1994 May 13; 269(19):13725-8

Regulation of biosynthesis of nitric oxide.

NICHOL CA, SMITH GK, DUCH DS.

Annu Rev Biochem. 1985; 54:729-64.

Biosynthesis and metabolism of tetrahydrobiopterin and molybdopterin.

NISHIDA K, HARRISON DG, NAVAS JP, FISHER AA, DOCKERY SP, UEMATSU M, NEREM RM, ALEXANDER RW, MURPHY TJ

J Clin Invest 1992 Nov;90(5):2092-6

Molecular cloning and characterization of the constitutive bovine aortic endothelial cell nitric oxide synthase.

NORTH AJ, MOYA FR, MYSORE MR, THOMAS VL, WELLS LB, WU LC, SHAUL PW

Am J Respir Cell Mol Biol 1995 Dec; 13(6): 676-82

Pulmonary endothelial nitric oxide synthase gene expression is decreased in a rat model of congenital diaphragmatic hernia.

NUSSLER AK, DI SILVIO M, BILLIAR TR, HOFFMAN RA, GELLER DA, SELBY R, MADARIAGA J, SIMMONS RL

J Exp Med 1992 Jul 1; 176(1): 261-4

Stimulation of the nitric oxide synthase pathway in human hepatocytes by cytokines and endotoxin.

OEMAR BS, TSCHUDI MR, GODOY N, BROVKOVICH V, MALINSKI T, LUSCHER TF.

Circulation. 1998 Jun 30;97(25):2494-8

Reduced endothelial nitric oxide synthase expression and production in human atherosclerosis.

OHARA T, OGATA H, TEZUKA F

Tohoku J Exp Med 1991 May; 164(1): 59-66

Histological study of pulmonary vasculature in fatal cases of persistent pulmonary hypertension of the newborn.

OZAKI M, KAWASHIMA S, YAMASHITA T, HIRASE T, NAMIKI M, INOUE N, HIRATA K, YASUI H, SAKURAI H, YOSHIDA Y, MASADA M, YOKOYAMA M.

J Clin Invest. 2002 Aug; 110(3):331-40

Overexpression of endothelial nitric oxide synthase accelerates atherosclerotic lesion formation in apoE-deficient mice.

OZELIUS LJ, BREAKEFIELD XO.

Nat Genet. 1994 Nov;8(3):207-9.

Co-factor insufficiency in dystonia-parkinsonian syndrome.

PALMER RM, FERRIGE AG, MONCADA S.

Nature. 1987 Jun 11-17; 327(6122): 524-6

Nitric oxide release accounts for the biological activity of endothelium-derived relaxing factor.

PALMER RM, ASHTON DS, MONCADA S

Nature 1988 Jun 16; 333(6174): 664-6

Vascular endothelial cells synthesize nitric oxide from L-arginine.

PALMER RM, MONCADA S

Biochem Biophys Res Commun 1989 Jan 16; 158(1): 348-52

A novel citrulline-forming enzyme implicated in the formation of nitric oxide by vascular endothelial cells.

PANDA K, ROSENFELD RJ, GHOSH S, MEADE AL, GETZOFF ED, STUEHR DJ

J Biol Chem 2002 Aug 23; 277(34): 31020-30

Distinct dimer interaction and regulation in nitric-oxide synthase types I, II, and III.

PANDA K, GHOSH S, STUEHR DJ.

J Biol Chem 2001 Jun 29; 276(26):23349-56

Calmodulin activates intersubunit electron transfer in the neuronal nitric-oxide synthase dimer.

PAPAPETROPOULOS A, RUDIC RD, SESSA WC.

Cardiovasc Res. 1999 Aug 15; 43(3): 509-20.

Molecular control of nitric oxide synthases in the cardiovascular system.

PARK JH, NA HJ, KWON YG, HA KS, LEE SJ, KIM CK, LEE KS, YONEYAMA T, HATAKEYAMA K, KIM PK, BILLIAR TR, KIM YM.

Nitric oxide (NO) pretreatment increases cytokine-induced NO production in cultured rat hepatocytes by suppressing GTP cyclohydrolase I feedback inhibitory protein level and promoting inducible NO synthase dimerization.

J Biol Chem. 2002 Dec 6; 277(49): 47073-9

PATEL, M AND DAY, B

Metalloporphyrin class of therapeutic catalytic antioxidants

TIPS 1999 Vol.20: 359-364

PIERCE,CM, S KRYWAWYCH, A J PETROS.

Ped Crit Care Med 1[1], 166. 2000.

Asymmetric dimethyl arginine in infants with persistent pulmonary hypertension of the newborn.

POU S, POU WS, BREDT DS, SNYDER SH, ROSEN GM.

J Biol Chem. 1992 Dec 5; 267(34):24173-6.

Generation of superoxide by purified brain nitric oxide synthase.

RAINE J, HISLOP AA, REDINGTON AN, HAWORTH SG AND SHINEBOURNE EA

Arch. Dis. Child. 66:398-402. 1991

Persistent pulmonary hypertension of the newborn

RAMAN CS, LI H, MARTASEK P, KRAL V, MASTERS BS, POULOS TL

Cell 1998 Dec 23; 95(7):939-50

Crystal structure of constitutive endothelial nitric oxide synthase: a paradigm for pterin function involving a novel metal center.

REES DD, PALMER RM, MONCADA S.

Proc Natl Acad Sci U S A. 1989 May; 86(9):3375-8

Role of endothelium-derived nitric oxide in the regulation of blood pressure.

REEVES JT, GROVES BM, TURKEVICH D

The case for treatment of selected patients with primary pulmonary hypertension.

Am Rev Respir Dis 1986 Aug;134(2):342-6

REID L, MEYRICK B

Hypoxia and pulmonary vascular endothelium.

Ciba Found Symp 1980; 78:37-60

RESTA TC, WALKER BR

Am J Physiol 1996 Mar;270(3 Pt 2):H888-96

Chronic hypoxia selectively augments endothelium-dependent pulmonary arterial vasodilation.

ROSENKRANZ-WEISS P, SESSA WC, MILSTIEN S, KAUFMAN S, WATSON CA, POBER JS.

J Clin Invest. 1994 May; 93(5): 2236-43.

Regulation of nitric oxide synthesis by proinflammatory cytokines in human umbilical vein endothelial cells. Elevations in tetrahydrobiopterin levels enhance endothelial nitric oxide synthase specific activity.

RUDOLPH, A.M.

Annu Rev Physiol 1979 41: 383-395

Fetal and neonatal pulmonary circulation

SANDERS SA, EISENTHAL R, HARRISON R.

NADH oxidase activity of human xanthine oxidoreductase--generation of superoxide anion.

Eur J Biochem. 1997 May 1; 245(3): 541-8

SAKAI N, KAUFMAN S, MILSTEIN S

Mol Pharmacol 1993 Jan; 43(1): 6-10

Tetrahydrobiopterin is required for cytokine-induced nitric oxide production in a murine macrophage cell line (RAW 264).

SASE K, MICHEL T.

Life Sci. 1995; 57(22): 2049-55.

Expression of constitutive endothelial nitric oxide synthase in human blood platelets.

SATO K, RODMAN DM, MCMURTRY IF

Am J Physiol 1999 Apr; 276(4 Pt 1): L571-81

Hypoxia inhibits increased ETB receptor-mediated NO synthesis in hypertensive rat lungs.

SCHMIDT HH, HOFMANN H, SCHINDLER U, SHUTENKO ZS, CUNNINGHAM DD, FEELISCH M.

No .NO from NO synthase.

Proc Natl Acad Sci U S A. 1996 Dec 10; 93(25): 14492-7

SCHMIDT K, WERNER ER, MAYER B, WACHTER H, KUKOVETZ WR

Biochem J 1992 Jan 15; 281 (Pt 2):297-300

Tetrahydrobiopterin-dependent formation of endothelium-derived relaxing factor (nitric oxide) in aortic endothelial cells.

SCHULZ R, NAVA E, MONCADA S.

Br J Pharmacol. 1992 Mar;105(3):575-80

Induction and potential biological relevance of a Ca(2+)-independent nitric oxide synthase in the myocardium.

SCHUMAN EM, MADISON DV.

Science. 1991 Dec 6;254(5037):1503-6

A requirement for the intercellular messenger nitric oxide in long-term potentiation.

SHAUL PW, YUHANNA IS, GERMAN Z, CHEN Z, STEINHORN RH, MORIN FC 3RD.

Am J Physiol. 1997 May; 272(5 Pt 1): L1005-12

Pulmonary endothelial NO synthase gene expression is decreased in fetal lambs with pulmonary hypertension.

SHAUL PW, FARRAR MA, MAGNESS RR.

Am J Physiol. 1993 Oct; 265(4 Pt 2):H1056-63.

Pulmonary endothelial nitric oxide production is developmentally regulated in the fetus and newborn.

SMITH JA, RADOMSKI MW, SCHULZ R, MONCADA S, LEWIS MJ

Br J Pharmacol 1993 Apr; 108(4):1107-10

Porcine ventricular endocardial cells in culture express the inducible form of nitric oxide synthase.

STEINHORN RH, RUSSELL JA, MORIN FC 3RD.

Am J Physiol. 1995 Apr;268(4 Pt 2):H1483-9.

Disruption of cGMP production in pulmonary arteries isolated from fetal lambs with pulmonary hypertension.

STOCKS AND HISLOP

Structure and Function of the respiratory system: Developmental aspects of their relevance to aerosol therapy.

In Drug Delivery to the Lung, Vol. 162 Ed. Visgaard H; Smaldone GC and O'Callaghan C part of Lung Biology in Health and Disease series. Exec. Ed. Claude Lenfant, Marcel Dekker Inc. New York, 2002.

STROES E, KASTELEIN J, COSENTINO F, ERKELENS W, WEVER R, KOOMANS H, LUSCHER T, RABELINK T

J Clin Invest. 1997 Jan 1; 99(1): 41-6.

Tetrahydrobiopterin restores endothelial function in hypercholesterolemia.

TAYEH MA, MARLETTA MA.

J Biol Chem. 1989 Nov 25; 264(33):19654-8

Macrophage oxidation of L-arginine to nitric oxide, nitrite, and nitrate. Tetrahydrobiopterin is required as a cofactor.

THOMAE KR, NAKAYAMA DK, BILLIAR TR, SIMMONS RL, PITT BR, DAVIES P

J Surg Res 1995 Sep; 59(3): 337-43

The effect of nitric oxide on fetal pulmonary artery smooth muscle growth.

THONY B, AUERBACH G, BLAU N.

Biochem J. 2000 Apr 1; 347 Pt 1:1-16.

Tetrahydrobiopterin biosynthesis, regeneration and functions.

TIEFENBACHER CP, BLEEKE T, VAHL C, AMANN K, VOGT A, KUBLER W.

Circulation. 2000 Oct 31; 102(18): 2172-9

Endothelial dysfunction of coronary resistance arteries is improved by tetrahydrobiopterin in atherosclerosis.

TOZZI CA, POIANI GJ, HARANGOZO AM, BOYD CD, RILEY DJ

J Clin Invest 1989 Sep;84(3):1005-12

Pressure-induced connective tissue synthesis in pulmonary artery segments is dependent on intact endothelium.

TSUTSUI M, MILSTIEN S, KATUSIC ZS.

Circ Res. 1996 Aug; 79(2): 336-42

Effect of tetrahydrobiopterin on endothelial function in canine middle cerebral arteries.

TULLOH RM, HISLOP AA, BOELS PJ, DEUTSCH J, HAWORTH SG.

Am J Physiol. 1997 May; 272(5 Pt 2): H2436-45

Chronic hypoxia inhibits postnatal maturation of porcine intrapulmonary artery relaxation.

TURLEY JE, NELIN LD, KAPLOWITZ MR, ZHANG Y, FIKE CD

Am J Physiol Lung Cell Mol Physiol 2003 Mar; 284(3): L489-500

Exhaled NO is reduced at an early stage of hypoxia-induced pulmonary hypertension in newborn piglets.

UEDA S, MATSUOKA H, MIYAZAKI H, USUI M, OKUDA S, IMAIZUMI T

J Am Coll Cardiol. 2000 Jan; 35(1):71-5

Tetrahydrobiopterin restores endothelial function in long-term smokers.

VALLANCE P.J.AND WEBB D,J.

Vascular endothelium in human physiology and pathophysiology 2000

Harwood Academic Publishers imprint, part of the Gordon and Breach Publishing Group.

VALLANCE P, COLLIER J, MONCADA S.

Lancet. 1989 Oct 28;2(8670):997-1000

Effects of endothelium-derived nitric oxide on peripheral arteriolar tone in man.

VAN GELDEREN EM, DEN BOER MO, SAXENA PR.

Naunyn Schmiedebergs Arch Pharmacol 1993 Oct; 348(4): 417-23

NG-nitro L-arginine methyl ester: systemic and pulmonary haemodynamics, tissue blood flow and arteriovenous shunting in the pig.

VANE JR, ANGGARD EE, BOTTING RM

N Engl J Med 1990 Jul 5; 323(1): 27-36

Regulatory functions of the vascular endothelium.

VASQUEZ-VIVAR J, DUQUAINE D, WHITSETT J, KALYANARAMAN B, RAJAGOPALAN S (A)

Arterioscler Thromb Vasc Biol. 2002 Oct 1;22(10):1655-61

Altered tetrahydrobiopterin metabolism in atherosclerosis: implications for use of oxidized tetrahydrobiopterin analogues and thiol antioxidants.

VASQUEZ-VIVAR J, MARTASEK P, WHITSETT J, JOSEPH J, KALYANARAMAN B. (B)

Biochem J. 2002 Mar 15;362(Pt 3):733-9

The ratio between tetrahydrobiopterin and oxidized tetrahydrobiopterin analogues controls superoxide release from endothelial nitric oxide synthase: an EPR spin trapping study.

VASQUEZ-VIVAR J, MARTASEK P, KALYANARAMAN B.

Circulation 102: II-63, 2000

BH4/BH2 ratio but not ascorbate controls superoxide and nitric oxide generation by eNOS (Abstract)

VASQUEZ-VIVAR J, HOGG N, MARTASEK P, KAROUI H, PRITCHARD KA JR, KALYANARAMAN B.

Tetrahydrobiopterin-dependent inhibition of superoxide generation from neuronal nitric oxide synthase.

J Biol Chem. 1999 Sep 17; 274(38):26736-42

VASQUEZ-VIVAR J, KALYANARAMAN B, MARTASEK P, HOGG N, MASTERS BS, KAROUI H, TORDO P, PRITCHARD KA JR.

Proc Natl Acad Sci U S A. 1998 Aug 4; 95(16):9220-5

Superoxide generation by endothelial nitric oxide synthase: the influence of cofactors.

VENEMA RC, JU H, ZOU R, RYAN JW, VENEMA VJ

J Biol Chem 1997 Jan 10; 272(2): 1276-82

Subunit interactions of endothelial nitric-oxide synthase. Comparisons to the neuronal and inducible nitric-oxide synthase isoforms.

WALTER R, BLAU N, SCHAFFNER A, SCHNEEMANN M, SPEICH R, STOCKER R, NAUJECK B, SCHOEDON G.

Am J Respir Crit Care Med. 1997 Dec; 156(6): 2006-10

Inhalation of the nitric oxide synthase cofactor tetrahydrobiopterin in healthy volunteers.

WANG, Y, AND CONCEANI F

Circ Res 1992 71: 320-33

Isolated pulmonary resistance vessels from fetal lambs: contractile behaviour and responses to indomethacin and endothelin-1

WANSTALL JC, KAYE JA, GAMBINO A.

Br J Pharmacol 1997 May; 121(2): 280-6

The in vitro pulmonary vascular effects of FK409 (nitric oxide donor): a study in normotensive and pulmonary hypertensive rats.

WEI CC, WANG ZQ, MEADE AL, MCDONALD JF, STUEHR DJ.

J Inorg Biochem. 2002 Sep 20; 91(4): 618-24.

Why do nitric oxide synthases use tetrahydrobiopterin?

WEI CC, WANG ZQ, WANG Q, MEADE AL, HEMANN C, HILLE R, STUEHR DJ.

J Biol Chem. 2001 Jan 5; 276(1): 315-9

Rapid kinetic studies link tetrahydrobiopterin radical formation to heme-dioxy reduction and arginine hydroxylation in inducible nitric-oxide synthase.

WERNER ER, BAHRAMI S, HELLER R, WERNER-FELMAYER G.

J Biol Chem. 2002 Mar 22; 277(12):10129-33

Bacterial lipopolysaccharide down-regulates expression of GTP cyclohydrolase I feedback regulatory protein.

WERNER ER, WERNER-FELMAYER G, MAYER B

Proc Soc Exp Biol Med 1998 Dec; 219(3): 171-82

Tetrahydrobiopterin, cytokines, and nitric oxide synthesis.

WERNER ER, WERNER-FELMAYER G, WACHTER H.

Proc Soc Exp Biol Med 1993 May; 203(1): 1-12

Tetrahydrobiopterin and cytokines.

WERNER ER, WERNER-FELMAYER G, FUCHS D, HAUSEN A, REIBNEGGER G, YIM JJ, WACHTER H.

Biochem J. 1991 Dec 15; 280 (Pt 3): 709-14

Impact of tumour necrosis factor-alpha and interferon-gamma on tetrahydrobiopterin synthesis in murine fibroblasts and macrophages.

WERNER-FELMAYER G, WERNER ER, FUCHS D, HAUSEN A, REIBNEGGER G, SCHMIDT K, WEISS G, WACHTER H

J Biol Chem 1993 Jan 25; 268(3): 1842-6

Pteridine biosynthesis in human endothelial cells. Impact on nitric oxide-mediated formation of cyclic GMP.

WERNER-FELMAYER G, WERNER ER, FUCHS D, HAUSEN A, REIBNEGGER G, WACHTER H

J Exp Med 1990 Dec 1; 172(6): 1599-607

Tetrahydrobiopterin-dependent formation of nitrite and nitrate in murine fibroblasts.

WEVER RM, VAN DAM T, VAN RIJN HJ, DE GROOT F, RABELINK TJ.

Biochem Biophys Res Commun. 1997 Aug 18;237(2):340-4.

Tetrahydrobiopterin regulates superoxide and nitric oxide generation by recombinant endothelial nitric oxide synthase.

WHARTON J, DAVIE N, UPTON PD, YACOUB MH, POLAK JM, MORRELL NW

Circulation 2000 Dec 19; 102(25): 3130-6

Prostacyclin analogues differentially inhibit growth of distal and proximal human pulmonary artery smooth muscle cells.

WILD LM, NICKERSON PA, MORIN FC 3RD

Ligating the ductus arteriosus before birth remodels the pulmonary vasculature of the lamb. Pediatr Res 1989 Mar;25(3): 251-7

WILLIAMS RL, COURTNEIDGE SA, WAGNER EF.

Cell 1988 Jan 15; 52(1): 121-31

Embryonic lethalities and endothelial tumors in chimeric mice expressing polyoma virus middle T oncogene.

WILLIAMS RL, RISAU W, ZERWES HG, DREXLER H, AGUZZI A, WAGNER EF.

Cell. 1989 Jun 16; 57(6): 1053-63

Endothelioma cells expressing the polyoma middle T oncogene induce hemangiomas by host cell recruitment.

WORT SJ, MITCHELL JA, WOODS M, EVANS TW, WARNER TD

J Cardiovasc Pharmacol 2000 Nov;36(5 Suppl 1):S410-3

The prostacyclin-mimetic cicaprost inhibits endogenous endothelin-1 release from human pulmonary artery smooth muscle cells.

XIA Y., TASI A-L., BERKA V., ZWEIER J.

Journal of Biol Chem 1998; 273 vol 40. 25804-25808

Superoxide generation from endothelial nitric oxide synthase

XIE L, SMITH JA, GROSS SS

J Biol Chem 1998 Aug 14; 273(33): 21091-8

GTP cyclohydrolase I inhibition by the prototypic inhibitor 2, 4-diamino-6-hydroxypyrimidine. Mechanisms and unanticipated role of GTP cyclohydrolase I feedback regulatory protein.

YANAGISAWA M, KURIHARA H, KIMURA S, TOMOBE Y, KOBAYASHI M, MITSUI Y, YAZAKI Y, GOTO K, MASAKI T.

Nature 1988 Mar 31; 332(6163): 411-5

A novel potent vasoconstrictor peptide produced by vascular endothelial cells.

YONEYAMA T, HATAKEYAMA K

Protein Sci. 2001 Apr; 10(4): 871-8

Ligand binding to the inhibitory and stimulatory GTP cyclohydrolase I/GTP cyclohydrolase I feedback regulatory protein complexes.

YONEYAMA T, HATAKEYAMA K.

J Biol Chem. 1998 Aug 7; 273(32): 20102-8.

Decameric GTP cyclohydrolase I forms complexes with two pentameric GTP cyclohydrolase I feedback regulatory proteins in the presence of phenylalanine or of a combination of tetrahydrobiopterin and GTP.

YONEYAMA T, BREWER JM, HATAKEYAMA K.

J Biol Chem. 1997 Apr 11;272(15):9690-6

GTP cyclohydrolase I feedback regulatory protein is a pentamer of identical subunits. Purification, cDNA cloning, and bacterial expression.

ZELLERS TM, VANHOUTTE PM.

Pediatr Res. 1991 Aug; 30(2): 176-80.

Endothelium-dependent relaxations of piglet pulmonary arteries augment with maturation.